U.PORTO

PHD IN PHARMACEUTICAL SCIENCES

PHARMACEUTICAL TECHNOLOGY SPECIALTY

Synthesis of Locust Bean Gum new derivatives and their application in nanoparticulate drug delivery systems

Luis Braz

D

2016

U.PORTO

Luis Braz . Synthesis of Locust Bean Gum new derivatives and their application in nanoparticulate drug delivery systems

D.FFUP **2016**

Synthesis of Locust Bean Gum new derivatives and their application in nanoparticulate drug delivery systems

Luis Braz

FACULDADE DE FARMÁCIA

This page was intentionally left in blank


U.PORTO
FACULDADE DE FARMÁCIA
UNIVERSIDADE DO PORTO


UAlg ESS
UNIVERSIDADE DO ALGARVE
ESCOLA SUPERIOR DE SAÚDE


CIQA


CBMR

Luis Manuel Lima Verde de Braz

Synthesis of Locust Bean Gum new derivatives and their application in nanoparticulate drug delivery systems

Thesis submitted in fulfilment of the requirements to obtain the PhD degree in Pharmaceutical Sciences,
Pharmaceutical Technology Speciality,
Faculty of Pharmacy of University of Porto

Work developed under supervision of Prof. Dr. Bruno Sarmento and co-supervision of Prof. Dr. Ana M Rosa da Costa and Prof. Dr. Domingos de Carvalho Ferreira

May, 2016

The full reproduction of this thesis is allowed for research purposes only, through a written declaration of the person concerned, to which he commits to.

Luis Manuel Lima Verde de Braz

“Don’t count the days, make the days count.”

Muhammad Ali

To Guida,

Diogo and Inês

This page was intentionally left in blank

ACKNOWLEDGEMENTS

I would like to express my deep gratitude to all the people and institutions that received, helped and supported me during this work. Thus, I would like to acknowledge:

My supervisor Professor Bruno Sarmento and my co-supervisors Professor Domingos Ferreira and Professor Ana Costa for all the support during the development of this work and thesis.

Professor Bruno Sarmento, my supervisor, from Instituto de Engenharia Biomédica (INEB) and Instituto de Investigação e Inovação em Saúde (I3S) da Universidade do Porto, Porto, Portugal, and from Instituto de Investigação e Formação Avançada em Ciências e Tecnologias da Saúde (IINFACTS) do Instituto Superior de Ciências de Saúde do Norte (ISCS-N) da Cooperativa de Ensino Superior Politécnico e Universitário (CESPU), Gandra Portugal, for accepting me as a PhD student, for the support and scientific guidance during the development of this work and the writing of the thesis. I also acknowledge his patience and, most of all, friendship.

Professor Domingos Ferreira, my co-supervisor, from Laboratório de Tecnologia Farmacêutica da Faculdade de Farmácia, Universidade do Porto (FFUP), Porto, Portugal, for the support, friendship, understanding and availability provided to make possible the development of this work.

Professor Ana Costa, my co-supervisor, from Centro de Investigação em Química do Algarve (CIQA), Universidade do Algarve, Faro, Portugal and from Faculdade de Ciências e Tecnologia, Universidade do Algarve (FCT-UAlg), Faro, Portugal, for accepting the challenge of being my PhD co-supervisor, for all the support and scientific guidance during the development of this work and the writing of the thesis. Also for her patience, for being very present during the bench work, especially during the challenging chemical modifications performed in locust bean gum. Thank you also for sharing with me the most difficult and most exultant moments during the performance of this work, and for her dedicated friendship.

Industrial Farense for kindly providing locust bean gum.

Professor Ana Grenha from Centro de Investigação em Biomedicina (CBMR) da Universidade do Algarve, Faro, Portugal and from Centro de Ciências do Mar (CCMAR) da Universidade do Algarve, Faro, Portugal and from FCT-UAlg, for all the support given during the development of this work, especially for lending a space in her laboratory and allow me to use her material and reagents.

All the colleagues at CBMR, particularly Susana Rodrigues for all the friendship and support during the development of this work. Thank you for feeding the cells and seeding the plates when I was unable to be there.

Professor João Lourenço from CIQA, FCT-UAlg and Centro de Química Estrutural (CQE), Instituto Superior Técnico, Universidade de Lisboa, Lisboa, Portugal for assistance in the X-ray diffraction analysis.

Professor Marta Covo from Research Unit on Applied Molecular Biosciences (UCIBIO) at Rede de Química e Tecnologia (REQUIMTE), Departmento de Química, and CENIMAT/I3N, Departmento de Ciência de Materiais, Faculdade de Ciências e Tecnologia, Universidade Nova de Lisboa, Caparica, Portugal, for assistance in the NMR analysis.

Professor Carlos Gamazo from Departamento de Microbiología y Parasitología da Universidad de Navarra (UNAV), Pamplona, Spain, for receiving me in his group at UNAV during my short stay, and for all the support in the *in vivo* studies performed there. Thank you for the short moment during all this time when I really felt like a PhD student.

Ana Camacho (now Professor Ana Camacho, congratulations!) from Departamento de Microbiología y Parasitología da Universidad de Navarra (UNAV), Pamplona, Spain, for assistance during the *in vivo* experiments performed in UNAV.

Marinella from CBMR for assistance in the day 0 blood sample collection in the *in vivo* assays performed in UAlg.

Patrícia Madureira from CBMR for assistance in the SDS-PAGE and immunoblotting analyses performed in UAlg.

All my colleagues at Escola Superior de Saúde da Universidade do Algarve (ESSUAlg) for their support and friendship.

My family, especially my wife, Guida, and my kids, Diogo and Inês, the reason for all this. Thank you for all the support in the good and bad moments. Diogo, sorry for having missed your 3rd birthday, but I'm glad I didn't miss your first official goal (against Benfica, just for the records!).

This work was supported by National Portuguese funding through FCT – Fundação para a Ciência e a Tecnologia, projects PTDC/SAU-FCF/100291/2008, PEst-OE/EQB/LA0023/2013, PEst-OE/QUI/UI4023/2011 and UID/Multi/04378/2013. PROTEC grant from Direção Geral do Ensino Superior (SFRH/PROTEC/67422/2010), and mobility grant from ShareBiotech are also acknowledged.

This page was intentionally left in blank

ABSTRACT

Polymeric nanoparticles have been demonstrating to be very promising in oral delivery of biopharmaceuticals, including for vaccination purposes. In this respect, they should focus on optimizing antigen association efficiency, provide stability, tailor the release and elicit high levels of long-lasting antibody and cellular immune responses. Nanoparticles may benefit oral immunization due to the predominant uptake of particulates by Peyer patches. The M cells have been pointed as the primary targets to consider for nanoparticles. After nanoparticle uptake, subsequent internalization by professional antigen presentation cells is expected to occur, mediating the following immune response. Additionally, nanoparticle matrix materials might further help on the potentiation of an immune response, and the use of mucoadhesive polymers, the surface chemistry and/or surface ligand conjugation play an important role. Locust bean gum (LBG) may contribute in a strong manner for the improvement of nanoparticle abilities regarding an application in oral immunization, as the chemical composition of this polysaccharide includes mannose residues that may provide a preferential targeting of M cells and/or dendritic cells.

The development of LBG-based nanoparticles for an application in oral immunization was, thus, proposed in this thesis. Nanoparticle production occurred by mild polyelectrolyte complexation, requiring the chemical modification of LBG. Three LBG derivatives were synthesized, namely a positively charged ammonium derivative (LBGA) and negatively charged sulfate (LBGS) and carboxylate (LBGC) derivatives. Glycidyltrimethylammonium chloride was the alkylating agent allowing to obtain LBGA, a *N,N*-dimethylformamide sulfur trioxide (SO_3·DMF) complex was the sulfating agent in the synthesis of LBGS, and 2,2,6,6-tetramethylpiperidine-1-oxyl the oxidizing agent used to produce LBGC. The derivatives were characterized by Fourier transform infrared spectroscopy, elemental analysis, nuclear magnetic resonance spectroscopy, gel permeation chromatography and x-ray diffraction. Since a pharmaceutical application was aimed, a toxicological analysis of the derivatives was required. The assessment of the metabolic activity of intestinal Caco-2 cells following exposure (3 h or 24 h) to LBG and derivatives was performed by the MTT test, demonstrating the general safety of LBG derivatives at concentrations up to 1.0 mg/mL, with the exception of LBGA. Similar observations resulted from a complementary cytotoxicity assessment evaluating cell membrane integrity (LDH release assay).

Several nanoparticle formulations were produced using LBGA or chitosan (either in the free amine, CS, or in the hydrochloride salt form, CSup) as positively charged polymers, and LBGC or LBGS as negatively charged counterparts. The nanoparticle formulations were obtained with production yields up to 58%, while sizes varied between 180 and 830

nm and zeta potential between -28 mV and +48 mV, depending on the qualitative and quantitative composition. Morphological characterization performed on chosen formulations (LBGA/LBGS and CSup/LBGS) by transmission electronic microscopy suggested that nanoparticles presented a solid and compact structure with spherical-like shape. CSup/LBGS nanoparticles, which were later selected for the subsequent stage of antigen association, demonstrated to be stable in suspension for at least 3 months when stored at 4 ºC. LBGA/LBGS and CSup/LBGS nanoparticle formulations induced high cell viability in Caco-2 cells after 3 h and 24 h of exposure, when tested at concentrations up to 1.0 mg/mL (MTT assay), which was a remarkable event particularly considering the observation of some toxicity of the bare LBGA derivative. The LDH release assay evidenced some cytotoxicity of the CSup/LBGS formulation (24 h; 1.0 mg/mL), not shown by the MTT assay.

Two model antigens (a particulate cellular extract of *Salmonella* Enteritidis HE, and a soluble antigen - ovalbumin, OVA) were associated to CSup/LBGS nanoparticles with efficiency around 30%. The process was verified to not induce any deleterious effect on antigen structural integrity, while the antigenicity was retained. Nanoparticles exhibited adequate physicochemical properties for an application in oral immunization (size of 180 – 200 nm; positive zeta potential of 10 – 13 mV) and demonstrated to restrain the release of the antigens. Regarding the latter, a very limited release of HE in both simulated gastric and intestinal fluids was observed, while OVA released a maximum of 40% in the former medium. *In vivo* studies encompassed the administration of either HE-loaded or OVA-loaded nanoparticles to BALB/c mice. During five (HE) or six (OVA) weeks after oral and subcutaneous immunization, the systemic (IgG1 and IgG2a) and mucosal (IgA) immunological responses were evaluated. The adjuvant effect of the CSup/LBGS nanoparticles in obtaining an immunological response after oral immunization was demonstrated, although this was only provided when the soluble antigen OVA was used. On the contrary, an absence of effect was observed when the particulate antigen HE was tested. Nanoparticles were further found to elicit a balanced Th1/Th2 immune response, which is a relevant observation regarding an effective immunological protection.

Overall, LBGS was the synthesized derivative showing better ability for complexation with chitosan regarding the objective of producing nanoparticles with adequate properties for oral immunization. Additionally, a preliminary indication on the potential of the system for oral immunization is provided, although this is dependent on the antigen type.

Keywords: Locust bean gum, oral immunization, ovalbumin, polymeric nanoparticles, *Salmonella* Enteritidis antigenic complex

RESUMO

As nanopartículas poliméricas têm demonstrado grande potencial na administração oral de biofármacos, incluindo em vacinação. Neste âmbito devem focar a otimização da eficiência de encapsulação, proporcionar estabilidade, modular a libertação e induzir níveis elevados e duradouros de resposta imunológica humoral e celular. As nanopartículas podem beneficiar esta abordagem devido à captura predominante de material particulado pelas placas de Peyer. As células M têm sido apontadas como principais alvos a considerar e, após internalização, é expectável a captura subsequente por células apresentadoras de antigénios profissionais, mediando a resposta imune que se segue. Adicionalmente, a matriz das nanopartículas pode potenciar a resposta imune e a utilização de polímeros mucoadesivos, com a sua química de superfície eventualmente aliada à conjugação superficial de ligandos, têm um papel importante. A goma de alfarroba (LBG) pode contribuir fortemente para melhorar a aplicação das nanopartículas em imunização oral, porque a sua composição química inclui resíduos de manose que podem proporcionar uma vetorização para as células M e/ou dendríticas.

O desenvolvimento de nanopartículas de LBG para imunização oral é assim proposta nesta tese. A produção das nanopartículas ocorreu por complexação polieletrolítica, requerendo a modificação química da LBG. Três derivados foram sintetizados, um derivado aminado carregado positivamente (LBGA) e os derivados sulfatado (LBGS) e carboxilado (LBGC), com carga negativa. O cloreto de glicidiltrimetilamónio foi o agente alquilante para obtenção da LBGA, o complexo de trióxido de enxofre e *N,N*-dimetilformamida (SO_3·DMF), o agente sulfatante na síntese da LBGS, e a 2,2,6,6-tetrametilpiperidina-1-oxil foi o agente oxidante na produção da LBGC. Os derivados foram caraterizados por espectroscopia de infravermelho de transformada de Fourier, ressonância magnética nuclear, análise elementar, cromatografia de permeação de gel e difração de raios-X. A intenção de uma aplicação farmacêutica implicou a análise toxicológica dos derivados. A avaliação da atividade metabólica de células Caco-2 após exposição (3 h ou 24 h) à LBG ou aos derivados sintetizados foi realizada por MTT, que mostrou que, com exceção da LBGA, os materiais induziram viabilidades acima dos 70% quando testados em concentrações até 1 mg/mL. Um ensaio complementar que avalia a integridade da membrana celular (libertação de LDH) conferiu resultados semelhantes.

Foram produzidas várias formulações de nanopartículas que utilizaram LBGA ou quitosano como polímero carregado positivamente e LBGC ou LBGS como polímero negativo. As nanopartículas foram obtidas com rendimento de produção até 58%, enquanto os tamanhos variaram entre 180 e 830 nm e o potencial zeta entre -28 mV e

+48 mV, dependendo da composição qualitativa e quantitativa. A caraterização morfológica realizada em algumas formulações (LBGA/LBGS e CSup/LBGS) por microscopia eletrónica de transmissão sugere que as nanopartículas apresentam uma estrutura sólida e compacta e forma aproximadamente esférica. As nanopartículas de CSup/LBGS, posteriormente selecionadas para a associação de antigénio, demonstraram manter a estabilidade físico-química por pelo menos 3 meses quando armazenadas a 4 ºC. As nanopartículas de LBGA/LBGS e CSup/LBGS revelaram ausência de citotoxicidade em células Caco-2 após 3 h e 24 h de exposição, quando em concentrações até 1.0 mg/mL (ensaio MTT), uma observação relevante considerando a forte citotoxicidade do derivado LBGA. O ensaio de libertação de LDH revelou maior citotoxicidade da formulação CSup/LBGS (24 h; 1.0 mg/mL), não observada no ensaio MTT.

Dois antigénios modelo (um extrato celular particulado de *Salmonella* Enteritidis – HE, e um antigénio solúvel – ovalbumina, OVA) foram associados às nanopartículas CSup/LBGS com eficácia aproximada de 30%. Um estudo de estabilidade revelou ausência de efeito negativo do processo de associação sobre a integridade estrutural do antigénio, mantendo a sua antigenicidade. As nanopartículas exibiram propriedades físico-químicas adequadas para uma aplicação em imunização oral (tamanho de 180 – 200 nm; potencial zeta positivo de 10 – 13 mV) e demonstraram retardar a libertação dos antigénios. Neste sentido, observou-se uma libertação muito limitada de HE em meios gástrico e intestinal simulados, enquanto a OVA libertou no máximo 40% no primeiro meio. Ensaios *in vivo* incluíram a administração de nanopartículas contendo HE ou OVA a ratinhos BALB/c. Durante cinco/seis semanas após imunização oral e subcutânea, a resposta imunológica sistémica (IgG1 e IgG2a) e mucosa (IgA) foi avaliada. O efeito adjuvante das nanopartículas de CSup/LBGS na resposta imunológica após imunização oral foi demonstrado, apesar de se ter verificado apenas para o antigénio solúvel OVA. Pelo contrário, verificou-se uma ausência de efeito quando se testou HE, um antigénio particulado. As nanopartículas proporcionaram ainda um equilíbrio na resposta Th1/Th2, o que é relevante para uma proteção imunológica eficiente.

De forma geral, o LBGS foi o derivado sintetizado que evidenciou maior capacidade para complexação com quitosano com vista à produção de nanopartículas com propriedades adequadas para imunização oral. Além disso, há uma indicação preliminar do potencial do sistema para imunização oral, apesar de este depender do tipo de antigénio.

Palavras-chave: complexo antigénico de *Salmonella* Enteritidis, goma de alfarroba, imunização oral, nanopartículas poliméricas, ovalbumina

LIST OF PUBLICATIONS AND COMMUNICATIONS

Publications

- **Braz, L.**, Dionísio, M., Grenha, A., 2011. Chitosan-based nanocarriers: effective vehicles for mucosal protein delivery. In: S.P. Davis (Ed.), Chitosan: manufacturing, properties and usage. Nova Science Publishers, New York. p. 365-412
- **Braz, L.**, Rodrigues, S., Fonte, P., Grenha, A., Sarmento, B., 2011. Mechanisms of chemical and enzymatic chitosan biodegradability and its application on drug delivery. In: G. Felton (Ed.), Biodegradable Polymers: Processing, Degradation and Applications. Nova Science Publishers, New York. p. 325-364
- **Braz, L.**, Grenha, A., Corvo, M., Lourenço, J.P., Ferreira, D., Sarmento, B., Rosa da Costa, A.M. Synthesis and characterization of Locust Bean Gum derivatives and their application in the production of nanoparticles, submitted for publication to Carbohydrate Polymers
- **Braz, L.**, Camacho, A., Grenha, A., Ferreira, D., Rosa da Costa, A.M., Gamazo, C., Sarmento, B., Chitosan/Sulfated Locust Bean Gum nanoparticles: *In vitro* and *in vivo* evaluation towards an application in oral immunization, submitted for publication to International Journal of Pharmaceutics

Oral communications

- **Braz, L.**; Grenha, A.; Sarmento, B.; Rosa da Costa, A. Novel Locust Bean Gum nanoparticles for protein delivery, XVIII International Conference on Bioencapsulation, Oporto – Portugal, September 2010
- **Braz, L.**, Grenha, A., Ferreira, D., Rosa da Costa, A.M., Sarmento, B. Locust Bean Gum based nanoparticulate system for oral antigen delivery. 9th Central European Symposium on Pharmaceutical Technology, Dubrovnik – Croatia, September 2012

Poster presentations

- **Braz, L.**; Grenha, A.; Sarmento, B.; Rosa da Costa, A. Synthesis of Locust Bean Gum New Derivatives for Drug Delivery Applications. 70th FIP World Congress of Pharmacy/Pharmaceutical Sciences, Lisbon – Portugal, August 2010
- **Braz, L.**, Grenha, A., Ferreira, D., Rosa da Costa, A.M., Sarmento, B. Modification of a galactomannan-based polysaccharide and application in drug delivery. I Simpósio Nacional de Nanociência e Nanotecnologia Biomédica, Lisbon – Portugal, May 2011

- **Braz, L.**, Grenha, A., Ferreira, D., Rosa da Costa, A.M., Sarmento, B. Cytotoxicity evaluation of Locust Bean Gum derivatives and their application in drug delivery. 3rd PharmSciFair, Prague – Czech Republic, June 2011
- Silva, A., Grenha, A., Rosa da Costa, A.M., **Braz, L.** Análise multifactorial dos parâmetros que influenciam o rendimento de purificação da goma de alfarroba. IV Congresso Ibero-Americano de Ciências Farmacêuticas, Lisbon – Portugal, June 2011
- **Braz, L.**, Grenha, A., Ferreira, D., Rosa da Costa, A.M., Sarmento, B. Locust Bean Gum derivatives for nanometric drug delivery. 19th Portuguese-Spanish Conference on Controlled Drug Delivery, Oporto – Portugal, October 2011
- **Braz, L.**, Grenha, A., Ferreira, D., Rosa da Costa, A.M., Sarmento, B. Locust Bean Gum based nanoparticles for oral antigen delivery. 2nd International Conference on Pharmaceutics and Novel Drug Delivery Systems, San Francisco - EUA, February 2012
- **Braz, L.,** Camacho, A., Grenha, A., Ferreira, D., Rosa da Costa, A.M., Sarmento, B., Gamazo, C. *Salmonella Enteritidis* oral immunization mediated by chitosan-sulphated locust bean gum nanoparticles. 11th International Conference of the European Chitin Society, Oporto - Portugal, May 2013
- **Braz, L.,** Grenha, A., Ferreira, D., Rosa da Costa, A.M., Sarmento, B. Ovalbumin-loaded sulphated locust bean gum nanoparticles for oral immunization. 3rd Conference on Innovation in Drug Delivery: Advances in Local Drug Delivery, Pisa - Italy, September 2013
- **Braz, L.,** Grenha, A., Ferreira, D., Rosa da Costa, A.M., Sarmento, B. Locust Bean Gum-based nanoparticles as antigens carriers. Nano2013.pt - II Simpósio Nacional de Nanociência e Nanotecnologia Biomédica, Lisbon – Portugal, October 2013
- **Braz, L.**; Grenha, A.; Ferreira, D.; Rosa da Costa, A.M.; Sarmento, B., Immunization study of OVA encapsulated in locust bean gum based nanoparticles, 9th World Meeting on Pharmaceutics, Biopharmaceutics and Pharmaceutical Technology, Lisbon - Portugal, April 2014

TABLE OF CONTENTS

LIST OF FIGURES

LIST OF TABLES

ABBREVIATIONS

ABTS: 3-ethylbenzthiazoline-6-sulfonic acid

AE: Association efficiency

AIDS: Acquired immune deficiency syndrome

ANOVA: One-way analysis of variance

APCs: Antigen-presenting cells

AS03: Adjuvant system 03

AS04: Adjuvant system 04

AUC: Area under the curve

BCA: Bicinchoninic acid

BCG: Bacillus Calmette-Guérin

BSA: Bovine serum albumin

CD: Cluster of differentiation

$CD4^+$: CD4 positive T cell

$CD8^+$: CD8 positive T cell

CpG DNA: Cytosine – phosphate – guanine deoxyribonucleic acid

CS: Chitosan

CSup: Ultrapure chitosan

DCs: Dendritic cells

DC-SIGN: Dendritic cell-specific intercellular adhesion molecule-3-grabbing non-integrin

DMEM: Dulbecco's modified Eagle's medium

DMF: Dimethylformamide

DMSO: Dimethyl sulfoxide

DNA: Deoxyribonucleic acid

DO: Degree of oxidation

DS: Degree of substitution

dsRNA: Double-stranded ribonucleic acid

EDTA: Ethylenediamine tetraacetic acid

ELISA: Enzyme-linked immunosorbent assay

FAE: Follicle associated epithelium

FBS: Fetal bovine serum

FDA: Food and drug administration

FTIR: Fourier transform infrared

GALT: Gut-associated lymphoid tissue

GlcNAc: *N*-acetylglucosamine

GPC/SEC^3: Triple detection gel permeation chromatography

GRAS: Generally recognized as safe

GTMAC: *N*-glycidyl-*N,N,N*-trimethylammonium chloride

HE: Immunogenic subcellular extract obtained from whole *Salmonella* Enteritidis

HPLC: High performance liquid chromatography

ICAM-3: Intercellular adhesion molecule 3

IFN-γ: Interferon-gamma

IgA: Immunoglobulin A

IgG1: Immunoglobulin G1

IgG2a: Immunoglobulin G2a

IL-10: Interleukin 10

IL-17: Interleukin 17

IL-2: Interleukin 2

IL-22: Interleukin 22

IL-4: Interleukin 4

IL-6: Interleukin 6

IPN: Interpenetrating polymer network

ISO: International Organization for Standardization

LBG: Locust bean gum

LBGA: Locust bean gum ammonium derivative

LBGC: Locust bean gum carboxylate derivative

LBGS: Locust bean gum sulfate derivative

LC: Loading capacity

LDH: Lactate dehydrogenase

LPS: Lipopolysaccharide

M cells: Microfold cells

M/G: Mannose/galactose ratio

ManNAc : *N*-acetylmannosamine

MBL: Mannose-binding lectin

MF59: Oil in water emulsion composed of squalene, polysorbate 80, sorbitan trioleate and citrate buffer

MHC I: Major histocompatibility complex I

MHC II: Major histocompatibility complex II

M_n: Number average molecular weight

MPLA: Monophosphoryl lipid A

MTT: Thiazolyl blue tetrazolium bromide

M_w: Weight average molecular weight

NMR: Nuclear magnetic resonance

NP: Nanoparticles

OD: Optical density

OVA: Ovalbumin

PAMP: Pathogen-associated molecular pattern

PBS: Phosphate buffered saline

PBS-T: Phosphate buffered saline-tween

PdI: Polydispersion index

PLGA: Poly(d,l-lactide-co-glycolide)

PPs: Peyer's patches

PRR: Pattern recognition receptors

PS: Proteins standard

PVA: Polyvinyl alcohol

PY: Production yield

R_g: Radius of gyration

SDS: Sodium dodecyl sulfate

SDS-PAGE: Sodium dodecyl sulfate - polyacrylamide gel electrophoresis

SGF: Simulated gastric fluid

SIF: Simulated intestinal fluid

SO_3.DMF: *N,N*-Dimethylformamide sulfur trioxide

SP-A: Surfactant protein A

SP-D: Surfactant protein D

ssRNA: Single-stranded ribonucleic acid

TCRs: T cell receptors

TEM: Transmission electron microscopy

TEMPO: 2,2,6,6-tetramethylpiperidine-1-oxyl

TGF-β: Transforming growth factor β

Th: T helper

Th1: T-helper type 1

Th17: T-helper type 17

Th2: T-helper type 2

Th3: T-helper type 3

TLR: Toll-like receptor

XRD: X-ray diffraction

CHAPTER 1

GENERAL INTRODUCTION

The information presented in this chapter was partially published in the following publications:

Braz, L., Dionísio, M., Grenha, A., 2011. Chitosan-based nanocarriers: effective vehicles for mucosal protein delivery. In: S.P. Davis (Ed.), Chitosan: manufacturing, properties and usage. Nova Science Publishers, New York. p. 365-412.

Braz, L., Rodrigues, S., Fonte, P., Grenha, A., Sarmento, B., 2011. Mechanisms of chemical and enzymatic chitosan biodegradability and its application on drug delivery. In: G. Felton (Ed.), Biodegradable Polymers: Processing, Degradation and Applications. Nova Science Publishers, New York. p. 325-364.

This page was intentionally left in blank

1. General introduction

1.1. Nanoparticles as carriers in drug delivery

The recent decades have brought to the market many new biomolecules that have been identified as having therapeutic potential. This boom is directly related with advances in the biotechnological industry, making available a very considerable number of molecules that are protein-based. These molecules are usually called biopharmaceuticals, meaning that they are biological in nature and manufactured using biotechnology (1). A considerably wide variety of molecules is included in this group, from protein and peptides, to antigens and nucleic acids. In many cases their promise is so high that they are thought to occupy in the future an undisputed place alongside other established therapies. Although therapeutically promising, biopharmaceuticals are very instable compounds and their administration is extremely challenging, due to inherent physicochemical and biopharmaceutical properties (2, 3). This is the main reason why parenteral delivery frequently represents the unique administration possibility, as is often verified for vaccines, for example. Nevertheless, the parenteral route involves an invasive and painful administration, thus not being easily accepted by the patients and many times leading to therapeutic incompliance (3, 4). A gap is, thus, clearly identified which needs to be filled, compelling researchers to invest in this area in order to find adequate alternatives that permit effective, safe, cheap and comfortable administration of biopharmaceutical molecules through other routes. Comparing with the modality of parenteral delivery, mucosal administration is advantageous as systemic pathway, mainly because it is non-invasive, reducing patient discomfort, but also because it generally does not require the involvement of skilled personnel for the administration, thus reducing the costs of the process (3, 5). In this manner, the development of non-injectable delivery systems for mucosal administration could enhance significantly patient's compliance, thereby leading to increased therapeutic benefits.

The therapeutic action of proteins and protein-based molecules is not only limited by the potential degradation in biological environments, but also compromised by their low ability to reach the therapeutic site of action (3, 6, 7). In fact, these limitations are related either with the presence of a great number of functional groups susceptible of chemical degradation, or with the high hydrophilic character of the proteins, which results in poor permeability (8, 9). In addition, drug delivery via mucosal routes faces other major restrictions, including specific mechanisms of defense, the possibility to induce immune reactions at the delivery site and, generally, limitations in the surface area available for

absorption (10). As such, a meaningful challenge for current pharmaceutical scientists has been the need to develop suitable vehicles that permit delivering macromolecules through alternative routes of administration. These drug delivery carriers should exhibit a sort of characteristics, including capacity for high drug association and the ability to enhance drug physicochemical stability, providing protection to encapsulated drugs from the moment of carrier production until release. Furthermore, in many cases, the carriers are expected to regulate the drug release profile, while allowing an intimate contact of molecules with mucosal barriers, contributing for their epithelial permeation. In such a task, there is a consensus in that the materials and methods used to prepare the referred vehicles play relevant roles (11, 12).

Directing the research efforts towards the development of adequate vehicles for the purpose of drug delivery through distinct routes of administration, resulted in the appearance of several drug delivery systems like nanoparticles and microspheres. Nanoparticulate-based technologies have reached a position of evidence and nanoparticles are one of the most approached systems. The International Organization for Standardization (ISO) defines nanoparticles as particles with at least one dimension less than 100 nm (13). This definition is however not consensual in the field of drug delivery and there are many authors considering that nanoparticles are carriers with dimensions between 10 and 1000 nm (14-17). The interest in nanosystems (submicron sized systems) relies on several differentiating features that include an increased surface-to-volume ratio, in many cases displaying surface functionality, which offers high potential for the association of biopharmaceuticals (15). Biological transport processes have been reported to be affected by the physical attributes of nanocarriers, both anatomically and down to the cellular ad subcellular levels (18). Actually, nanocarriers have been reported to increase drug absorption by reducing the resistance of the epithelium to drug transport in a localized area or by carrying the drug across the epithelium (19). In this regard, transport has been described as more favorable for nanoparticles than for microparticles (2, 20, 21). In addition, colloidal carriers are reported to have improved capacity to interact with mucosal epithelial membranes (20), maximum interaction being reported to occur for systems within 50 – 500 nm (8). Colloidal carriers have also shown several times the ability to control the drug release profile of encapsulated molecules (22-24). Importantly, specifically regarding the delivery of biopharmaceuticals, an improvement of molecule stability, bioavailability, targeting, uptake and biological activity has been shown (24-26). **Table 1.1** summarizes the advantages and drawbacks of nanoparticles for drug delivery applications.

Table 1.1 - Advantages and limitations of nanoparticles for drug delivery applications.

Advantages	**Limitations**
High surface/volume ratio	Undefined physical shape
Ease of surface modification	Limited capacity to co-associate other functional molecules
Maximised contact with mucosae	Unknown toxicity profile
High drug concentration in desired site	Lack of suitable large-scale production methods
Ability to enter cells	Low stability in some biological fluids
Protection of encapsulated molecules	Tendency for aggregation
Possibility to provide controlled release	Limited loading capacity (unsuitable for less potent drugs)
Possibility of targeted delivery	Small size can provide access to unintended environments

1.1.1. Methods for nanoparticle production

Although rather different materials may be used to produce nanoparticles, including metals and ceramics, polymers have been one of the most used of the material classes. The literature describes many methods to produce polymeric nanoparticles. Naturally, each method has its own *pros* and *cons*, and the choice of a particular methodology will mainly depend on specific characteristics of the drug to be encapsulated and the material to be used as matrix (3). The techniques may be categorized into top-down or bottom-up approaches. Top-down processes involve the size-reduction of large particles to the nanometre range, which can be achieved by milling or high pressure homogenization. These processes have much lower application when compared with bottom-up techniques, which involve the assembly of molecules in solution to form defined nanostructures (27, 28). However, it is important to mention that delivery systems resulting from bottom-up technologies usually display size polydispersity (29), which in some cases limits nanoparticle usefulness. In fact, it is assumed that in a polydisperse system, larger nanoparticles might have higher drug loading capacity, while smaller nanoparticles are expected to have higher efficiency at delivering drugs to tissues or cells.

In a limit situation, this means that, even if the drug carrier has high association efficiency, the efficacy of the delivery may be poor (30). Therefore, fabrication processes should be rigorously optimized to provide a compromise between satisfactory association efficiency and the most suitable size for the established objective. Interestingly, a recent technological development related to a top-down process termed particle replication in non-wetting templates, which is a modified soft lithography technique, has demonstrated independent control over nanoparticle size, as well as other parameters that include shape, modulus (stiffness) and surface chemistry (29, 31).

Bottom-up techniques might also be classified according to whether the formulation of nanoparticles involves a polymerization reaction or is achieved directly from a preformed polymer (32). Methods involving polymerization are divided in emulsion polymerization and interfacial polymerization (32). When nanoparticles are prepared from preformed polymers, which is the most common approach, the diversity of techniques increases, involving methods based on emulsification, polymer desolvation, or intermolecular electrostatic interactions (11, 32). Contrary to low molecular weight drugs, biopharmaceuticals possess organized structures (proteins for example may have secondary, tertiary, or even quaternary structure) with labile bonds and side chains of chemically reactive groups. This specific structure defines the exact properties and activities of the molecules and, therefore, it is crucial to ensure its preservation during the association procedures, as its disruption or the modification of side chains can lead to loss of activity of the molecule. This fragile nature requires that methods selected for association do not damage the molecule structure, reduce their biological activity, or render them immunogenic (3).

Methods based on the establishment of intermolecular electrostatic interactions are one of the most reported and are applied when the matrix of nanoparticles is composed by at least one polyelectrolyte, that is, a polymer that exhibits charged groups when in solution. The principle of this methodology is the ability of polyelectrolytes to establish stable links with oppositely charged groups (33). Two different methods are described based on electrostatic interaction. *Ionic gelation* is the used denomination when the polyelectrolyte is a polymer with gelling ability (such as chitosan or alginate, for instance) and its gelation is induced by small anionic molecules, such as phosphate, citrate and sulfate groups. A very typical example is that of chitosan nanoparticles prepared by interaction of chitosan amino groups with the phosphate groups of tripolyphosphate (34). In turn, *polyelectrolyte complexation* is the name of the technique when the groups mediating the interaction are provided by two oppositely charged polyelectrolytes, instead of involving one small molecule (35). The latter approach is often referred to as complex coacervation or

interfacial coacervation (36, 37), and includes for example chitosan/alginate (38), chitosan/carrageenan (39) or chitosan/dextran sulfate (40) nanoparticles. **Figure 1.1** displays a schematic representation of the method of polyelectrolyte complexation to produce nanoparticles. The assembly of nanoparticles is easily and immediately observed upon pouring a solution of one polyelectrolyte over a solution of the oppositely charged polyelectrolyte, under mild stirring.

The popularity of the method is mainly due to the fact that it usually involves a complete hydrophilic environment and mild preparation conditions (41), avoiding the use of organic solvents or high shear forces and making association of labile drugs, such as biopharmaceuticals, an easier task (33, 42).

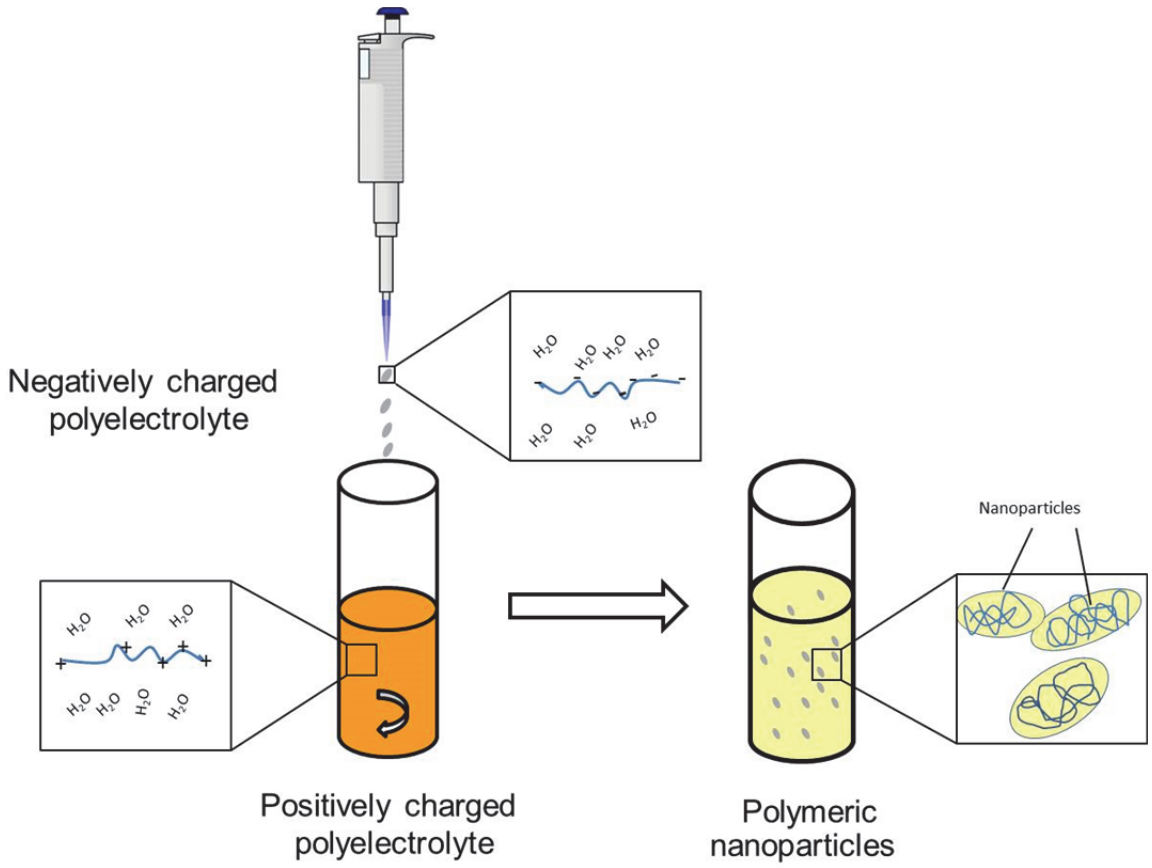

Figure 1.1 – Schematic representation of the preparation of nanoparticles by the method of polyelectrolyte complexation.

The literature indicates that, in order to obtain nanocarriers with pre-established characteristics by this method, an optimization of the process should be performed

focusing aspects such as the concentration of polyelectrolytes, the stirring conditions and the conditions of centrifugation (43).

1.1.2. Materials for nanoparticle production

The selection of appropriate materials for drug delivery approaches should be driven by several requirements, including biocompatibility, biodegradability, versatility and low overall costs of production (11, 44). As mentioned above, polymeric nanoparticles are one of the most representative of nanomedicines, as polymers are among the most versatile building units, permitting an easy tailoring of their properties to meet specific requirements (44). By definition, polymeric nanoparticles can be produced using either synthetic or natural polymers. The former are reported frequently, but in many cases they display unsatisfactory biocompatibility, which limits potential clinical applications (45). On the contrary, natural polymers comply more easily with the requirements mentioned above (46). Actually, it has been claimed that one of the ways of avoiding the potential toxicity of nanocarriers, an issue believed to be one of the most relevant in preventing diverse clinical applications so far, may be using natural materials (45). Moreover, these have some remarkable merits over synthetic ones, namely improved capacity for cell adhesion and mechanical properties similar to natural tissues (47).

The class of natural polymers is divided in proteins and polysaccharides. The latter have found a wide range of applications, as there is an extensive variety of materials available for exploration, comparing with proteins. Furthermore, many polysaccharides are obtained from plants or marine organisms, therefore being less probable to induce adverse immunological reactions, as compared with proteins (44). Polysaccharides are complex carbohydrates, composed of monosaccharides joined together by glycosidic bonds (44, 48). The most common basic units composing these carbohydrate polymers include several monosaccharides such as D-glucose, D-fructose, D-galactose, L-galactose, D-mannose, L-arabinose and D-xylose. Some polysaccharides comprise in their structure simple sugar acids (glucuronic, mannuronic and iduronic acids) and also monosaccharide derivatives, like the amino sugars D-glucosamine and D-galactosamine, as well as their derivatives *N*-acetylneuraminic acid and *N*-acetylmuramic acid (49). The presence of several of these sugar units on the side chain of carbohydrate polymers makes them good candidates for targeted delivery by carbohydrate recognizing receptors found on the surface of several cells (50, 51).

Polysaccharides might have algal, plant, microbial or animal origin, but they all share general properties of natural polymers, including the propensity for biocompatibility, low cost and hydrophilicity (45, 48, 52). **Table 1.2** presents the *pros* and *cons* of polysaccharides as nanoparticle matrix materials.

Table 1.2 – *Pros* and *cons* of polysaccharides as nanoparticle matrix materials (53).

Advantages	**Limitations**
Structural flexibility, stability	Inter-batch variability
Low cost	Limited availability (if widely used)
Bioadhesion capacity	Complex and varied composition
Hydrophilicity	Difficult to process
Biocompatibility, biodegradability	Immunogenicity

Importantly, polysaccharides are economical, readily available, usually biodegradable and with few exceptions, also biocompatible (46, 54). These are the reasons justifying that they assume a relevant role as matrix materials for drug delivery systems and, namely, nanoparticles. Owing to the potential to exhibit biodegradability, carriers based on polysaccharides are expected to be easily eliminated from the organism, as a consequence of their metabolization into small sugar units that integrate conventional metabolic processes, thereby permitting elimination or re-absorption (45). Polysaccharides present diverse physicochemical properties, deriving from multiple chemical structures that also translate into different molecular weights (M_w) and intrinsic characteristics. Ionic nature, for instance, is one of the greatest items of variation, as cationic, anionic and neutral polysaccharides can be found (46, 48). The hydrophilic character is particularly important, as it allows the production of nanoparticles by methods not involving organic solvents. Additionally, polysaccharides also benefit from a great structural flexibility, forming either linear or branched structures and easily permitting chemical modifications (44, 55). The more sophisticated applications of these polymers to produce nanoparticles, which include controlled or triggered release, or even targeted delivery, frequently demand chemical modifications of polysaccharides. These usually encompass the introduction of ionic or hydrophobic groups, degradable bonds, spacers or targeting moieties (44). The ability to adhere to biological surfaces comprises a relevant

advantage in drug delivery applications (48), as these frequently imply an interaction with cell surfaces. In this regard, the reactive functional groups of polysaccharides allow the formation of non-covalent bonds with cell surfaces, affording enhanced residence time and, consequently, increased drug absorption (45, 52). Notwithstanding the relevance of the advantages mentioned above, some drawbacks should also be taken into account, such as the possibility of generating immunogenic responses and the polymer variability related to origin and supplier (47). Regarding the latter, plant-derived polysaccharides pose potential challenges, as structural differences might occur according to the location and plant collection season (46).

As understood from what is described above, although polysaccharides have been traditionally included in formulations as inert materials, modern pharmaceutical design involves these excipients in increasingly relevant roles. In this manner, their application usually intends to endow the dosage forms with multi-functional abilities, such as controlled release, stabilization, emulsification or bioadhesiveness, among others (46, 48). Nevertheless, the set of polysaccharide properties confers a relevant versatility that adds to a wide range of biological abilities, thus generally contributing to an increased application in drug carrier production.

The application of polysaccharides in the production of nanoparticles by polyelectrolyte complexation or ionic gelation is widely reported (34, 38-40, 56, 57). As these methods require hydrophilic materials that exhibit opposite charges, in addition to an absence of toxicity, chitosan is the only natural polycationic polysaccharide that satisfies these needs (52). On the contrary, there are many negatively charged polysaccharides that can be used for this end, including alginate, hyaluronic acid, dextran sulfate, chondroitin sulfate and carrageenan, among many others. However, the interest on using other materials that do not exhibit charge has also been demonstrated occasionally and, in this regard, the synthesis of charged derivatives of these polysaccharides has been reported to serve the strategy, as described for pullulan (58, 59).

Below, the general characteristics of the polysaccharides locust bean gum and chitosan, which were used in this work to produce nanoparticles by polyelectrolyte complexation, are detailed.

1.1.2.1. Locust bean gum

Locust bean gum (LBG) is a non-starch polysaccharide, mainly comprised of a high molecular weight (approximately 50 000 – 3 000 000 Da) neutral galactomannan consisting in a linear chain of (1-4)-linked β-D-mannopyranosyl units with (1-6)-linked α-D-galactopyranosyl residues as side chains (60), as depicted in **Figure 1.2**.

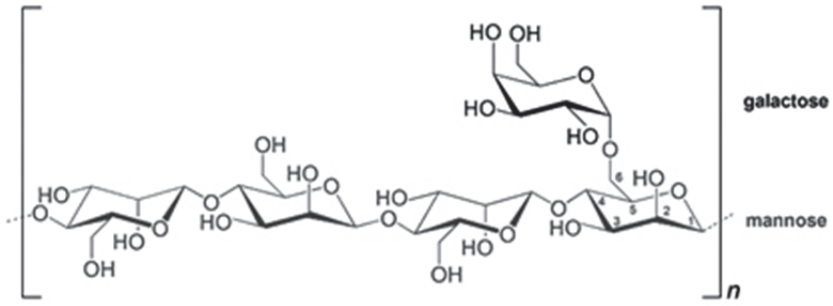

Figure 1.2 – Chemical structure of locust bean gum.

The polysaccharide is extracted from the seeds of the carob tree (*Ceratonia siliqua*), where it acts as a reserve material utilized during germination. It is also referred in the literature by several other synonyms, such as carob bean gum, carob seed gum, carob flour or even *ceratonia* (61) and consists in a white to yellowish white, nearly odorless, powder. The carob is a large tree that grows to about 10 m high in 10-15 years, and starts to bear good quantities of pods around this age, although it may not be fully grown until it is 50 years old. It is very abundant in the Mediterranean region, although its location also extends to various regions of North Africa, South America, and Asia. Its fruit is a long brown pod containing very hard brown seeds, the kernels, which represent approximately 10% of the weight of the fruit. In the processing of carob gum, these seeds are first dehusked by treating the kernels with dilute sulfuric acid or with a thermal mechanical treatment. The seeds are then split lengthwise and the germ portion is separated from the endosperm. Following, the isolated endosperm (42-46% of the seed weight) undergoes grinding, sifting, grading, and packaging (native LBG). The gum may still be simply washed with ethanol or isopropanol to control the biological load (washed LBG) or be further clarified by dispersion in hot water, recovery by precipitation with isopropanol or ethanol, filtering, drying and milling (clarified LBG). The clarified gum has higher galactomannan content, and no longer contains the cell structure. The commercial samples of LBG contain approximately 80-85% galactomannan, 5-12% moisture, 1.7-5%

acid-soluble matter, 0.4-1% ash, and 3-7% protein; the samples of clarified LBG contain approximately 3-10% moisture, 0.1-3% acid-soluble matter, 0.1-1% ash, and 0.1-0.7% protein (60, 62-64).

Galactomannans include several polysaccharides, such as LBG, guar gum and tara gum, which mainly differ in the mannose/galactose (M/G) ratio and the substitution pattern of side-chain units. The M/G ratio varies depending on the distribution of the galactose units over the mannose backbone, being approximately 4:1 for LBG, as results from reported mannose and galactose contents varying within 73-86% and 27-14%, respectively (60, 65). This is an approximate ratio, as it is strongly affected by the varying origins of the polymer and plant growth conditions during production (46). This ratio is the main characteristic affecting galactomannans solubility, as higher water solubility is afforded by higher galactose content (66), because it introduces an entropic and a steric barrier to the ordered packing of mannose segments that leads to aggregate formation (67). Galactose grafts to the mannose chain are known to not be spaced regularly, instead assuming random locations on the linear backbone and leading to low-substituted (“smooth”) and densely-substituted (“hairy”) zones (68). These low-substituted blocks of the backbone permit, consequently, the formation of strong intramolecular hydrogen bonds that reduce the hydration of the gum (69). Displaying an M/G ratio of approximately 4:1, LBG presents limited solubility, having propensity to form aggregates in cold water, as the long segments of unsubstituted mannose, which can be as large as 50 mannose units, are prone to undergo aggregation (47, 67, 69). LBG forms very viscous solutions at relatively low concentrations (70). When in solution, galactomannans have an extended rod-like conformation and occupy a large volume of gyration. In a process dependent on the molecular weight, these gyrating molecules collide with each other and with clusters of solvent molecules to produce solutions of high viscosity (69). Being non-ionic in nature, LBG viscosity and solubility are little affected by pH changes within the range of 3-11, as well as by the addition of salts (62, 63). In this context, chemical modifications of galactomannans to perform carboxylation, hydroxylalkylation and phosphorylation have been approached to overcome solubility limitations (71, 72).

Plant resources are renewable and, therefore, one of their important advantages relies on the possibility to have constant material supply, which is ensured if the plants are cultivated or harvested in a sustainable manner. However, plant-based materials also pose potential challenges that include the production of small quantities that may present structural differences depending on the location of the plants from which they originate, as well as the collecting season. In this context, several studies have evidenced that the chemical structure and molecular weight of LBG vary systematically with the type of

cultivar and growth conditions (46, 47). Furthermore, dehulling and milling processes, as well as dissolution temperature, are reported to influence the chemical (mannose and galactose content) and rheological properties of LBG (47, 68, 73, 74). This probably justifies, at least in part, why LBG is considered polydisperse from a chemical point of view, presenting three types of structural variation: 1) degree of galactose substitution, 2) patterning of galactose side groups and 3) chain length; all directly related with biosynthesis mechanisms (47). This is possibly one of the major limitations compromising a more frequent application of LBG in the pharmaceutical field. LBG is Generally Recognized as Safe (GRAS) by the Food and Drug Administration (FDA) and is approved in most areas of the world (European Union, United States of America, Japan, Australia, etc.), being used as thickening, gelling and stabilizing agent in both food and cosmetic industries (75, 76). In food industry it is a food additive, coded as E-410 in the European Union (77). Recently it has been indicated as a very useful excipient for pharmaceutical applications mainly due to its ability as controlled release excipient in tablets. However, other relevant properties and abilities have been demonstrated which contribute for its increasing use. The synergistic interaction between xanthan gum and LBG leading to the formation of thermally reversible gels is well-known. This effect has been ascribed to a denaturant effect of LBG that disturbs the helix-coil equilibrium of xanthan, displacing it from an ordered conformation to a more flexible one, facilitating the formation of heterotopic junctions between both polymers (78). A mucoadhesive behaviour has been indicated for this polysaccharide (79), although of lower potency comparing with others like chitosan. Additionally, there are indications on LBG biodegradability (64, 75), especially if administered orally, as enzymatic degradation mediated by β-mannanase (80, 81) or colonic bacteria (82) is expected to occur. Low toxicity and availability at low cost (75, 76, 83) have also been referred, contributing for the increased interest on the polymer.

1.1.2.1. Chitosan

Chitosan is a (1–4)-linked 2-amino-2-deoxy-β-D-glucan (**Figure 1.3**) that is obtained from the deacetylation of chitin, the second most abundant natural polymer after cellulose (84). The most usual source of chitin is the exoskeleton of crustaceans, but it exists in insects and fungi. Despite the widespread occurrence, up to now the main commercial sources of chitin have been crab and shrimp shells. Chitosan is the polymer considered to be obtained when chitin is deacetylated to such a degree that it becomes completely soluble in dilute aqueous acidic systems (85). The partial deacetylation is performed under

alkaline conditions (86) and results in the appearance of primary amino groups (87). Chitosan has also been reported to be obtained through biotechnological processes (88, 89). As shown in Figure 3, this polysaccharide is composed of repeating units of *N*-acetylglucosamine and D-glucosamine. Contrary to most polysaccharides, such as agar, dextran, pectin, cellulose and agarose, which are acidic in nature, chitin and chitosan are basic polysaccharides (90).

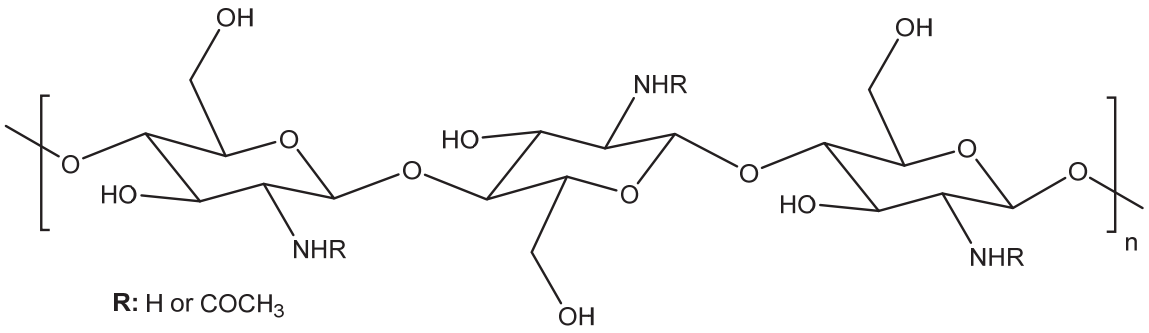

Figure 1.3 – Chemical structure of chitosan.

Chitosan comprises a series of polymers with different molecular weight and degree of deacetylation, characteristics which have been proving determinant in its behaviour (84, 85). Although these features are determined by the conditions selected during preparation/extraction of polymers, they can be further modified at a later stage. For example, the deacetylation degree can be lowered by reacetylation (91) and the molecular weight can be lowered by acidic depolymerization (92).

In fact, the main difference between chitin and chitosan is the number of acetyl groups. Although it is apparently a small difference, it turns to important variances in physicochemical properties, including solubility (chitin is insoluble in water and in the most common organic solvents and, hence, not useful for pharmaceutical purposes, whereas chitosan is soluble in acidic solutions), biodegradability and mucoadhesive capacity (93, 94). Displaying a pK_a of approximately 6.5, chitosan is insoluble in water and solutions of alkaline pH, while it becomes soluble in aqueous acidic solutions due to the protonation of most amino groups (89). This behaviour has been referred in some occasions to strongly affect the biomedical applications of the polymer, because it is insoluble at physiological pH (7.4), but it is a fact that it has been often demonstrated that chitosan-based formulations improve the therapeutic effect of the associated macromolecules, upon *in vivo* administration through physiological routes (24, 93, 95-99). This demonstrates that

the presence of chitosan in the site of action as a dissolved form is not a critical issue regarding the therapeutic action of the carried molecules, although it is certainly decisive in the preparation of formulations. Directly regarding the influence of deacetylation degree on solubility, highly deacetylated chitosans (85% or more) are readily soluble in solutions with pH up to 6.5 (94).

Chitosan is included in marketed dietary supplements, as it attaches to fat and prevents its absorption, inducing weight loss (100). It is well known as a non-toxic, biocompatible and biodegradable polymer (101, 102), characteristics that render it very attractive for the biomedical and pharmaceutical fields. Given the structural similarity to glycosaminoglycans, it has been widely proposed for biomedical applications, including wound healing and tissue engineering (89). Additionally, it has long been a reference in the field of drug delivery, mainly owing to the reported mucoadhesive properties (103) and the ability to enhance the permeability of drugs (23, 93, 95, 96, 98, 104-109). The electrostatic interactions occurring between cationic amino groups of chitosan and the negatively charged mucin have been reported as the main driving force for its strong mucoadhesion (110). There is, thus, a direct relation between mucoadhesive capacity and the deacetylation degree, because highly deacetylated chitosan has more positively charged amino groups available to mediate the interaction with the negatively charged mucus components, leading to increased mucoadhesion (107). This explains that most scientific research reporting the pharmaceutical application of chitosan is performed with highly deacetylated chitosan. The ability to improve the permeability of drug molecules is described to be related with both transcellular and paracellular transport. While in transcellular pathway the effect is mostly related with the mucoadhesive capacity, in the case of the paracellular route it is attributed to a specific interaction with tight junctions, leading to their transient opening (111). In the latter case, although it is suggested that the temporary disruption of tight junctions is due to multiple mechanisms, it was demonstrated that a specific type of transmembrane proteins (claudins) is possibly playing a major role (112).

1.2. Nanoparticle application in oral immunization

1.2.1. General concepts in immunization

The search for successful vaccination has become one of the driving forces of global health strategies, because it is an effective approach to overcome diseases, presenting low incidence of side effects and great preventive actions (113). Despite this, society, cultural and individual beliefs, along with concerns about adverse effects, led to the creation of anti-vaccine movements that resulted in disruptions and even cessation of vaccine programs. These occurrences have consequently led to increased morbidity and mortality (114, 115).

The history of vaccination is plenty of attempts to treat numerous infectious diseases which are responsible for approximately 25% of global mortality, especially in children with age below five years (116, 117). The production of a successful vaccine is, however, devoid of triviality and requires a strong knowledge anchored on safety, feasibility, cost and, above all, demonstration of protective efficacy (**Figure 1.4**) (118).

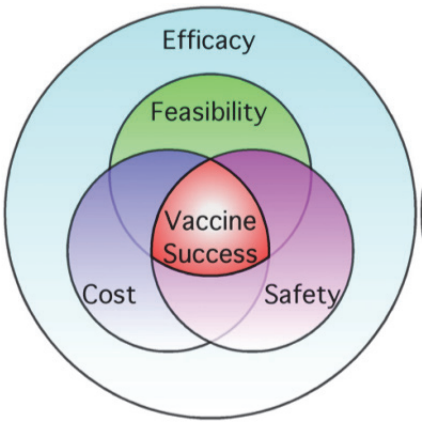

Figure 1.4 – Contribution of efficacy, safety, feasibility and cost to the development of vaccines (118).

Several types of vaccines are available in the market, exhibiting varied degrees of immunogenicity, stability and safety (119): live attenuated, killed whole, toxoid, and component (subunit) vaccines (120). Live attenuated vaccines are usually created from the naturally occurring pathogen itself. These vaccines are prepared from strains that are almost or completely devoid of virulence, but are capable of inducing a protective immune response (121). This is due to their ability to multiply in the host and provide continuous

antigenic stimulation over a period of time, thus often requiring just a single boost (122). Nevertheless, the application of these vaccines comprises some limitations, which include the possibility to cause severe infections in immunocompromised individuals (120), high risk of reverting back to the virulent form (122), and the need for an effective cold chain for their distribution. The latter is a clear limitation to their application in developing countries, as these might lack the necessary infrastructure (123). Examples of live attenuated vaccines are smallpox, polio (Sabin), measles, mumps, rubella, varicella and adenovirus (119, 122). Inactivated (killed) vaccines (such as influenza, hepatitis A, polio (Salk)) (119, 122) contain killed or inactivated microorganisms. These are not able to cause infection, but they are still able to stimulate a protective immune response, however usually requiring multiple doses to maintain immunity (122, 124). Toxoid vaccines consist in inactivated toxins but stimulate the production of neutralizing antibodies (tetanus, diphtheria) (122, 125). Subunit vaccines use a defined portion of the pathogen, such as proteins, peptides or nucleic acids (120, 122), and their interest mainly relies on the provided increased safety, as these cannot revert to a virulent form, as well as on the observed lack of contaminants remaining from the original pathogenic organism (122). Despite of this, the application of these formulations results in poor immunogenic effect when administered alone (120), demanding the use of an adjuvant in order to enhance the immunological response (122, 126).

Adjuvants are a highly heterogeneous group of compounds which share the characteristic of providing a modulation or/and enhancement of immune response (127). The mechanism mediating the interaction of adjuvants with the immune system is highly variable, as is the type of induced immunomodulation process, which consists, in short, in Th1, Th2, Th3, Th17 or/and T regulatory mediated response. The Th1 subset is characterized by the secretion of cytokines such as interleukin 2 (IL-2) and interferon-γ (IFN-γ), to assist in cell-mediated immune response. The Th2 subset assists preferentially in antibody immune responses after secreting cytokines like interleukin 4 (IL-4) (120). Th3 cells secrete interleukin 10 (IL-10) and/or transforming growth factor β (TGF-β), which are immunosuppressive cytokines that inhibit the proliferation of and cytokine production by effector T cells, including Th1 cells and Th2 cells (128). Th17 cells secrete interleukin 17 and 22 (IL-17 and IL-22, respectively) and play an important role in host defense against bacterial and fungal infection, especially at mucosal surfaces (129). Several functions for regulatory T cells include are suggested, which include prevention of autoimmune diseases by maintaining self-tolerance; suppression of allergy, asthma and pathogen-induced immunopathology; feto-maternal tolerance; and oral tolerance (130). Adjuvants are described to act through different mechanisms, including the formation of a depot for

the antigen, acting as an intermediate to target the antigen to immune cells, a mechanism that is assumed to occur when antigen delivery is mediated by particulate delivery systems, and even the stimulation of immune cells themselves (120, 131). Many compounds and strategies are described as adjuvants (120), but only aluminum-based mineral salt (alum), MF59 (an o/w emulsion composed of <250 nm droplets formed when squalene (4.3% v/v), polysorbate 80 (0.5% v/v) and sorbitan trioleate (0.5% v/v) are emulsified in citrate buffer), Adjuvant System 03 (AS03) (o/w emulsion + α tocopherol) and Adjuvant System 04 (AS04) (composed of monophosphoryl lipid A (MPLA) and alum) are approved for human usage (120, 122, 131, 132).

In addition to the urgent need to develop vaccines for emerging diseases, such as Zika or Ebola, there are well-known infectious diseases like malaria, tuberculosis and acquired immune deficiency syndrome (AIDS), that are still lacking an effective vaccine (133-135). The Bacillus Calmette-Guérin (BCG) vaccine has been available for many years against tuberculosis and the first vaccine against malaria was approved in 2015, but they are both referred as having low-medium efficacy (134, 135). This evidences the need for innovative strategies to the development of effective vaccines.

1.2.2. Oral immunization

The majority of vaccines available nowadays are administered through injection. The need for this procedure increases general vaccination costs and requires trained personnel to perform the administration, apart from being painful and uncomfortable, which often results in diminished patient compliance. In addition, the administration itself presents safety risks related to infection, needle reuse and disposal (119, 136), not to mention the need for cold-chain distribution (123). Oral vaccination emerges, in this context, as a strategy to overcome some of the mentioned drawbacks, benefiting from the general advantages of oral administration, but also basing its success on specific immune features of the intestine which revealed crucial for immunization. **Table 1.3** presents the main advantages and disadvantages of oral administration.

Contrary to parenteral immunization, which is mainly effective at producing systemic immune responses, oral vaccines elicit both systemic and mucosal immunity, further providing much higher patient's compliance and being more easily distributed, which is relevant for developing countries (119, 137, 138). Additionally, it is estimated that 90% of all mammalian infections originate at mucosal surfaces and, thus, mucosal sites are the primary access locations for most human pathogens (138). This reinforces the relevance

of inducing mucosal immunity towards limiting or preventing pathogen entry, thereby avoiding infection (139, 140).

Table 1.3 – Advantages and disadvantages of oral administration (141).

Advantages	**Disadvantages**
Large surface area offered for drug absorption (200 m^2)	Acidic gastric environment
Readily accessible and non-invasive	High metabolic activity
Rich blood supply	Drug diffusion limited by mucus barrier and intestinal motility
Ease of administration	Low permeability of epithelium
Possibility of prolonged retention	Possibility of food interaction
Patient acceptance and compliance	Individual variability
	Tolerogenicity

Notwithstanding the importance of the above considerations, oral vaccine delivery faces the major challenge of antigen uptake, as the intestine is designed to prevent invasion of foreign molecules, via epithelial tight junctions and high levels of enzymatic activity (142). In addition, many microbial antigens are hydrophilic molecules, thus having low epithelial permeability (8). As a result, the fate of many orally administered vaccines is gastrointestinal degradation, requiring high antigen doses or several repeated administrations to supply sufficient antigen for the induction of immune protection (126). In this context, and further considering the poor immunogenic activity of antigens administered through the oral route, the association of these macromolecules with nanoparticulate carrier systems has been demonstrating to be a promising approach, eliciting adequate immune responses (143).

However, there is still an important barrier to overcome, consisting in the constant intestinal fluid secretion, that may cause rapid removal of the applied delivery vehicles. It has, therefore, been proposed in several occasions that intestinal immunization could be improved by the use of appropriate bioadhesins, such as lectins, that bind specifically to

the mucosal surface and increase the carrier/antigen residence time (144). The decoration with suitable ligands could, in addition, mediate specific recognition by receptors on antigen presenting or sampling cells that direct the type and intensity of the subsequent immune response (145).

The immune response takes place, for example, in the course of an infection. It starts with an attraction of leukocytes to the infected region and interaction of the pathogen with the immune cells driven by pathogen-associated molecular pattern (PAMP) molecules, which have characteristic molecular patterns of infectious agents. These molecules are recognized by innate immune receptors called pattern recognition receptors (PRR) present on epithelial cells and antigen-presenting cells (APCs) and cause cell activation and subsequent migration (146). Toll-like receptors (TLRs) and C-type lectin receptors are the PRR families most involved in immune responses (147). While the former are expressed either on the cell surface or inside the endosomes (148), the latter are expressed on cell surface (149). **Table 1.4** presents the different TLRs and their specific ligands.

Table 1.4 – Toll-like receptors (TLRs) and their specific ligands (150).

TLRs	Ligands
TLR-1/ TLR-2	Triacylated lipopeptides
TLR-2/ TLR-6	Diacylated lipopeptides
TLR-3	Viral dsRNA
TLR-4	Lipopolysaccharide
TLR-5	Flagellin
TLR-7	Viral ssRNA
TLR-8	Viral ssRNA
TLR-9	Bacterial or viral CpG DNA
TLR-11	Profilin
TLR-10, 12, 13	Unknown

CpG DNA: cytosine – phosphate – guanine deoxyribonucleic acid; dsRNA: double-stranded ribonucleic acid; ssRNA: single-stranded ribonucleic acid

C-type lectin receptors are a set of cell surface receptors that are specialized on the recognition of carbohydrate molecules, including mannose, *N*-acetylglucosamine, L-fucose, glucose and galactosamine, among others (151), as depicted in **Table 1.5**.

Table 1.5 – Some of the most frequent C-type lectins and their specific ligands (152, 153).

C-type lectin	Ligands
Mannose receptor	Mannose, fucose, *N*-acetylglucosamine
Dectin-1	*β*-Glucan
Dectin-2	Mannose
DC-SIGN	Mannose, ICAM-3
MBL	Mannose, glucose, L-fucose, ManNAc, GlcNAc
SP-A	Glucose, mannose, L-fucose, ManNAc
SP-D	Glucose, mannose, maltose, inositol

DC-SIGN: dendritic cell-specific intercellular adhesion molecule-3-grabbing non-integrin; GlcNAc: *N*-acetylglucosamine; ICAM-3: Intercellular adhesion molecule 3; ManNAc : *N*-acetylmannosamine; MBL: mannose-binding lectin; SP-A: surfactant protein A; SP-D: surfactant protein D

The professional APCs comprise B lymphocytes, macrophages and dendritic cells (DCs) (136, 154), being the latter essential in generating the adaptive response. DCs uptake antigens, frequently with mediation of the mannose receptor, also known as CD206, that is overexpressed in their surface (155), and initiate a cascade of events that in most cases ends up with the elimination of pathogens. The antigens are degraded into peptides and these are presented on DCs surface using specific receptors of the major histocompatibility complex (MHC) I or II. While processing antigens, DCs initiate their maturation process and migrate to the lymph nodes, where they present the antigen (known as signal 1) and costimulatory signals (known as signal 2) to T cells (146). The antigen is presented together with the MHC of DCs to the T cell receptors (TCRs), while the costimulatory signals are the interaction of CD80 and CD86 DCs co-stimulatory molecules with CD28 T cell receptor. DCs mostly express CD80 and CD86 co-stimulatory molecules when capturing an antigen PAMP-related, which demonstrates the danger associated to that antigen. When DCs present the antigen to T cells without these costimulatory signals, T cell anergy (tolerance mechanism) to that antigen occurs (150, 156). The antigens presented by DCs through the MHC-I are recognized by $CD8^+$ T cells which are then converted into cytotoxic T cells, giving rise to a cell-cytotoxic immune response. Once activated, the cytotoxic T cells are responsible for lysing infected cells, thereby avoiding the growth of the microorganism. Furthermore, antigens presented by MHC-II are recognized by $CD4^+$ T cells, which differentiate in T helper (Th) cells. These cells promote, by releasing specific cytokines, both the cellular immune response and antibody response (120, 146). In turn, the B cells recognize extracellular antigens through immunoglobulins (Ig) present on their surface, causing their activation. B cells, aided by

Th cells, undergo extensive proliferation and generate both high-affinity memory B cells and long-lived plasma cells (157), the latter being capable to secrete large amounts of specific antibody (158). During this process, memory T and B cells are produced, which can quickly proliferate and eliminate the infecting agent (146).

Immune responses occurring in the intestinal area are mediated by the so called gut-associated lymphoid tissue (GALT). This comprises diffusely-scattered cells in the lamina propria, intra-epithelial lymphocytes, isolated lymphoid follicles present throughout the intestine and, most importantly, Peyer's patches (PPs) (141, 159). The latter are the structures where immune cells of the intestinal mucosa are mainly located (154), being privileged targets for mucosal vaccination due to their crucial role in intestinal mucosal immunity (160). The immune cells from the PPs, such as the DCs, are separated from the lumen by the Follicle Associated Epithelium (FAE) (159), which is composed of enterocytes, goblet cells and microfold cells (M cells) (136, 154). Several works suggest that PPs are the predominant site of uptake of nano- and microparticles, a process in which the antigen-sampling M cells play an important role (136). The M cells are, however, present in a small number in the intestinal tract, representing only 1 out of 10 million epithelial cells (approximately 5% in humans) (161). In parallel, they constitute 10–30% of the epithelial cells of the FAE above the PPs (162). These cells are considered the main entrance for pathogens invading the organism (163, 164) and are characterized by a disorganized brush border and a reduced mucus layer at the apical side, because in FAE there are less mucus secreting goblet cells than on the rest of the intestinal epithelium (165, 166). Furthermore, M cells contain small cytoplasmatic vesicles, few lysosomes and short microvilli (136, 159), and there is evidence that they can transport the antigen without any degradation, even in the absence of a protective carrier (167). Importantly, although the clear existence of a mannose receptor has not been described yet, M cells have been reported to favorably recognize mannose units and mannosylated carriers have been described to target M cells (80, 168, 169). The basolateral chamber of M cells is deeply invaginated forming a pocket hosting APCs: lymphocytes, macrophages and DCs (136, 154). These characteristics of M cells make them particularly suited for the task of antigen uptake, because they favor antigen interactions with the apical membrane, provide optimized antigen endocytosis, shorten and facilitate antigen access to the basolateral compartment, and finally favor rapid and straightforward interactions between immune cells and APCs that are present at the basal side (154). Therefore, M cells have been signaled as potentials targets to take into account in the design of oral vaccination strategies.

1.2.3. The role of nanoparticles: Locust bean gum as potential adjuvant

Polymeric nanoparticles have been demonstrating to be very promising in oral delivery of biopharmaceuticals, as many works report their effective role in the enhancement of oral drug bioavailability by facilitating cell internalization (19, 170). Their reduced size provides an intimate contact with epithelia and, in several occasions, they have shown the capacity to carry the encapsulated molecules through the epithelium (8, 19).

With respect to oral vaccination, the design of suitable antigen delivery systems should focus on optimizing antigen association efficiency, ensuring the maintenance of its stability during association, tailoring release kinetics and eliciting high levels of long-lasting antibody and cellular immune responses. Nanoparticles may provide extra benefits in oral immunization strategies, because PPs have shown to be a predominant site for uptake of particulates (136). Given their role in intestinal mediated immunization, M cells are the primary targets to consider and it has been demonstrated that particle uptake depends on various factors, such as particle size, surface charge, concentration, stability and ligand conjugation (170). In this context, it is important to highlight that nanoparticles have been showing to be better taken up by M cells as compared to microparticles (171-173). Once M cell uptake is observed, subsequent uptake by professional APCs, such as macrophages and DCs, is expected to occur, mediating the following immune response. Importantly, a great advantage of formulating antigens in nanocarriers lies in the exploitation of the intrinsic capacity of the referred phagocytic cells (macrophages, DCs, etc.), located in the PPs, to internalize foreign particulate materials (174). Another remarkable issue comes from studies on mucosal vaccination that have demonstrated that particulate antigens are often more immunogenic than antigens in solution, under the indication that particulate antigens are more likely to be trafficked across the mucosa and taken up by APCs (175).

A careful selection of nanoparticle matrix materials might further help on the potentiation of an immune response. In this context, mucoadhesive polymers may help on the prolongation on the intestinal residence time (176), potentiating the uptake by M cells. Importantly, the physicochemical characteristics of polymeric nanoparticles can be modulated by tuning polymer properties and surface chemistry, while their specificity may also be augmented by surface ligand conjugation (15). LBG, one of the polysaccharides used in this work for nanoparticle production, may contribute in a strong manner for the improvement of nanoparticle abilities regarding an application in oral immunization mediated by nanoparticles. The greatest potentiality that is identified comes from the proper chemical structure, which is composed of mannose and galactose residues. Given

the favorable contact with mannose residues, mentioned above, LBG might act as vector with preferential targeting ability towards these cells. Furthermore, it has mucoadhesive characteristics (79), although these are not as significant as those described for chitosan, which is the other polysaccharide used as matrix material in nanoparticle production. Finally, as dendritic cells are described to express mannose receptors (155), LBG nanoparticles are also expected to have a privileged contact with these cells, after being sampled by M cells.

CHAPTER 2

MOTIVATIONS AND OBJECTIVES

This page was intentionally left in blank

2. Motivations and Objectives

Successful vaccination approaches are required to face some of the most threatening diseases worldwide. Additionally, as many of the most concerning situations occur in developing countries, alternatives to the parenteral administration, that has costly requirements (cold chain, sterility, skilled personnel, etc.), are demanded (119, 123, 136). Oral immunization has thus been reaching a position of evidence in this regard, not only because the oral route is the main port of entry of pathogens and permits easy administration (138), but also due to specific structural abilities of the intestinal area (Peyer's patches, M cells, antigen presenting cells) regarding immunization approaches (136, 154). Some of these structures are known to establish a preferential contact with particulates (136). Therefore, the use of nanoparticles as antigen carriers has been proposed as a valuable strategy to induce immunological responses. These nanoparticles may be further functionalized or display in their structure moieties that provide an extra improvement of the targeting ability. In this regard, the use of locust bean gum (LBG) as matrix material may contribute for the improvement of nanoparticle abilities regarding oral immunization due to the mannose content that mediates a privileged contact with M cells and dendritic cells (80, 155, 169). Mucoadhesive materials may also be beneficial, providing prolonged intestinal residence time (176), and thus, potentiating the uptake by M cells. LBG has been reported to exhibit mucoadhesive characteristics (79), although other polysaccharides, like chitosan, are known to display much stronger mucoadhesiveness (103).

Taking into account the motivations referred above, this work is aimed at producing nanoparticles based on LBG for an application in oral immunization. To demonstrate the feasibility of the approach, *Salmonella* Enteritidis antigenic complex (HE) and ovalbumin (OVA) were used as model antigens.

To accomplish the referred general objective, several partial objectives were considered, which are disclosed below:

1) To synthesize charged derivatives of LBG (sulfated, carboxylated and ammonium) and confirm the effective derivatization using adequate techniques;

2) To produce LBG-based nanoparticles by polyelectrolyte complexation and select a formulation with suitable properties for antigen association and application as carrier in oral immunization;

3) To associate the model antigens HE and OVA and investigate their release profile in media relevant for oral delivery applications;

4) To evaluate the cytotoxicity of the synthesized LBG derivatives and LBG-based nanoparticles in human intestinal epithelial cells (Caco-2);

5) To evaluate *in vivo* the immunological response to a selected formulation of LBG-based nanoparticles associating the model antigens individually.

In this manner, it is expected to develop a natural, biocompatible polymeric nanoparticulate system which displays ability for the efficient association of antigens and suitable physicochemical properties for an application in oral vaccination.

CHAPTER 3

LOCUST BEAN GUM DERIVATIVES AND PRODUCTION OF NANOPARTICLES

The information presented in this chapter was submitted for publication in Carbohydrate Polymers:

Braz, L., Grenha, A., Corvo, M., Lourenço, J.P., Ferreira, D., Sarmento, B., Rosa da Costa, A.M. Synthesis and characterization of Locust Bean Gum derivatives and their application in the production of nanoparticles, submitted for publication

This page was intentionally left in blank

3. Synthesis and characterization of Locust Bean Gum derivatives and their application in the production of nanoparticles

3.1. Introduction

Biopolymers, among them polysaccharides, are an attractive class of polymers, as they are derived from natural sources, normally easily available, relatively cheap, many times biodegradable, and that can be modified by suitable chemical reagents. The most common basic unit of polysaccharides is the monosaccharide D-glucose, although D-fructose, D-galactose, L-galactose, D-mannose, L-arabinose, D-xylose, and the amino sugars D-glucosamine and D-galactosamine, as well as simple sugar acids, like glucuronic acid and iduronic acid, and sulfated monosaccharides are also frequently present (62).

Locust bean gum (LBG), also known as carob bean gum, is obtained from the endosperm of carob tree (*Ceratonia siliqua*) seeds, where it is a reserve material. The tree is very abundant in the Mediterranean region, including the Algarve. The gum corresponds to a galactomannan, and commercial samples of LBG contain approximately 80-85% galactomannan, while the remaining content is ascribed to proteins and impurities. LBG is reported as biocompatible, biosorbable, biodegradable, non-teratogenic and non-mutagenic, and its degradation products are excreted readily. Classified by the FDA as GRAS material, it is approved in most areas of the world for use in the food industry as thickener, stabilizer, emulsifier, and gelling agent (E410), as well as in the pharmaceutical industry as excipient in drug formulations, and in biomedical applications (60, 62-64). LBG is mainly comprised of a high molecular weight (approximately 50 000 – 3 000 000 Da) neutral galactomannan consisting in a linear chain of (1-4)-linked β-D-mannopyranosyl units with (1-6)-linked α-D-galactopyranosyl residues as side chains. The mannose and galactose contents have been reported to be 73-86% and 27-14%, respectively, which corresponds to a mannose:galactose (M/G) ratio of approximately 4:1 (60). For that reason, and in spite of the uneven distribution of galactose units along the mannose backbone, leading to low-substituted (“smooth”) and densely-substituted (“hairy”) zones (68), LBG is typically represented as shown in **Figure 1.2** (chapter 1, general introduction). Being non-ionic in nature, its viscosity and solubility are little affected by pH changes within the range of 3-11, as well as by the addition of salts (62, 63).

Recently, there has been a growing interest in the chemical functionalization of polysaccharides, particularly those non-animal derived, mainly by making use of the free

hydroxyl groups distributed along their backbone, in order to create derivatives with tailored properties for desired applications (48). Carboxymethylation of polysaccharides is a well-known etherification process achieved by reaction with monochloroacetic acid, and leading to products with a variety of promising properties, like increased hydrophilicity, water solubility, and solution clarity. Carboxymethyl cellulose, guar gum, LBG, and xanthan gum have been successfully used in the production of novel drug delivery systems, like beads, microparticles, and nanoparticles (177). The sodium carboxymethyl ether of LBG was combined with polyvinyl alcohol (PVA) for the production of interpenetrating polymer network (IPN) hydrogel microspheres of buflomedil hydrochloride, regarding a controlled drug delivery (178). The introduction of carboxyl groups in a galactomannan isolated from the seeds of *Leucaema leucocephala*, with an M/G ratio around 1.3, was successfully performed using 2,2,6,6-tetramethylpiperidine-1-oxyl (TEMPO) as oxidizing agent. This reagent acts by oxidizing the free C-6 position of the monosaccharide units, which, in this case, was demonstrated to be more effective on the mannopyranose units than on the galactose ones. As expected, the modified polymer, an anionic polyelectrolyte, showed greater water solubility than the original material. The fact that in the course of this oxidation reaction aldehyde groups form as intermediate, allowed the obtainment of an amphiphilic polymer by reductive amination with an amine bearing a long alkyl chain (179). Cellulose (180) and cashew gum (181) were also converted in the corresponding polyuronic acids by the above method. Sulfated LBG derivatives with various degrees of substitution were obtained by the chlorosulfonic acid/pyridine method, which presented significant chain stiffness, due to the electrostatic effect (182). A mixed carboxymethyl sulfate derivative of LBG was prepared by carrying out a sulfation reaction with SO_3.DMF complex followed by carboxymethylation. Ionotropic gelation of this LBG derivative induced by basic aluminum chloride in the presence the potent analgesic tramadol hydrochloride, led to the formation of hydrogel beads incorporating the drug. These hydrogels disintegrated very quickly in an acidic solution, liberating almost all of their content in 15 min, thus constituting a promising system for immediate dosage release formulations leading to instant analgesic action (183).

In this chapter, the chemical modification of LBG, aiming at the obtainment of charged derivatives intended for the development of nanoparticulate carriers by polyelectrolyte complexation, is described. Two anionic (sulfate and carboxylate) and one cationic (trimethylammonium) derivatives were prepared. The former two were obtained by an adaptation of a method applied in the sulfation of other polysaccharides, using an SO_3·DMF complex as sulfating agent (184), and using the above described oxidizing agent TEMPO (179), respectively. The latter was synthesized by reaction with the

alkylating agent glycidyltrimethylammonium chloride (GTMAC), adapting a described procedure (185).

3.2. Materials and methods

3.2.1. Materials

Locust bean gum (LBG) was a kind gift from Industrial Farense (Faro, Portugal). Chitosan (CS, low molecular weight, deacetylation degree = 75 – 85%), glacial acetic acid, chlorosulfuric acid ($HClSO_3$), dimethylformamide (DMF), *N*-glycidyl-*N,N,N*-trimethylammonium chloride (GTMAC), sodium hydroxide (NaOH), potassium hydroxide (KOH), 2,2,6,6-tetramethypiperidine-1-oxyl (TEMPO), sodium bromide (NaBr), sodium hypochlorite solution (NaClO), sodium borohydride ($NaBH_4$), sodium nitrate ($NaNO_3$), sodium dihydrogen phosphate (NaH_2PO_4), sodium azide (NaN_3), dialysis tubing (pore size 2000 Da), phosphotungstate dibasic hydrate, glycerol, phosphate buffered saline (PBS) pH 7.4 tablets, Dulbecco's modified Eagle's medium (DMEM), penicillin/streptomycin (10000 units/mL, 10000 µg/mL), non-essential amino acids, L-glutamine 200 mM, trypsin-EDTA solution (2.5 g/L trypsin, 0.5 g/L EDTA), trypan blue solution (0.4%), thiazolyl blue tetrazolium bromide (MTT), lactate dehydrogenase (LDH) kit, sodium dodecyl sulfate (SDS), dimethyl sulfoxide (DMSO), hydrochloric acid (HCl 37%), sodium chloride (NaCl) and potassium dihydrogen phosphate (KH_2PO_4) were purchased from Sigma-Aldrich (Germany). Ethanol was supplied by VWR. Potassium bromide (KBr) was obtained from Riedel-del-Haën (Germany). Fetal bovine serum (FBS) was obtained from Gibco (USA). Ultrapure water (Mili-Q Plus, Milipore Iberica, Madrid, Spain) was used throughout. All other chemicals were reagent grade.

3.2.2. Cell line

The Caco-2 cell line was obtained from the American Type Culture Collection (Rockville, USA) and used between passages 77-93. Cell cultures were grown in 75 cm^2 flasks in a humidified 5% CO_2/95% atmospheric air incubator at 37 ºC. Cell culture medium was DMEM supplemented with 10% (v/v) FBS, 1% (v/v) L-glutamine solution, 1% (v/v) non-essential amino acids solution and 1% (v/v) penicillin/streptomycin. Medium was changed every 2-3 days and cells were subcultured weekly.

3.2.3. Synthesis of Locust Bean Gum derivatives

3.2.3.1. Purification of Locust Bean Gum

The purification of LBG envisaged the removal of the protein content (3-7%) commonly present in commercial samples (60). To do so, a standard procedure was followed (73, 78), in which LBG (5.0 g) was slowly dispersed in distilled water (1000 mL) previously heated to 85 ºC, the dispersion being stirred for 1h. Then, the dispersion was cooled to room temperature and, subsequently, centrifuged (22 000 x *g*, 20 ºC, 1 h). The supernatant was collected and added to an equal volume of ethanol. The precipitate was collected by vacuum filtration and added again to an equal volume of ethanol. After subsequent collection by vacuum filtration, the precipitate was dried in a vacuum oven at 30 ºC during 72 h affording 3.9 g of white powder. The residue was grinded and stored until further use.

3.2.3.2. Sulfation of Locust Bean Gum

Sulfation of LBG was performed by a method established for the sulfation of other polysaccharides (184).

The sulfation agent, SO_3·DMF, was prepared by slowly dropping 5 mL of $HClSO_3$ into 25 mL of stirred DMF under cooling in an ice water bath, and continuing the stirring for 1.5 h. The obtained solution was stored in the refrigerator until further use.

Method 1

Purified LBG (500 mg) was dispersed in DMF (35 mL) and stirred at 60 ºC for 30 min, in order to provide the dispersion of LBG into the solvent. Then, the SO_3·DMF complex was added (9.3 mL) and the mixture reacted for 4 h under magnetic stirring. Subsequently, the mixture was cooled down to room temperature in an ice bath, neutralized with 30% NaOH solution until precipitation, and concentrated under reduced pressure at 60 ºC to evaporate the solvent. The residue was dissolved in distilled water (30 mL) and dialyzed against distilled water (5 L). The water was changed every 24 h and, after 3 days, the solution was concentrated under reduced pressure at 40 ºC. Then, ethanol was added into the concentrated solution, in order to precipitate the solute, and the dispersion was concentrated under reduced pressure at 40 ºC. The previous step was repeated twice,

and the last evaporation was performed until full evaporation of the solvent. The obtained powder was dried in a vacuum oven at 40 ºC for 3 days, affording 407 mg of brownish powder that was grinded and stored until further use.

Method 2

Purified LBG (500 mg) was slowly dispersed in distilled water (100 mL) previously heated to 85 ºC, and the dispersion was stirred for 1 h. After that time, the dispersion was cooled to room temperature and poured into an equal volume of ethanol. The precipitate was collected, added to DMF (300 mL) and centrifuged (22 000 x *g*, 20 ºC, 20 min). The precipitate was recovered and added to DMF (100 mL), resting overnight. This dispersion was then filtered and the residue was again added to DMF (35 mL), this new mixture being stirred at 60 ºC for 30 min, in order to provide the dispersion of LBG into the solvent. Then, the SO_3·DMF complex was added (9.3 mL) and the mixture reacted for 4 h under magnetic stirring. Subsequently, the mixture was cooled down to room temperature in an ice bath, neutralized with 30% NaOH solution until precipitation, and concentrated under reduced pressure at 60 ºC to evaporate the solvent. The residue was dissolved in distilled water (30 mL) and dialyzed against distilled water (5 L). The water was changed every 24 h and, after 3 days, the solution was concentrated under reduced pressure at 40 ºC. Then, ethanol was added into the concentrated solution, in order to precipitate the solute, and the dispersion was concentrated under reduced pressure at 40 ºC. The previous step was repeated twice, and the last evaporation was performed until full evaporation of the solvent. The obtained powder was dried in a vacuum oven at 40 ºC for 3 days, affording 363 mg of brownish powder that was grinded and stored until further use.

3.2.3.3. Carboxylation of Locust Bean Gum

The carboxylation of LBG was performed by oxidation with TEMPO (179). Purified LBG (500 mg) was dissolved in 200 mL of distilled water under stirring at 80 ºC for 30 min. After cooling down, the volume was adjusted to 200 mL and the solution was cooled in an ice bath. Then, TEMPO (10 mg) and NaBr (50 mg) were added to the solution under stirring. A 15% sodium hypochlorite solution (3.0 mL) with pH adjusted to 9.3 with 2 M HCl solution was mixed with the polymer solution. The pH was maintained at 9.3 by addition of a 0.05 M aqueous NaOH solution for 4 h. To stop the reaction, sodium borohydride (75 mg) was added and the solution was stirred for 45 min. Then the pH of the mixture was

adjusted to 8 by addition of HCl before precipitation by 2 volumes of ethanol in presence of NaCl (up to 10 g/L). The polymer was isolated by filtration under reduced pressure, washed several times with ethanol, filtered and dried in a vacuum oven at 30 ºC during 3 days. A white powder (529 mg) was obtained, grinded and stored until further use.

3.2.3.4. Quaternary ammonium salt of Locust Bean Gum

The introduction of quaternary ammonium groups in LBG was achieved by alkylation with glycidyltrimethylammonium chloride (GTMAC), as follows (185): an aqueous solution (10 mL) of KOH (0.550 g), was prepared in a round bottom flask, under stirring, at 60 ºC. Then, purified LBG (506 mg) and 3.72 mL of GTMAC were added. After 5 h, an equal amount of GTMAC was added to the mixture, which was allowed to react until the completion of 24 h. It was then diluted with 20 mL of miliQ water, allowed to cool down to room temperature, and neutralized with HCl (2M). The resulting solution was dialyzed for 3 days, the water being replaced every 24 h. Then, the LBGA solution was concentrated under reduced pressure at 40 ºC and ethanol was added into the concentrated solution, in order to precipitate the solute. The dispersion was concentrated under reduced pressure at 40 ºC and ethanol was added again and evaporated under the same conditions until full evaporation of the solvent. The obtained powder was dried in a vacuum oven at 40 ºC for 3 days, affording 423 mg of white powder that was grinded and stored until further use.

3.2.4. Chemical characterization of Locust Bean Gum derivatives

3.2.4.1. Fourier transform infrared (FTIR) spectroscopy

For recording FTIR spectra of purified LBG and their derivatives, samples were grounded with KBr in a mortar and compressed into discs. For each spectrum, a 32-scan interferogram was collected in transmittance mode with a 4 cm^{-1} resolution in the 4,000-400 cm^{-1} region.

3.2.4.2. Elemental analysis

Elemental analysis data were obtained in a Thermo Finnigan, FLASH EA 1112 Series (C, N, S) or in a Fisons Instruments, EA 1108 CHNS-O (O) elemental analyzer.

3.2.4.3. Nuclear magnetic resonance (NMR) spectroscopy

All NMR spectra were acquired in a Bruker Avance III 400 spectrometer equipped with a temperature control unit and a pulse gradient unit capable of producing magnetic field pulsed gradients in the z-direction of 56.0 G/cm, operating at 400.15 MHz for hydrogen, 100.61 MHz for carbon, using a multinuclear reverse 5 mm probe (TXI). The samples where dissolved in D_2O. ^1H NMR spectra were recorded with 8.22 KHz spectral window digitized with 64 K points. The ^{13}C spectrum was recorded between 0 and 238 ppm using 24,000 Hz spectral window digitized into 64 K points.

3.2.4.4. GPC/SEC^3 analysis

Triple detection Gel Permeation Chromatography (GPC/SEC^3) analysis was performed in a modular system constituted by a degasser, HPLC pump (K-1001) and RI detector (K-2300) from Knauer, and a viscometer and RALLS from Viscotek (Trisec Dual Detector Model 270), using two PL aquagel-OH mixed 8 μm, 300 x 7.5 mm columns.

For purified LBG, LBGC and LBGS the eluent was 0.2 M $NaNO_3$, 0.01M NaH_2PO_4, 0.1% w/v NaN_3, pH=7, at 1mL/min; the samples were dissolved in the eluent at 1 mg/mL. For LBGA the eluent was 0.5 M $NaNO_3$, 0.01M KH_2PO_4, 0.1% w/v NaN_3, pH=2, at the same rate; the sample was dissolved at 1mg/mL in 10^{-2} M HCl.

3.2.4.5. X-ray diffraction (XRD)

Powder X-ray diffractograms were recorded on a Panalytical X'Pert Pro diffractometer, operating at 45 kV and 35 mA. The patterns of the pristine and modified samples were recorded in the range 5-45 degrees (2θ) with a step size of 0.0167 and a time per step of 2 000 seconds, using CuKα radiation filtered by Ni and an X'Celerator detector. Prior to the analysis, samples were reduced to a fine powder by grinding in a mortar.

3.2.5. Production of Locust Bean Gum-based nanoparticles

All nanoparticles were prepared by polyelectrolyte complexation method which consists in the electrostatic interaction between the positive and negative charges of the different polymers (35), as depicted in **Figure 1.1** (chapter 1, general introduction).

3.2.5.1. CS/LBGS and CS/LBGC nanoparticles

Five mass ratios of CS/LBGC (1:0.75; 1:1; 1:1.25; 1:1.5 and 1:2), and CS/LBGS (1:1; 1:1.25; 1:1.5; 1:2 and 1:2.5) were used to prepare the nanoparticles by polyelectrolyte complexation. The stock solution of CS, dissolved in 1% (w/w) acetic acid, was prepared to reach a final concentration of 1.0 mg/mL, while those of LBGC and LBGS, dissolved in ultrapure water, had a final concentration of 2.0 mg/mL. The solutions were filtered with a 0.45 µm filter prior to use. The formulations were prepared by slowly adding 1.8 mL of LBGC or LBGS to 1.0 mL of CS under gentle magnetic stirring at room temperature, as shown in **Figure 1.1** (chapter 1, general introduction). The concentration of CS was kept constant at 1.0 mg/mL for the preparation of all formulations, while that of LBGC or LBGS was modified to obtain the different ratios.

The suspensions of nanoparticles were mixed by magnetic stirring for 10 min and then centrifuged in eppendorfs having a layer of 10 µL of glycerol, in order to facilitate the following step of resuspension. The isolation of nanoparticles was performed by centrifugation (Thermo Scientific-Heraeus Fresco 17, Germany) at 16 000 x *g*, for 30 min at 15 ºC. After discarding the supernatants, the nanoparticles were resuspended with 200 µL of ultrapure water.

3.2.5.2. LBGA/LBGS nanoparticles

Three mass ratios of LBGA/LBGS were used to prepare the nanoparticles by polyelectrolyte complexation, in particular 2/1, 1/1 and 1/2. The stock solution of LBGA, dissolved in ultrapure water, was prepared to reach a final concentration of 0.5 mg/mL, while that of LBGS, dissolved in ultrapure water, had a final concentration of 1.0 mg/mL. The solutions were filtered with a 0.45 µm filter prior to use. The formulations 2/1, 1/1 and 1/2 were prepared by slowly adding 1.8 ml of LBGS to 1.0 ml of LBGA under gentle magnetic stirring at room temperature, as shown in **Figure 1.1** (chapter 1, general introduction). The concentration of LBGA was kept constant at 0.5 mg/mL for the preparation of all formulations, while that of LBGS was modified to obtain the different ratios.

As described before, the suspensions of nanoparticles were mixed by magnetic stirring for 10 min and then centrifuged in eppendorfs with a layer of 10 µL of glycerol, in order to facilitate the following step of resuspension. The isolation of nanoparticles was performed by centrifugation (Thermo Scientific-Heraeus Fresco 17, Germany) at 16 000 x *g*, for 30

min at 15 ºC. After discarding the supernatants, the nanoparticles were resuspended with 200 µL of ultrapure water.

3.2.6. Characterization of Locust Bean Gum-based nanoparticles

3.2.6.1. Size, polydispersion index and ζ potential

The size, ζ potential and polydispersion index (PdI) determination of the nanoparticles were performed on freshly prepared samples. Size and PdI were measured by dynamic light scattering and zeta potential was measured by laser Doppler anemometry, using a Zetasizer Nano ZS (Malvern instruments, Malvern, UK). To prepare the samples, 20 µL of each formulation were diluted in 1 mL of ultrapure water.

3.2.6.2. Production yield

For determination of nanoparticle production yield, the nanoparticles were prepared as described in the previous sections, but without the use of the 10 µL of glycerol. After discarding the supernatant of each formulation, the pellets were frozen and then dried on a freeze-dryer (Alpha RVC, Christ, Germany). The yield of nanoparticle production (PY) was calculated as follows:

PY = (Nanoparticle sediment weight/Total solids weight) x 100

where nanoparticle sediment weight is the weight after freeze-drying and total solids weight is the total amount of solids added for nanoparticle formation.

3.2.6.3. Morphological analysis

The morphological examination of LBGA/LBGS nanoparticles was conducted by transmission electron microscopy (TEM; JEM-1011, JEOL, Japan). The samples were stained with 2% (w/v) phosphotungstic acid and placed on copper grids with carbon films (Ted Pella, USA) for TEM observation.

3.2.7. Safety evaluation

The *in vitro* cell viability and cytotoxicity of bulk LBG, purified LBG and the synthesized derivatives was assessed in Caco-2 cells by the MTT assay and the LDH release assay, respectively. LBGA/LBGS nanoparticles were evaluated using the MTT assay.

The cells were seeded at a density of 1×10^4 cells/well in 96-well plates, in 100 µL of the same medium used for culture in cell culture flasks, and were grown at 37 °C in a 5% CO_2 atmosphere for 24 h before use.

The effect of polymeric solutions and nanoparticle suspensions was evaluated for 3 h and 24 h at three different concentrations (0.1, 0.5 and 1.0 mg/mL). A SDS solution (2%, w/v) was used as a positive control of cell death, while cells incubated with DMEM served as negative control. An additional control (DMEM+H_2O) consisting in a mixture of DMEM and H_2O in the same ratio used for the samples was used, in order to evaluate the contribution of polymers on cell viability. All formulations and controls were prepared as solution/suspensions in pre-warmed cell culture medium without FBS immediately before application to the cells.

To initiate the assay, culture medium of cells at 24 h in culture was replaced by 100 µL of fresh medium without FBS containing the test samples or controls. A constant ratio (3:1) between the culture medium and the solution/suspension of the materials was used. After 3 or 24 h of cell exposure, samples/controls were removed and 30 µL of the MTT solution (0.5 mg/mL in PBS, pH 7.4) was added to each well. After 2 h, any generated formazan crystals were solubilised with 50 µL of DMSO. Upon complete solubilisation of the crystals, the absorbance of each well was measured by spectrophotometry (Infinite M200, Tecan, Austria) at 540 nm and corrected for background absorbance using a wavelength of 650 nm (186).

The relative cell viability (%) was calculated as follows:

$$\text{Viability (\%)} = (A - S)/(CM - S)\times 100$$

where A is the absorbance obtained for each of the concentrations of the test substance, S is the absorbance obtained for the 2% SDS and CM is the absorbance obtained for untreated cells (incubated with cell culture medium). The latter reading was assumed to correspond to 100% cell viability. The assay was performed at least for three occasions with six replicates at each concentration of test substance in each instance.

Considering the general mild effect observed in the MTT assay, the LDH release assay was performed on polymeric solutions and nanoparticle suspensions, after 24 h exposure to a concentration of 1.0 mg/mL. This is a colorimetric assay that quantitatively measures LDH, a stable cytosolic enzyme that is released upon cell lysis. Released LDH in culture supernatants is measured with a 30-min coupled enzymatic assay that results in the conversion of a tetrazolium salt into a red formazan product. The amount of color formed is proportional to the number of lysed cells (187).

Samples from the culture medium in the seeding plates were centrifuged (16 000 x *g*, 5 min, 15 ºC), and 50 µL were collected and reacted with 100 µL of the LDH reagent at room temperature and protected from light. The reaction was stopped after 30 min by adding 15 µL HCl 1M. Absorbance was measured by spectrophotometry at a wavelength of 490 nm with background correction at 690 nm. The relative LDH release (%) was calculated as follows, considering 100% release for samples incubated with the lysis solution (positive control of cell death):

$$\text{LDH release (\%)} = A_{test}/A_{control} \times 100$$

where A_{test} is the absorbance of the test sample and $A_{control}$ is the absorbance of positive control of cell death. The assay was performed in at least three occasions, with three replicates in each instance.

3.2.8. Statistical analyses

The t-test and the one-way analysis of variance (ANOVA) with the pair wise multiple comparison procedures (Holm-Sidak method) were performed to compare two or multiple groups, respectively. All analyses were run using the SigmaStat statistical program (Version 3.5, SyStat, USA) and differences were considered to be significant at a level of $P < 0.05$.

3.3. Results and discussion

Since commercial LBG contains about 3-7% protein in its constitution (60), it is essential to go through a purification step prior to use, in order to avoid interference in the modification reactions to be performed. Therefore, it was purified using a method based on previously published protocols (73, 78), with a yield of approximately 78%. This purified LBG was the material used for subsequent work, unless stated otherwise.

3.3.1. Synthesis and chemical characterization of Locust Bean Gum derivatives

The syntheses of the three charged LBG derivatives were made by adaptation of procedures described in the literature for the modification of other polysaccharides (179, 184, 185). To perform the sulfation reaction, SO_3·DMF was chosen as sulfating agent (184), as it presents advantages over methods involving the manipulation of either pyridine or sulfur trioxide (188-190). For the synthesis of the sulfate derivative, two approaches were performed as described in the methodology. The difference mainly resided in the processing of LBG prior to the addition of SO_3·DMF. For the introduction of trimethylammonium groups in LBG, GTMAC was used as alkylating agent, which proved to be efficient in the alkylation of other polysaccharides (58, 185, 191, 192). The reaction mechanisms are as follows:

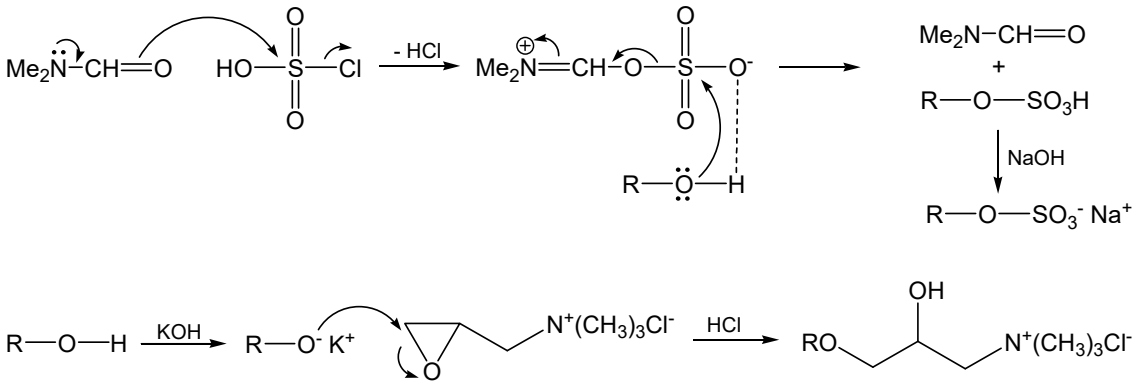

For the transformation of LBG into the corresponding polyuronic acid, TEMPO, a stable nitroxyl radical, was chosen as oxidizing agent (179). This has proved to possess a high

efficiency in the conversion of high molecular weight polysaccharides. A highly selective oxidation of C-6 primary hydroxyl to carboxylic groups can be achieved in an aqueous solution of the polysaccharide at pH 9-11 with NaClO and catalytic amounts of TEMPO and NaBr (179-181). The mechanism is as follows:

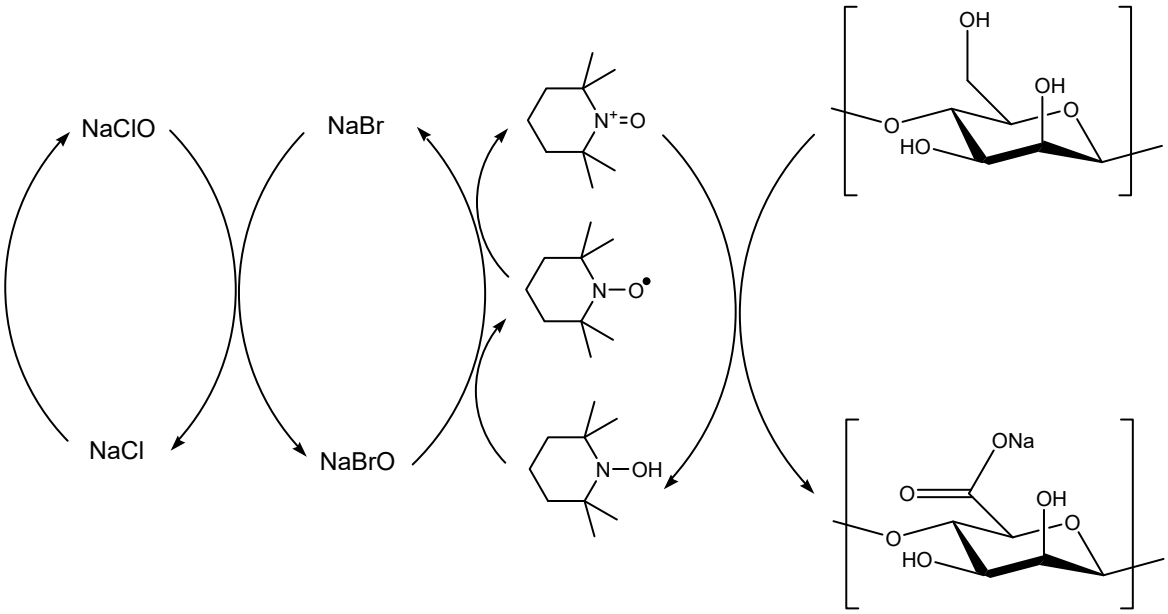

The methods described above are summarized in **Figure 3.1**.

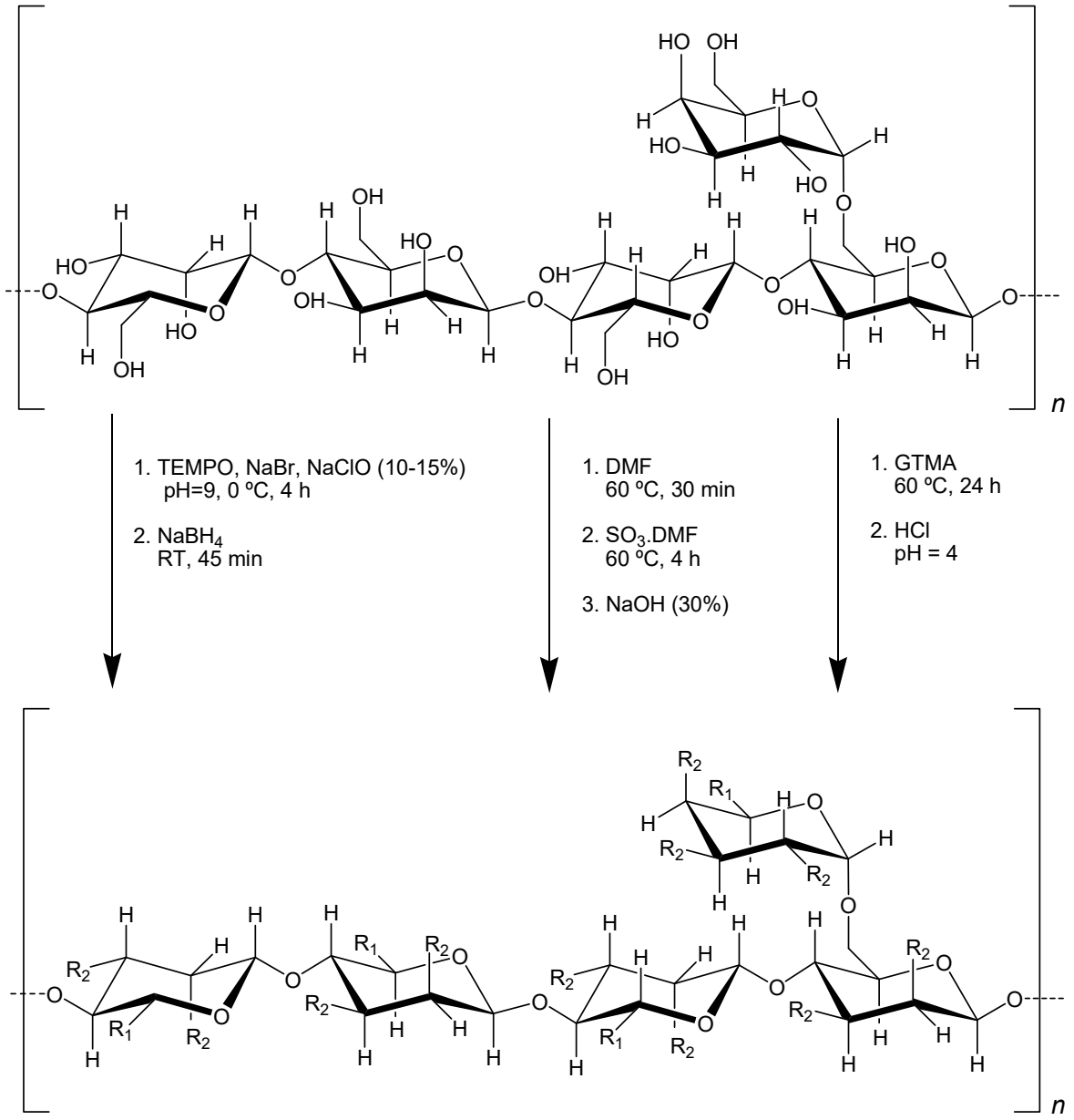

LBGC: R_1 = COOH / CH_2OH; R_2 = OH

LBGS: R_1 = $CH_2OSO_3^-$ / CH_2OH; R_2 = OSO_3^- / OH

LBGA: R_1 = $CH_2OCH_2CH(OH)CH_2N^+(CH_3)_3$ / CH_2OH;
R_2 = $OCH_2CH(OH)CH_2N^+(CH_3)_3$ / OH

Figure 3.1 – Scheme of the chemical modifications introduced in LBG.

As shown in **Figure 3.2**, LBG sulfate functionalization (LBGS) was confirmed by FTIR, through the appearance of a S=O asymmetric stretching band (184) at 1255 cm^{-1} and that of C-O-S symmetric stretching (189) at 817 cm^{-1}. In the carboxylate derivative (LBGC), the absorption bands at 1601 cm^{-1} and 1415 cm^{-1} are attributed to asymmetric and symmetric

stretching vibration of $–COO^-$, respectively (181). Since the quaternary ammonium groups do not display characteristic IR absorption bands (193), evidence for formation of the amino functionalized derivative (LBGA) comes from the broadening of the band at 1088 cm^{-1} (ether C-O symmetric stretching) and the new bands at 1479 and 914 cm^{-1} (C-H scissoring in methyl groups of the ammonium and ether C-O asymmetric stretching, respectively) (192).

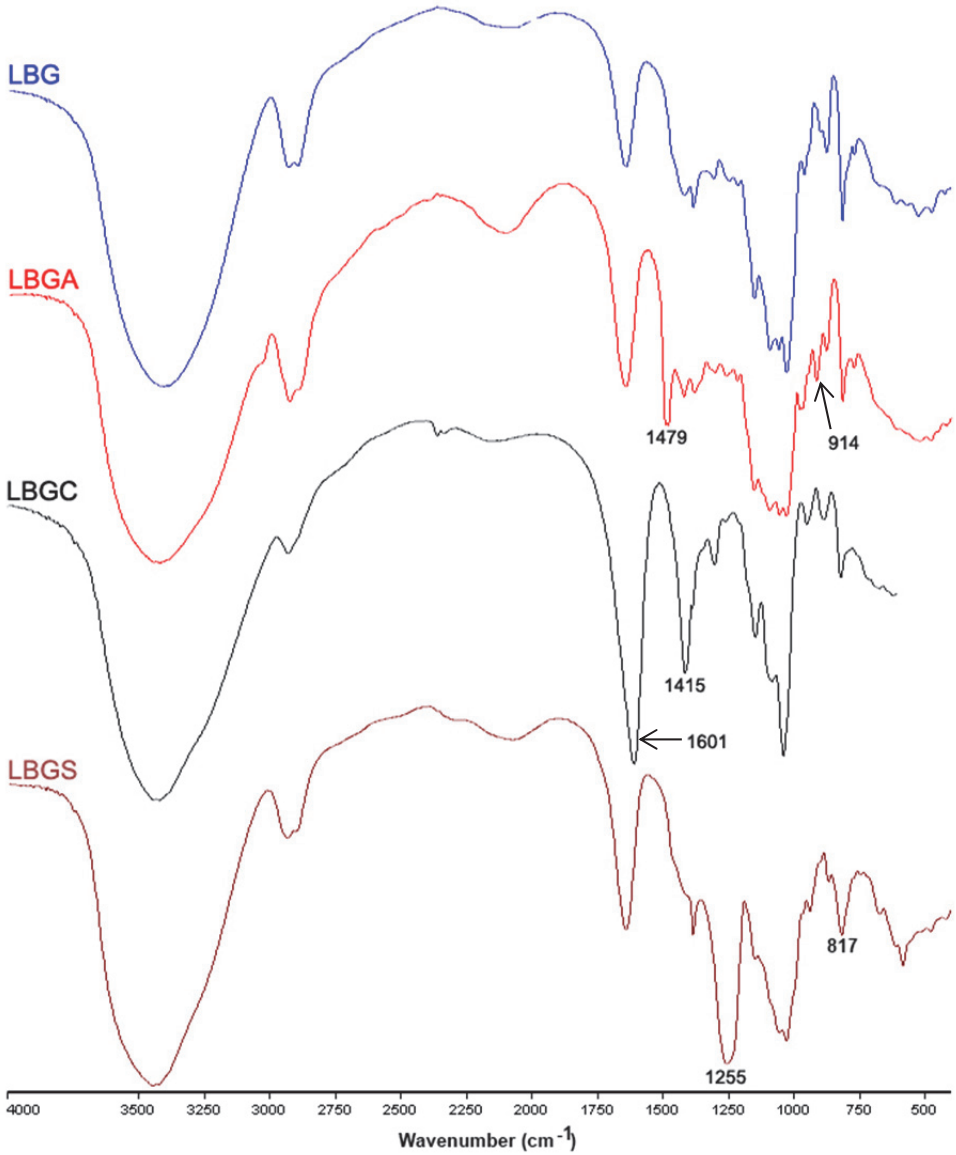

Figure 3.2 – FTIR spectra of purified Locust Bean Gum (LBG) and its ammonium (LBGA), carboxylate (LBGC) and sulfate (LBGS) derivatives.

In the elemental analysis, the weight percentages found for the analysed elements are compiled in **Table 3.1**.

Table 3.1 – Elemental analysis data from the sulfate (LBGS), carboxylate (LBGC) and ammonium (LBGA) derivatives of locust bean gum (LBG).

Element (%)	Polymer					
	LBGS (M1)*	**LBGS (M2-B1)***	**LBGS (M2-B2)***	**LBGS (M2-B3)***	**LBGC**	**LBGA**
N	---	---	---	---	---	3.84
C	25.55	35.06	23.94	28.42	37.39	43.39
S	7.77	3.50	9.78	7.41	---	---
O	---	---	---	---	48.96	---

*B1, B2 and B3 refer to LBGS derivatives from batches 1, 2 and 3, respectively; M1 and M2 refer to LBGS derivatives synthesized with methods 1 and 2, respectively

For LBGS, different degrees of substitution were obtained, even under the same reaction conditions. For the sample of LBGS obtained by the first method (method 1), a C:S molar ratio of 8.78 was obtained, which corresponds to a degree of substitution (DS) of 3.5. Therefore, if the sulfate groups are assumed to be in the form of sodium salts, a molecular formula between $C_{30}H_{47}S_3O_{34}Na_3$ and $C_{30}H_{46}S_4O_{37}Na_4$, to which corresponds a mean molecular weight of 1166 g/mol, is derived. On the other hand, the samples of LBGS obtained by the second method (method 2) presented a high variability on C:S molar ratio, ranging from 26.76 in batch 1 to 6.55 in batch 2, and batch 3 presenting a value of 10.24. These values correspond to values of DS of 1.22, 4.63, and 3, and to the mean molecular weights of 932, 1282, and 1111 g/mol, respectively. As indicated in the methods and stated above, the difference between the two methods only refers to a preliminary treatment of LBG before the sulfation reaction. In the second method, a better dispersion of LBG was promoted before the contact with the sulfating agent in an attempt to improve the reaction. The need for this pre-treatment was motivated by the poor solubility of LBG in DMF. Since in the sulfation reaction the polymer is used as a dispersion in the solvent, it would be expected that a more effective dispersion would favour the reaction. Notwithstanding and quite surprisingly, it was observed that, although the pre-treatment afforded the highest value of DS (4.63), it also gave the lowest substitution (1.22), while in

its absence an intermediate value of DS was obtained. This variation in DS translates, in the FTIR spectra of the various samples, in different intensities of the band at 1255 cm^{-1} relative to other bands in the spectrum, with more substituted samples presenting a more intense band (**Figure 3.3**).

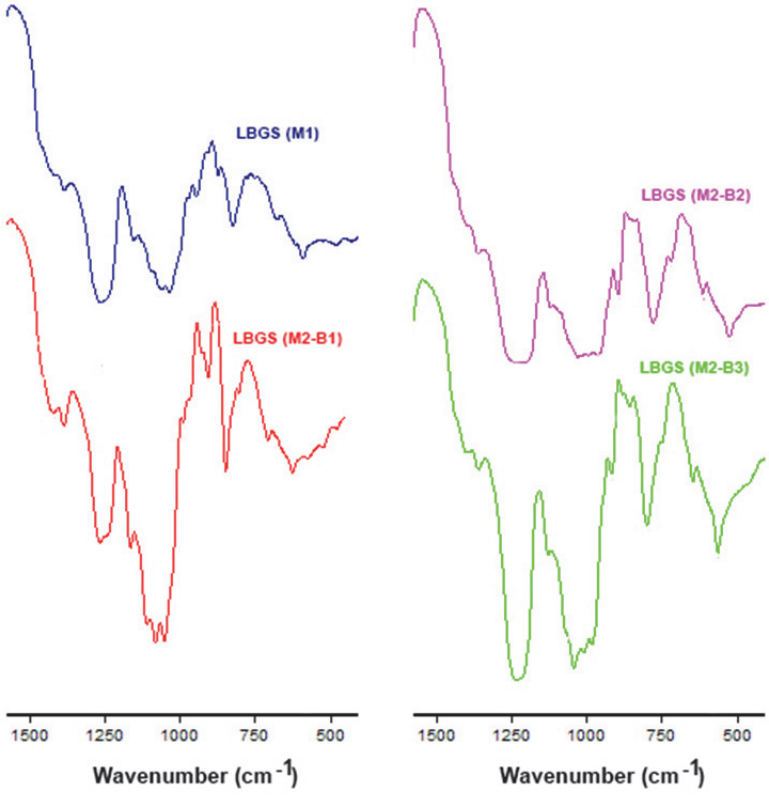

Figure 3.3 – FTIR spectra of Locust Bean Gum sulfate derivatives (LBGS) obtained in method 1 (M1) and method 2 (M2). B1, B2 and B3 refer to batch 1, 2 and 3, respectively.

Assuming that a better dispersion of LBG leads to a higher reaction efficiency and affords higher values of DS, it seems that the dispersibility of LBG in the reaction medium does not directly correlate to the method used in its dispersion. One reason for the observed variability in DS may be the fact that, contrary to what is observed in the reactions described below (oxidation and alkylation), in which LBG progressively dissolves as the reactions proceed, in this case a total solubilisation is never reached. This renders the outcome of this reaction quite unpredictable and, therefore, this issue will have to be tackled in future work. In fact, the reaction of LBG activated by pre-soaking in DMF and dispersed in the same solvent, with solid SO_3·DMF complex, bellow 15 ºC, led to a DS of approximately 4 (183). On the other hand, sulfation of LBG dispersed in formamide with

SO_3·pyridine complex, under diverse conditions of reaction time, temperature, and amount of sulfating agent, led to DS varying between approximately 2 and nearly 5 (182). Again the soaking of LBG with the solvent prior to the reaction led to an intermediate DS relative to the range obtained without any pre-treatment, although in the latter case a different reagent and solvent were used. Nevertheless, only one batch per reaction conditions seems to have been obtained in both these works, and therefore the state of dispersion of LBG in each case may very well be the factor governing the substitution obtained, instead of the parameters analysed. Moreover, in the latter work, no correlation or trend between molecular weights of the obtained derivatives or depolymerisation of the parent polysaccharide and degree of substitution is observed. On the contrary, a very erratic dispersion of molecular weights with growing DS is obtained, pointing to a random behaviour in this reaction. For LBGC, a C:O ratio of 1.02 was found, which corresponds to a degree of oxidation (DO) of 4, meaning that all the free C-6 must have been oxidized. Assuming all carboxylate groups to be in the sodium salt form, the molecular formula would be $C_{30}H_{38}O_{29}Na_4$, and the molecular weight 955 g/mol. This value is not surprising, in view of the effectiveness of the oxidizing system, although somewhat higher than DO values observed for other galactomannans, which typically lay below 70% of the free units (181). In LBGA, the C:N molar ratio was found to be 13.16, corresponding to a DS of 4.24. If all the ammonium groups are in the form of chloride salt, this corresponds to a molecular formula between $C_{54}H_{106}O_{29}N_4Cl_4$ and $C_{60}H_{120}O_{30}N_5Cl_5$, and the mean molecular weight of 1454 g/mol. This corresponds to a full reaction of the free C-6 hydroxyl groups, along with reaction on some secondary hydroxyls, in line with what was observed by us in a similar modification performed in pullulan (58).

Figure 3.4 presents the ^{1}H-NMR spectra of LBG and its three derivatives (LBGA, LBGS, and LBGC). In the spectrum of LBG (**Figure 3.4 a**), there are three signals (5.21, 4.93, and 3.74 ppm) resolved from the envelope of peaks between 3.8 and 4.4 ppm. The former two are attributed to the anomeric protons H-1 of galactose and mannose units, respectively, while the latter is due to the proton in the C-5 of mannose. In the spectrum of LBGA (**Figure 3.4 b**) all the signals shifted upfield as a consequence of the alkylation of hydroxyl groups, probably mostly the ones in C-6, as these are the most reactive. Due to this shifting, the anomeric protons signals disappeared bellow the strong signal of HOD, and the C-5 proton is probably now absorbing at 3.41. Nevertheless, this attribution may not be correct, since the sample enormously swelled upon addition of D_2O, reaching a very dilute state and affording a spectrum with low signal intensities. A noteworthy aspect of this spectrum is the intense singlet at 3.15 ppm, which indicates the presence of the trimethylammonium methyl groups. The high intensity of this peak is consistent with the

obtained DS of over 4. Another change denoting the presence of the *N*-(2-hydroxypropyl)-*N,N,N*-trimethylammonium groups in LBGA is the shoulder in the HOD signal, at nearly 4.38 ppm, corresponding to the absorbance of the CH(OH) proton.

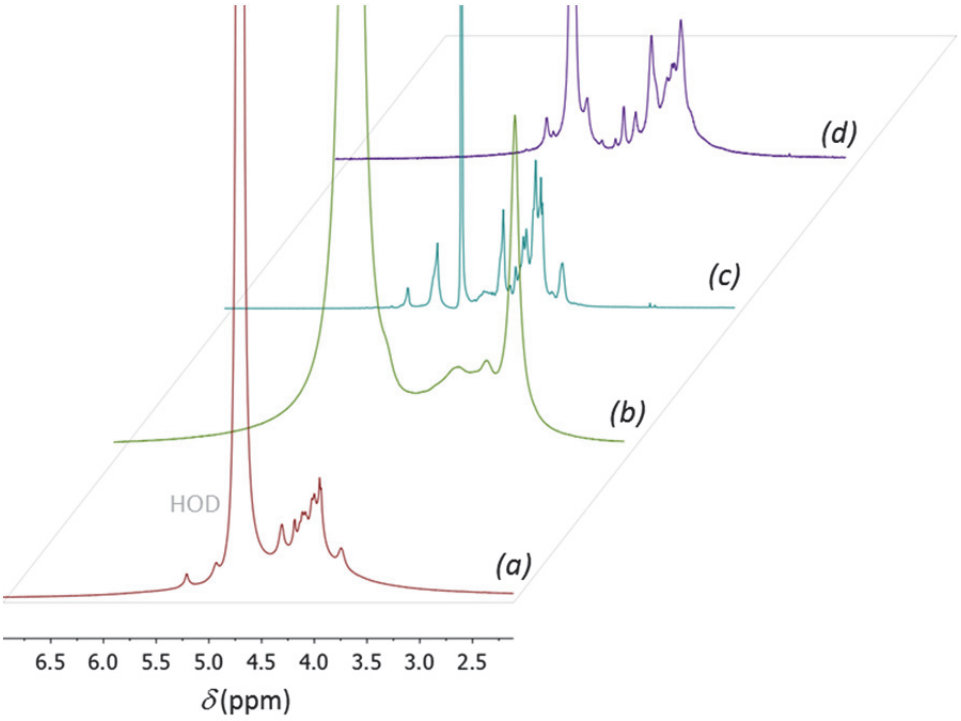

Figure 3.4 – ^{1}H-NMR of (a) LBG, (b) LBGA, (c) LBGS, and (d) LBGC; the big singlet centered at 4.7 ppm is due to HOD (identified in grey).

The spectrum of LBGS (**Figure 3.4 c**) does not differ much from the one of the parent polysaccharide, which is not totally unexpected, since this corresponds to a sample with a low value of DS (batch 1 in method 2). Still, a new broad signal centred at 4.46 ppm appeared, corresponding to the downshift of the H-6 of pyranosyl units with sulfate groups attached. The fact that this spectrum was acquired in a more concentrated sample caused a reduction of the HOD signal relative to the remaining ones, allowing the integration of the two H-1 signals. The area below the signal corresponding to the H-1 of mannose is approximately four times higher than that below the peak of the anomeric proton of galactose, thus confirming the M:G ratio of 4:1. Superimposed with the former signal is that of the downshifted peak of the galactose H-4 from substituted units. However, this is a very faint signal, as the DS of this sample is low and substitution occurred mostly in the most reactive primary hydroxyl groups of the C-6 carbons, therefore not compromising this estimation. The spectrum of LBGC (**Figure 3.4 d**) is characterized by an upfield shift

of most of the signals and therefore not much information may be derived from it. However, that is not the case of the ^{13}C-NMR of this derivative (**Figure 3.5**), in which the signals of the C-6 of galactose and unsubstituted mannose units, expected to appear at 61-62 ppm, are absent, in line with the full oxidation of these carbons estimated from the elemental analysis data. Also a relatively broad signal appeared at nearly 176 ppm, due to a poor resolution of the signals of the carboxylic acid carbons in galactose and mannose units. Moreover, no signals attributable to aldehydic carbons (190-200 ppm) are observed in the spectrum, thus confirming the complete oxidation to carboxylic acid.

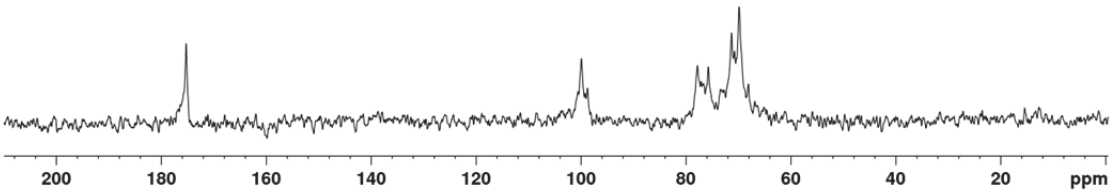

Figure 3.5 – ^{13}C-NMR of LBGC.

Table 3.2 presents the average molecular weights, polydispersity index (PdI), and radius of gyration (*R*g) of LBG and its derivatives. For the parent polysaccharide (LBG), these are in general agreement with the literature (60, 74). Upon chemical modification, an increase in both molecular weight and R_g was observed in LBGA, and a big decrease in these parameters was patent in LBGC and LBGS. The increase identified in LBGA is attributable to the presence of the introduced pendant chains, which lead to an increase in the molar mass of the repeating unit and force the polymer, once in solution, and similarly to what happens in the crystalline state (XRD results), to adopt a conformation that is suitable to accommodate such bulky groups. The results observed in the LBGC and LBGS derivatives suggest the occurrence of depolymerization during the chemical modification, a common observation when the conditions of either the oxidation (181) or the sulfation reaction (189) are applied. The latter was already stated in a similar modification performed in pullulan (58). Moreover, no additional dehydration reactions, with intra- and/or intermolecular crosslinking leading to a fraction of high molecular weight chains, observed in sulfation reactions carried out at higher temperatures (188), occurred in this case. The results obtained for LBGS were very similar among the two synthetic methods (methods 1 and 2).

Table 3.2 – GPC analysis of purified Locust Bean Gum (LBG), and its ammonium (LBGA), carboxylate (LBGC) and sulfate (LBGS) derivatives.

Polymer	M_n (Da)	M_w (Da)	PdI	R_g (nm)
LBG	327 300	589 100	1.80	71.61
LBGA	500 600	871 000	1.74	86.05
LBGC	73 790	119 500	1.62	28.19
LBGS	21 380	26 510	1.24	14.21

M_n: number average molecular weight; M_w: weight average molecular weight; PdI: polydispersity index; R_g: radius of gyration

Figure 3.6 shows the XRD patterns of the pristine and modified LBG samples. The pattern of LBG, with a broad peak centered at *ca.* 20º 2θ with shoulders at *ca.* 7.5 and 15º 2θ, reflects the predominantly amorphous nature of the material. These shoulders vanish in the pattern of LBG modified with sulfate, probably due to some changes in the organization of the polymer chains imposed by the sulfate groups. In what concerns the ammonium derivative, the pattern clearly shows an increase of intensity for higher d-spacings, which is compatible with an increase of the distance between the polymer chains, due to the long chain bearing the ammonium group (58). When compared with the other modifications, the introduction of carboxylate groups gives rise to the highest degree of disruption of the long-range order of the LBG polymer chains. The intensity of the peak that appears at 20º 2θ in the pattern of the original polymer (LBG) is substantially reduced and new broad peaks are now present at ca. 12 and 25º 2θ. This is not surprising, as the conversion of galactose and mannose units into the corresponding uronic acids would enormously affect the conformation of the polysaccharide chains and, consequently, the way they pack in the solid phase.

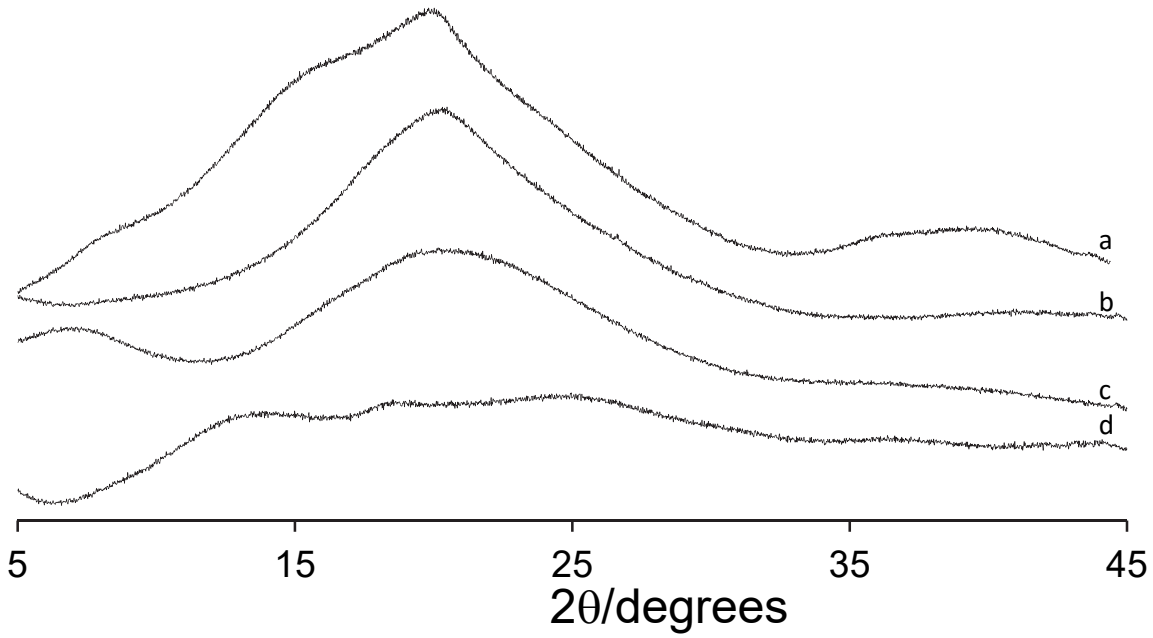

Figure 3.6 – XRD patterns of (a) pristine locust bean gum (LBG), (b) sulfated LBG (LBGS), (c) ammonium LBG (LBGA), and (d) carboxylated LBG (LBGC).

3.3.2. Characterization of nanoparticles

The production of LBG derivatives described above endowed the polymer with charged groups, enabling the preparation of nanoparticles by polyelectrolyte complexation. This is a mild method occurring in hydrophilic medium, devoid of aggressive conditions such as organic solvents or high shear forces, and involving electrostatic interactions between oppositely charged polymers (108, 194). Three derivatives were synthesized which were used in the production of different formulations of nanoparticles. The negatively charged sulfate and carboxylate derivatives were complexed with chitosan to produce CS/LBGS and CS/LBGC nanoparticles, respectively. In turn, the ammonium derivative was complexed with the sulfate derivative in the innovative approach of producing LBG-only nanoparticles (LBGA/LBGS). The results regarding the physicochemical characterization of the referred nanoparticle formulations are displayed and discussed below.

3.3.2.1. CS/LBGS and CS/LBGC nanoparticles

The first approach towards the formulation of CS/LBGS and CS/LBGC nanoparticles involved the production of carriers having higher or at least the same amount of LBG derivative comparing to chitosan. In this regard, the starting mass ratios selected for the production of the referred formulations of nanoparticles were 1:1, 1:1.5 and 1:2. In the course of the experiments, the need to test other ratios was identified, not necessarily being coincident for each formulation, thus justifying the slight differences observed between the two formulations.

Table 3.3 displays the physicochemical characteristics of CS/LBGS nanoparticles. For the production of these nanoparticles, LBGS corresponding to method 1 was used. With CS/LBGS mass ratios varying between 1:1 and 1:2.5, and recalling that CS amount remains constant in all formulations, it was verified that nanoparticle size generally increased with increasing amounts of LBGS. The minimum size was 364 nm (CS/LBGS = 1:1, w/w) and the highest size was 589 nm (CS/LBGS = 1:2.5, w/w) ($P < 0.05$).

Table 3.3 - Physicochemical characteristics and production yield of CS/LBGS unloaded nanoparticles (mean ± SD; n ≥ 3). Different letters represent significant differences in each parameter ($P < 0.05$).

CS/LBGS (w/w)	Size (nm)	PdI	Zeta potential (mV)	Production yield (%)
1:1	364.1 ± 30.0 ^{a}	0.34 ± 0.09	+45.6 ± 1.2 ^{d}	37.3 ± 5.6 ^{h}
1:1.25	403.7 ± 37.7 ^{ab}	0.40 ± 0.06	+40.0 ± 0.8 ^{e}	58.1 ± 2.7 ^{i}
1:1.5	pp*	1.0 ± 0.0	-5.9 ± 4.4 ^{f}	n.d.
1:2	500.3 ± 59.6 ^{bc}	0.47 ± 0.08	-23.9 ± 2.7 ^{g}	56.6 ± 7.2 ^{i}
1:2.5	589.0 ± 69.5 ^{c}	0.54 ± 0.03	-28.5 ± 5.0 ^{g}	n.d.

n.d.: not determined; pp: precipitate; *slight precipitation compromised the measurement of this parameter

The registered increase in size as higher amount of LBGS is included in the formulations as compared with CS, might be explained by the increase of total mass of polymers that is present. This effect was also reported in other works using the same nanoparticle production method (39, 195). Precipitation was found to occur for an intermediate formulation (CS/LBGS = 1:1.5, w/w), being coincident with a zeta potential close to zero (-5.9 mV) that possibly is not sufficient to provide particle repulsion, thus leading to

aggregation. A clear Tyndall effect was observed in all the other nanoparticle formulations. The formulations 1:1 and 1:1.25 (w/w) exhibited a strong positive zeta potential of more than 40 mV. The incorporation of a higher amount of LBGS, from formulation 1:1 to 1:1.25 (w/w) resulted in a corresponding decrease in the zeta potential from +46 mV to +40 mV ($P < 0.05$). The formulations 1:2 and 1:2.5 (w/w) presented a complete shift in the zeta potential as the nanoparticles became negatively charged with zeta potential reaching -29 mV. Again, the incorporation of a higher amount of LBGS led to a nominal decrease in the zeta potential, although this is not statistically significant. This absolute shift of nanoparticle charge occurring between the formulations 1:1.25 and 1:2 (w/w) reflects the higher amount of LBGS that is present in the nanoparticles but also demonstrates that both polymers have different charge density. Zeta potential results are perfectly in line with the charge ratios that were calculated for each formulation of nanoparticles, as is depicted in **Figure 3.7**. This figure shows the effect of charge ratios on the zeta potential of CS/LBGS nanoparticles prepared with varying polymeric ratios.

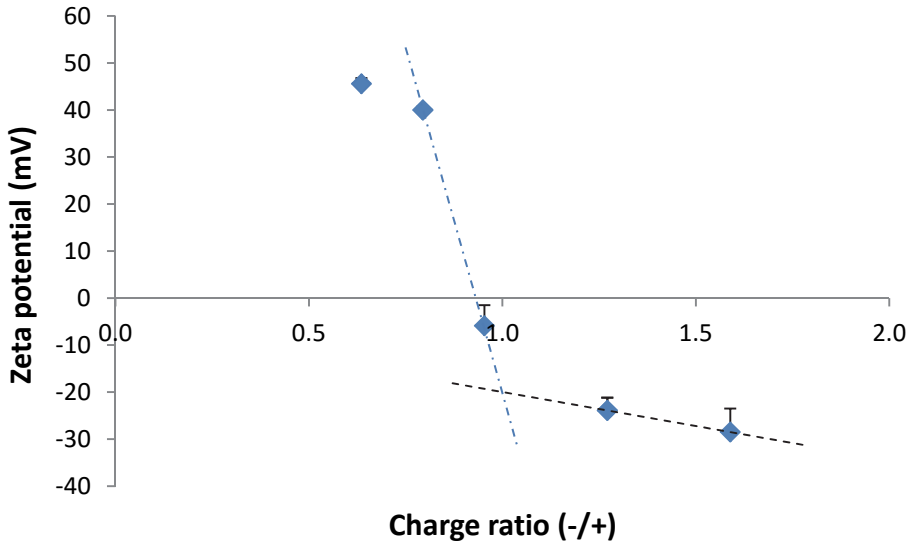

Figure 3.7 – Effect of charge ratio (-/+) on the zeta potential of CS/LBGS nanoparticles.

For each polymer, by dividing the charge of the repeating unit by its molar mass, a charge per mass ratio may be obtained. CS has a higher charge per mass ratio than LBGS (4.72 x 10^{-3} *vs* 3.00 x 10^{-3} charges/g, respectively), which justifies why formulations CS/LBGS = 1:1 and 1:1.25 (w/w) have a -/+ charge ratio below 1. The strong positive zeta potential (> 40 mV) of these nanoparticles is due to the predominance of positive charges. In turn, the occurrence of precipitation in the formulation 1:1.5 (w/w) was coincident with a charge

ratio around 1, justifying that the determined zeta potential was close to neutrality. In fact, although a 1:1 -/+ charge stoichiometry might not imply the occurrence of complete charge neutralization, due to different charge spacing in the intervenient species and to steric limitations (195), one may assume a preferential interaction between the sulfate and the ammonium groups, both weakly hydrated, instead of with the strongly hydrated counterions (196). This leads to mainly an intrinsic charge matching in detriment of an extrinsic charge compensation and, thus, to a small deviation from neutrality. Finally, the continued addition of the negative polymer (formulations CS/LBGS = 1:2 and 1:2.5, w/w) produced an excess of negative charges, resulting in -/+ charge ratio above 1 and, consequently, negatively charged nanoparticles. A similar behavior concerning the charge ratios leading to either the precipitation or the formation of nanoparticles, was previously described (195).

The polydispersity index varied between 0.3 and 0.5, which is considered high. Regarding the production yield, very reasonable values for this nanoparticle production methodology, were obtained. A yield of 37% was registered for formulation 1:1 (w/w) which increased to 58% ($P < 0.05$) for formulation 1:1.25 (w/w). This is a result of the proper mechanism of nanoparticle formation, based on the neutralization of chitosan amino groups by the sulfate groups of LBGS. The incorporation of a higher amount of LBGS provides an additional amount of sulfate groups that interacted with chitosan, thus forming a higher amount of nanoparticles (106). However, this effect occurs up to a certain limit. As observed, further increasing the amount of LBGS led to precipitation, certainly because of the demonstrated neutralization of charges, as referred above. On keeping increasing LBGS mass, nanoparticles are again formed (CS/LBGS 1:2 and 1:2.5, w/w), this time with an opposite charge and a high yield (57% for formulation 1:2, w/w).

The results obtained for CS/LBGC nanoparticles were rather different comparing to those described above regarding CS/LBGS formulations. In this case, as shown in **Table 3.4**, the initially approached formulation of CS/LBGC 1:1 (w/w) resulted in a size of 479 nm, which is more than 30% higher than the corresponding CS/LBGS formulation ($P < 0.05$). The formulation 1:1.5 (w/w) already presented precipitation, similarly to 1:2 (w/w) and therefore the intermediate formulation 1:1.25 (w/w) was produced.

Table 3.4 - Physicochemical characteristics and production yield of CS/LBGC unloaded nanoparticles (mean ± SD; n ≥ 3). Different letters represent significant differences in each parameter ($P < 0.05$).

CS/LBGC (w/w)	Size (nm)	PdI	Zeta potential (mV)	Production yield (%)
1:0.75	489.9 ± 63.6 [a]	0.45 ± 0.04	+45.5 ± 13.0 [b]	49.0 ± 5.0 [d]
1:1	479.1 ± 30.8 [a]	0.51 ± 0.07	+42.2 ± 7.4 [b]	54.3 ± 7.0 [d]
1:1.25	828.8 ± 299.8 [a]	0.64 ± 0.15	+28.8 ± 7.3 [b]	n.d.
1:1.5	pp*	1.0 ± 0.0	-2.5 ± 8.3 [c]	n.d.
1:2	pp*	1.0 ± 0.0	-15.2 ± 7.4 [c]	n.d.

n.d.: not determined; pp: precipitate; *slight precipitation compromised the measurement of this parameter

The registered size revealed a strong increase to 829 nm, although this is not statistically significant as is accompanied by an extremely high standard deviation, which indicates reproducibility issues. This formulation also presented a high polydispersity index and thus was not characterized for production yield. An attempt was also performed to produce nanoparticles at a CS/LBGC ratio of 1:0.75 (w/w), but the characteristics were very similar, under all aspects, to those of ratio 1:1 (w/w). The polydispersity index was around 0.5 – 0.6, which is even higher than those registered for CS/LBGS nanoparticles, reinforcing the difficulty in producing suitable nanoparticles with the LBGC derivative. The zeta potentials are highly positive (around +45 mV), which probably contributes to the system stability. The determination of the charge ratios involved in each formulation of nanoparticles is depicted in **Figure 3.8**.

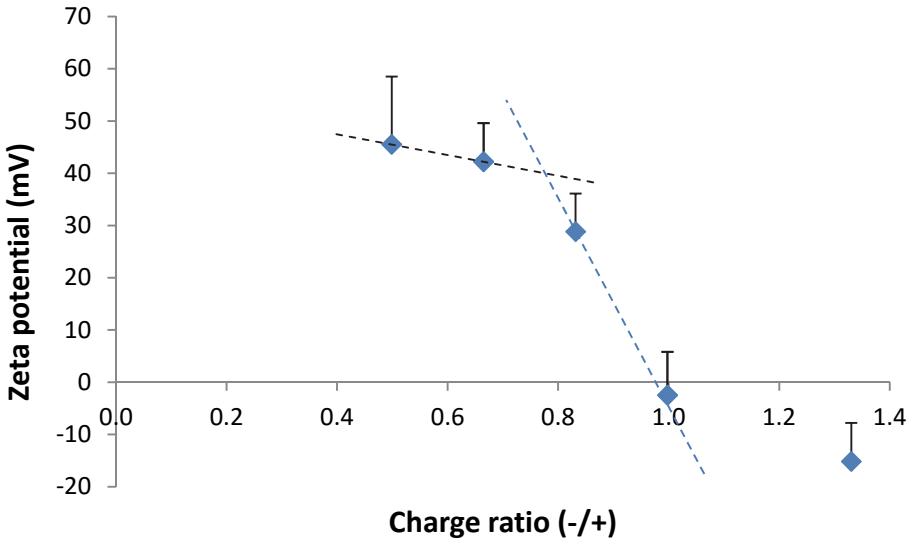

Figure 3.8 – Effect of charge ratio (-/+) on the zeta potential of CS/LBGC nanoparticles.

As observed, formulations 1:0.75 and 1:1 (w/w) have a -/+ charge ratio between 0.5 and 0.7 which does not translate into significant differences in the zeta potential. Nanoparticles 1:1.25 (w/w) displayed a -/+ charge ratio of 0.85 which induced a nominal decrease of the zeta potential to +29 mV, although not to a statistically significant level. As observed above for CS/LBGS nanoparticles, reaching a -/+ charge ratio around 1 (formulation 1:1.5, w/w) resulted in precipitation. However, in this case the continued addition of the negative polymer to formulate CS/LBGC = 1:2 (w/w) nanoparticles still resulted in precipitation, despite the -/+ charge ratio of 1.4. It is important to highlight that, while the resulting zeta potential for this formulation was of -15 mV, in the CS/LBGS corresponding formulation was -24 mV, which possibly permitted enough repulsion to stabilize the formed nanoparticles.

The determined production yields are satisfactory for this methodology, as referred above, being around 50%. When comparing the zeta potentials of these nanoparticles with those obtained for CS/LBGS nanoparticles (**Table 3.3**), a similar trend is observed. In this regard, increasing the amount of LBGC present in the formulation reflects in a decrease of the surface charge, owing to the higher amount of negative groups being incorporated. Similarly to CS/LBGS nanoparticles, the formulation 1:1.5 is the one showing neutrality (zeta potential of -2.5 mV) and the further incorporation of LBGC led to a decrease in the surface charge. The precipitation verified for the latter was possibly due to the fact that the existing surface charges were not sufficient to ensure particle repulsion. The resemblance of the trend, particularly regarding the shift of the zeta potential (occurring for mass ratio of

1:1.5), suggests the similarity of charge density in both derivatives. In fact, LBGS has a charge per mass ratio of 3.00 x 10^{-3} charges/g, as stated before, and LBGC has 3.14 x 10^{-3} charges/g.

3.3.2.2. LBGA/LBGS nanoparticles

One of the great novelties of producing LBG charged derivatives is the possibility of using these to produce, for the first time, LBG-only nanoparticles. Given the difficulties in producing nanoparticles with the LBGC derivative, as stated above, it was decided to produce the LBG-only nanoparticles using just LBGS as negative counterpart. The nanoparticles were produced by complexation of this derivative (method 2 – 50/50 mixtures of batches 2 and 3) with the ammonium derivative (LBGA) by the same methodology reported in the other cases (polyelectrolyte complexation).

After observing the precipitation of the formulation LBGA/LBGS 1:1 (w/w), possibly resulting from a (-/+) charge ratio of 1.09, formulations 1:2 (w/w) and 2:1 (w/w) were approached, which results are depicted in **Table 3.5**.

Table 3.5 - Physicochemical characteristics and production yield of LBGA/LBGS unloaded nanoparticles (mean ± SD; n ≥ 3). Different letters represent significant differences in each parameter ($P < 0.05$).

LBGA/LBGS (w/w)	Size (nm)	PdI	Zeta potential (mV)	Production yield (%)
1:2	206.6 ± 5.0 [a]	0.13 ± 0.03	-27.8 ± 1.4 [c]	30.0 ± 8.6 [e]
1:1	pp	-	-	-
2:1	368.3 ± 19.3 [b]	0.38 ± 0.05	+48.1 ± 1.5 [d]	16.7 ± 3.8 [f]

pp: precipitate

The formulation containing the highest amount of LBGS registered a size of 207 nm and a low polydispersity index of 0.13. Naturally, the zeta potential was negative (-28 mV), reflecting the higher content of negatively charged derivative, which translated into a (-/+) charge ratio of 2.17. As expected, the formulation having more LBGA exhibited a strongly positive zeta potential (+48 mV; $P < 0.05$), as a result of the (-/+) charge ratio of 0.54.

However, this particular formulation presented higher size (368 nm) along with higher polydispersity index ($P < 0.05$). At a first evaluation, the size differences could be considered unexpected. In fact, for the preparation of these nanoparticles, LBGA is kept constant at 0.5 mg/mL and LBGS concentration is adapted to meet the desired ratio. Therefore, formulation 1:2 (w/w) accounts with a total polymeric mass of 1.5 mg while formulation 2:1 (w/w) accounts with 0.75 mg. In line with this, formulation 1:2 (w/w) was perhaps expected to have a higher size. However, if one considers the molecular weight of the derivatives, reported in section 3.3.1, LBGA has a much higher M_n than LBGS (500 600 *vs* 21 380). In this regard, it becomes justifiable that nanoparticles having double amount of LBGA comparing with LBGS are those displaying the higher size.

Regarding the production yield, this was very different between the two formulations. While formulation 1:2 (w/w) resulted in 30%, formulation 2:1 (w/w) presented 17% ($P < 0.05$). This difference is probably due to variances in the molecular weight of the two derivatives. In formulation 1:2 (w/w), there is a determined amount of a high molecular weight polymeric chain and a double amount of a shorter macromolecule that possibly presents higher diffusion. On the contrary, in formulation 2:1 (w/w) the amount of the polymer with higher molecular weight is double comparing with that of the smaller polymer, thus resulting in a lower number of interactions and limiting the amount of nanoparticles formed.

LBG-only nanoparticles were morphologically characterized by TEM and the specific formulation LBGA/LBGS 1:2 (w/w) was considered representative for this end. As shown in **Figure 3.9** the nanoparticles present a spherical shape and have a compact structure.

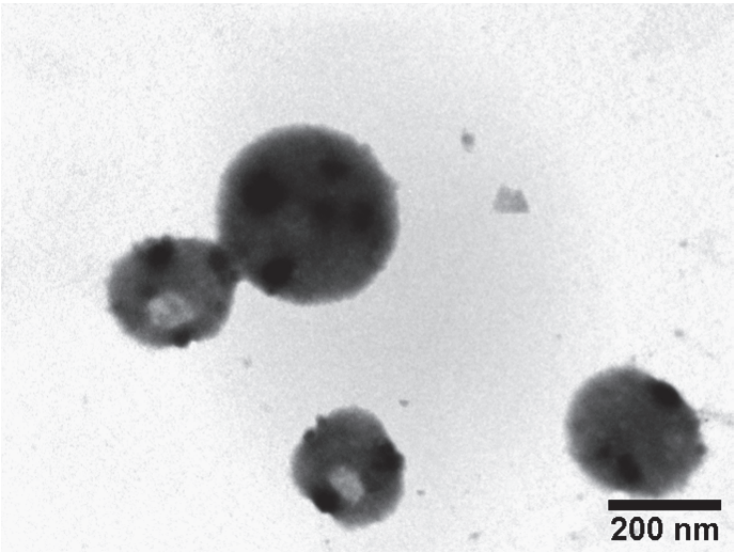

Figure 3.9 – TEM microphotograph of LBGA/LBGS = 1:2 (w/w) nanoparticles.

3.3.3. Safety evaluation

Addressing the biocompatibility of materials to be used in drug delivery is a major issue in formulation development (52, 197, 198). Additionally, current international guidelines indicate the need to contextualize biocompatibility with a specific route of administration and dose of the material (198). According to the guidelines issued by the International Organization for Standardization (ISO), testing biocompatibility implies the performance of a complete set of assays, addressing at first cellular morphology, membrane integrity and metabolic efficiency, among other tests (197, 199-201). In this work we performed two of the most used assays to test the toxicological effect of materials, which are the metabolic assay MTT and the membrane integrity assay based on LDH release. The MTT assay assesses cell metabolic efficiency, relying on the evaluation of enzymatic function. To do so, after the exposure to the test materials, cells are incubated with yellow tetrazolium (MTT) salts which are reduced to purple-blue formazan crystals by active mitochondrial dehydrogenases (197). In this manner, a higher concentration of the formazan dye corresponds to a higher amount of metabolically active cells, which is usually interpreted as higher cell viability. The LDH release assay provides a mean to determine the amount of LDH in cell culture medium upon exposure to potential toxicants. As LDH is a cytoplasmic enzyme, its presence in the cell culture medium is an indicator of irreversible cell death due to cell membrane damage (202, 203). The assay thus evaluates cell membrane integrity and complements the results obtained by the MTT assay.

Caco-2 cells are derived from a human colorectal carcinoma and are the most frequently used as *in vitro* intestinal cell culture model. The epithelial cells in the intestinal region are a heterogeneous population of cells that include enterocytes or absorptive cells, goblet cells that secrete mucin, endocrine cells and M cells, among others. The most common epithelial cells are the enterocytes that are responsible for the majority of the absorption of both nutrients and drugs in the small intestine (204, 205). Despite their colonic origin, Caco-2 cells undergo spontaneous differentiation in culture conditions to assume the characteristics of small intestinal cells. These include morphological and functional attributes, rendering the cell line a model of mature enterocytes (206). Owing to these features, Caco-2 cells are the most reported in the studies of drug absorption and toxicity (207, 208).

In this work, Caco-2 cells were used to evaluate the toxicological profile of LBG and the synthesized derivatives. **Figure 3.10** and **Figure 3.11** represent the Caco-2 cell viability obtained after exposure to the mentioned materials at different concentrations, for a period of 3 h and 24 h. Cell viability values were calculated in relation to the 100% cell viability considered for the incubation with DMEM (negative control of cell death). The evaluation of LBG-based samples generally evidenced a mild effect on cell viability, considered to be devoid of biological relevance. In fact, with the exception of LBGA, all the other samples resulted in viabilities above 70% after 3 h or 24 h of exposure, when tested at concentrations varying within 0.1 and 1.0 mg/mL. While at 3 h values remained above 88% in all conditions, the prolonged exposure until 24 h induced slight alterations. However, these were in most cases devoid of physiological relevance and the only remarkable effect resides in the decrease of the viability induced by the contact with LBGC at the highest concentration tested (1.0 mg/mL) ($P < 0.05$) to a value around 70%. Importantly, this is the value considered by ISO 10993-5 (201) as the level below which a toxic effect is assumed to occur.

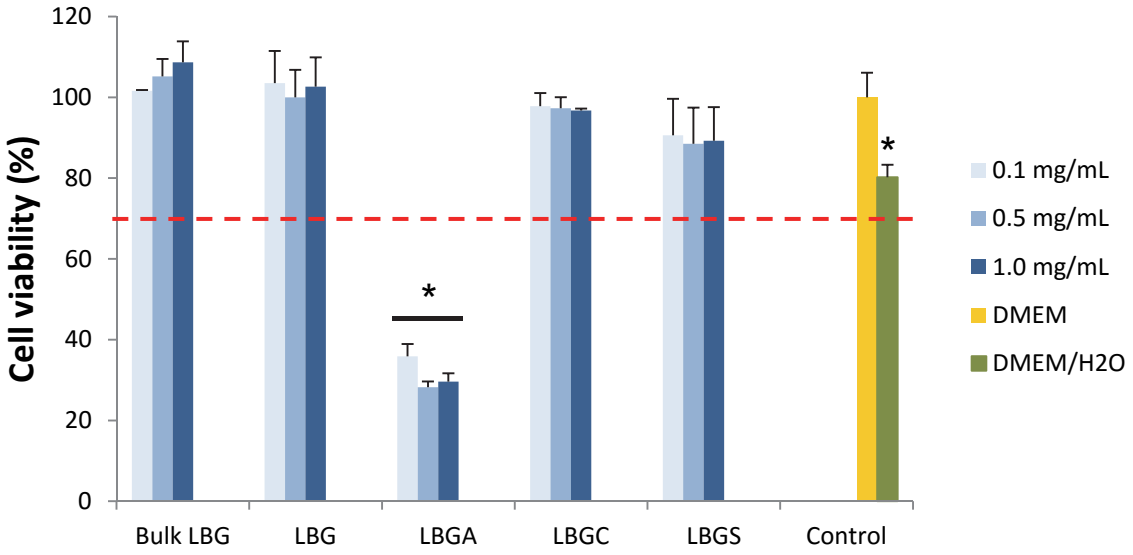

Figure 3.10 - Caco-2 cell viability measured by the MTT assay after 3 h exposure to increasing concentrations of bulk Locust Bean Gum, purified Locust Bean Gum (LBG) and its ammonium (LBGA), carboxylate (LBGC) and sulfate (LBGS) derivatives. Data represent mean ± SEM (n ≥ 3, six replicates per experiment at each concentration). Dashed line indicates 70%. * $P < 0.05$ compared with DMEM.

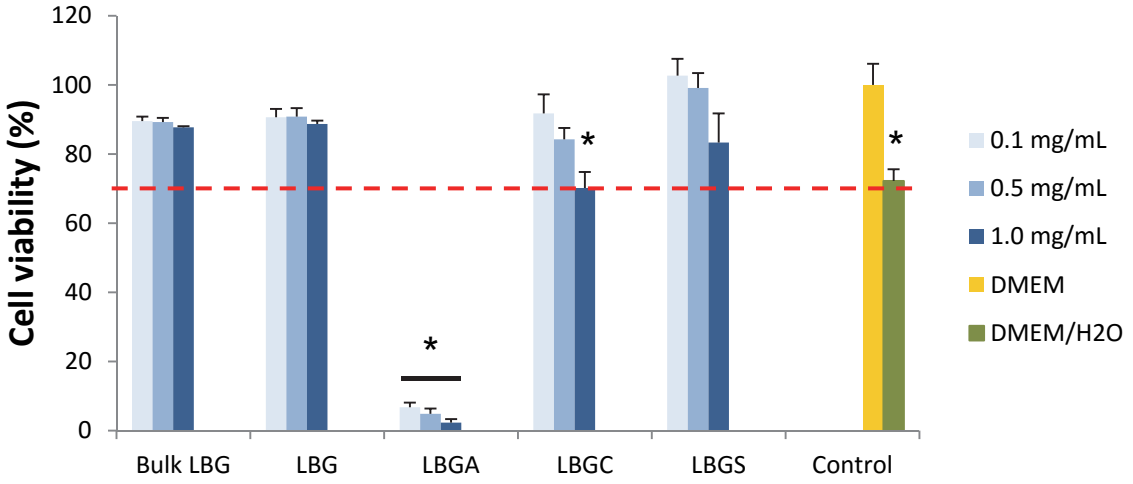

Figure 3.11 - Caco-2 cell viability measured by the MTT assay after 24 h exposure to increasing concentrations of bulk Locust Bean Gum, purified Locust Bean Gum (LBG) and its ammonium (LBGA), carboxylate (LBGC) and sulfate (LBGS) derivatives. Data represent mean ± SEM (n ≥ 3, six replicates per experiment at each concentration). Dashed line indicates 70%. * $P < 0.05$ compared with DMEM.

Although not directly proposed herein as matrix material *per se,* unmodified LBG was also tested, because its application in drug delivery has been reported, in many occasions addressing oral delivery strategies (83, 209-219), but data on its effect on epithelial cells

are not available on the literature. Moreover, a comparison between bulk LBG and LBG was performed, revealing no significant differences, which indicates an absence of effect of the purification process in the cytotoxic profile of the material. It is important to mention that the results shown for LBGS sample correspond to the derivative obtained by the second method of synthesis (method 2 – batch 1), which were similar to those registered for the derivative obtained in the first method (method 1; data not shown).

As mentioned before, LBGA is the material that presents the most distinct behavior, appearing as the exception to the mild effect observed for the tested materials. In fact, as shown in **Figure 3.10**, a strong decrease of cell viability to approximately 30% is obtained for any of the tested concentrations already upon a 3 h exposure. The effect is even more drastic after 24 h, when a very low level of cell survival was registered ($P < 0.05$; **Figure 3.11**). Regarding concentration, there are no evidences of a statistically significant concentration-dependent effect. The influence of surface charges on cytotoxicity remains largely unresolved and sometimes the literature reports contradictory results. This is possibly due to different characteristics of basic materials being used and also to dissimilar assay conditions, which are frequently not described in sufficient detail. Nevertheless, there are many indications suggesting that surface charge has a role on cellular uptake (220, 221) and on the toxicological effect of substances. In this context, positively charged materials have been frequently found to be more cytotoxic than neutral or negatively charged counterparts, because positive charges provide a means for stronger interaction with cell surfaces, in many cases associated with internalization of the material (221-225). These statements are coincident with the results of our work, since the neutral (bulk LBG and LBG) and negatively charged materials (LBGC and LBGS) are devoid of a toxic effect. Another parameter that could be indicated as playing a significant role on toxicity consists on the molecular weight of the polymers. In this regard, although it could be suggested that smaller sizes have higher probability to be internalized by the cells, the literature has been reporting no correlation (226). In this work, the molecular weight of the polymers also seems to not be driving the cytotoxic behavior, as LBGS is the smallest molecule and shows no toxic effect.

Comparing to LBGA, a very similar toxicological profile was observed for an ammonium derivative of another polysaccharide, pullulan, which was synthesized using the same methodology (58, 59). In that case, the assessment was performed in Calu-3 cells (bronchial cell line) and cell viabilities around 50-60% were observed after 3 h, decreasing to 40% at 24 h. Although a time-dependent effect is also clearly observed, the effect on cell viability is not as strong as for LBGA. The first consideration to take into account is the fact that the assessment was performed in different cell lines, which might translate into

different sensitivity. Additionally, different charge density of the polymers might be indicated as possible justification. In this regard, LBGA has a DS of 4.24, while the corresponding pullulan derivative (ammonium pullulan) has a DS of 2 (58). A higher number of positive charges results in stronger interactions and, thus, in lower cell viability. Complementing this idea, a work reporting the cytotoxic effect of cationic pullulan microparticles on human leukemic K562(S) cells, has established that toxicity increased with the increase molar concentration of amino groups (227). In the work reporting the cytotoxic evaluation of pullulan derivatives, a sulfate derivative of that polysaccharide was also assessed. Similarly to what was observed for LBGS, the registered cell viability was well above 80% (59).

Considering that polymer samples were solubilized in water and diluted with cell culture medium prior to incubation with the cells, an additional control was performed consisting in a mixture of DMEM and H_2O in the same ratio used for the samples. This enables a real evaluation of the contribution of the polymers on the final cell viability. As observed in **Figure 3.10** and **Figure 3.11**, the cell viability induced by this control varied between 72% and 80%. Upon 3 h of contact there is a statistically significant difference between the control (DMEM + H_2O) and all samples but with LBGS (**Figure 3.10**). In fact, higher cell viability is observed upon exposure to bulk LBG, LBG and LBGC, suggesting a positive effect of the presence of the polymers. Interestingly, after 24 h exposure (**Figure 3.11**), a shift is observed in the effect induced by LBGC and LBGS. In the former, the prolonged contact with the cells at the two highest concentrations reverts the positive effect on cell viability observed at 3 h. For LBGS, the results demonstrate that at the two lowest concentrations, the more prolonged contact improves cell viability, which was not registered at 3 h.

One of the most important information provided by the evaluation performed with the MTT assay, is that only the more prolonged exposure to the highest concentration tested (1.0 mg/mL; 24 h) induced a relevant decrease of Caco-2 cell viability (exception for LBGA). Therefore, it was deemed important to complement the results at these conditions by means of the quantification of the amount of LDH released by Caco-2 cells. To perform this assay, DMEM was used as negative control of LDH release and a lysis buffer was used as positive control. Thus, the negative control (DMEM) corresponds to a normal cell death, while the positive control (lysis buffer) represents 100% cell death.

Figure 3.12 shows the results of LDH release after 24 h exposure to the materials at the concentration of 1.0 mg/mL. No statistically significant differences were observed between the negative control (DMEM), bulk LBG, LBG, LBGC and LBGS, which means that these

materials do not compromise Caco-2 cell membrane integrity, as no increased LDH release was induced as compared with that observed upon incubation with cell culture medium (DMEM). On the contrary, the contact with LBGA resulted in 90% LDH release, which is considered comparable to that induced by the lysis buffer, thus indicating a high cytotoxic effect that results in cell membrane disruption. The results obtained in this assay reinforce those found in the MTT tests, confirming the high cytotoxicity of LBGA.

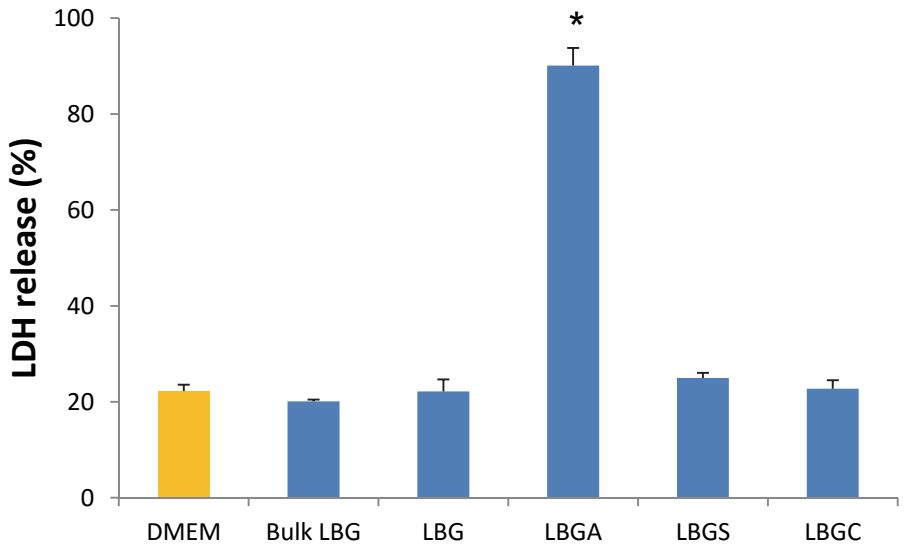

Figure 3.12 – Caco-2 cell viability measured by the LDH release assay after 24 h exposure to 1 mg/mL solutions of bulk Locust Bean Gum, purified Locust Bean Gum (LBG) and its ammonium (LBGA), carboxylate (LBGC) and sulfate (LBGS) derivatives. Data represent mean ± SEM (n ≥ 3, three replicates per experiment). * $P < 0.05$ compared with DMEM.

The overall results obtained with these complementary cytotoxicity assays indicate that, with the exception of LBGA, LBG and negatively charged derivatives, present no cytotoxicity towards this *in vitro* intestinal model. This was observed even for the highest concentration tested (1.0 mg/mL) and for prolonged contact (24 h), suggesting their relative safety for an application as matrix materials of oral drug delivery systems.

Complementarily, the effect on cell viability provided by LBGS (method 2 – batch 1) was assessed in Calu-3 and A549 cells (respiratory epithelial cells) and the results, displayed in **Figure 3.13** and **Figure 3.14**, are in line with those observed for Caco-2 cells.

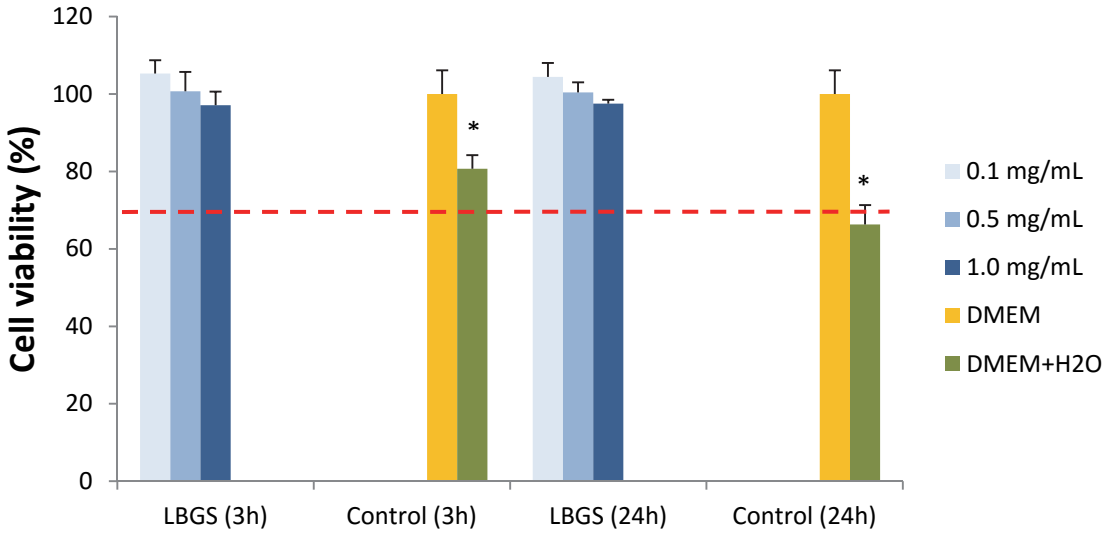

Figure 3.13 – A549 cell viability measured by the MTT assay after 3 h and 24 h exposure to increasing concentrations of sulfate locust bean gum (LBGS) derivative. Data represent mean ± SEM (n ≥ 3, six replicates per experiment at each concentration). Dashed line indicates 70%. * $P < 0.05$ compared with respective control (DMEM).

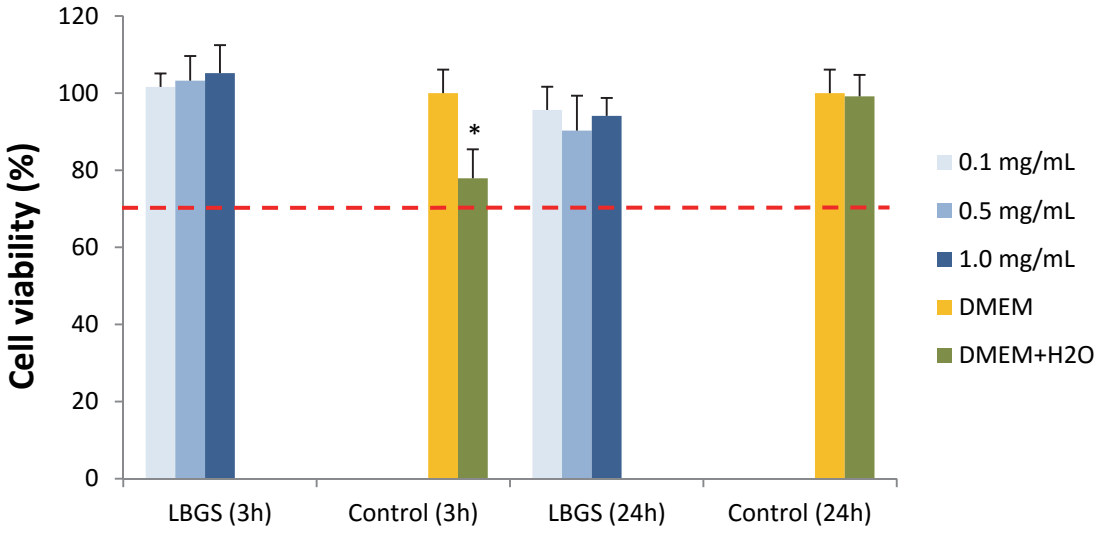

Figure 3.14 – Calu-3 cell viability measured by the MTT assay after 3 h and 24 h exposure to increasing concentrations of sulfate locust bean gum (LBGS) derivative. Data represent mean ± SEM (n ≥ 3, six replicates per experiment at each concentration). Dashed line indicates 70%. * $P < 0.05$ compared with respective control (DMEM).

Proposing materials for drug delivery applications requires testing the developed carriers and not only assume the apparent absence of cytotoxicity of the polymers. In this regard, it is consensual that carriers exhibit new and unique properties, thus generating potential

different risks as compared to the raw materials of the same chemistry (228), as observed in other works (58, 59). In this regard, in addition to the evaluation of the polymer and the synthesized derivatives, a preliminary evaluation of LBG-based nanoparticles was further performed using the MTT assay. Although several formulations were proposed and developed herein, that corresponding to LBG-only nanoparticles was selected for this step due to the novelty of the polymer in nanoparticle production.

The viability of Caco-2 cells upon exposure to LBGA/LBGS nanoparticles is shown in **Figure 3.15** (3 h) and **Figure 3.16** (24 h). The two developed formulations (LBGA/LBGS 2:1 and 1:2, w/w) were assessed. For formulation 2:1 (w/w) the comparison of results obtained for each tested time revealed a statistically significant difference between concentrations 0.1 and 1.0 mg/mL ($P < 0.05$). Formulation 1:2 (w/w) did not evidence significant differences between all concentrations at the two tested times. A similar observation was made after comparing the same concentrations for different times (3 h and 24 h). The most remarkable result is that no significant effect on cell viability is observed for both formulations at all concentrations, up to 24 h. Actually, the registered viability was over 80% in all cases, which, as said before, is considered very acceptable according to the ISO10993-5 (201).

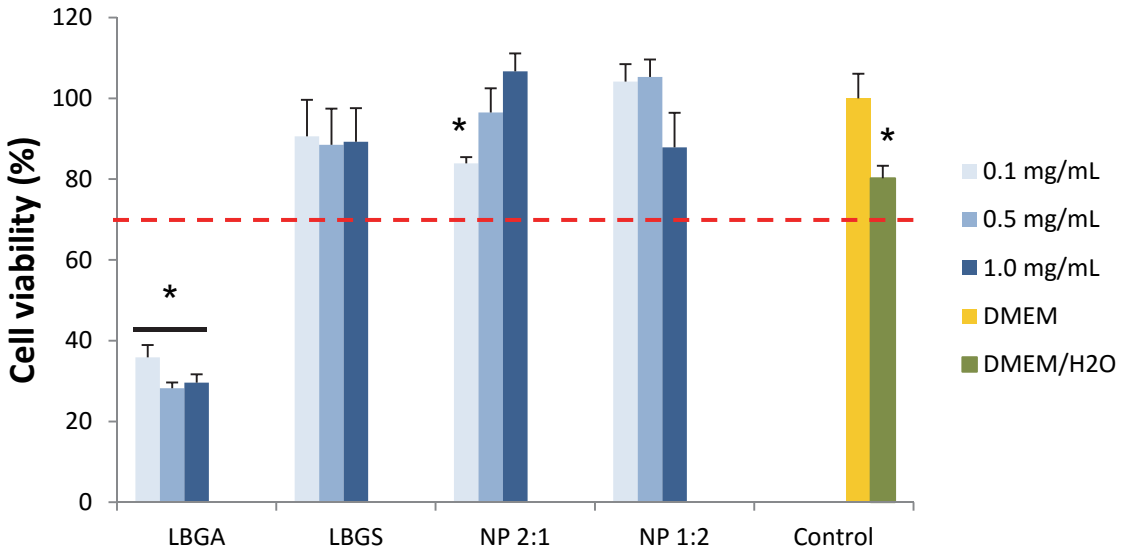

Figure 3.15 – Caco-2 cell viability measured by the MTT assay after 3 h exposure to increasing concentrations of ammonium Locust Bean Gum (LBGA) derivative, sulfate Locust Bean Gum (LBGS) derivative and LBGA/LBGS nanoparticles (NP). Data represent mean ± SEM (n ≥ 3, six replicates per experiment at each concentration). Dashed line indicates 70%. * $P < 0.05$ compared with DMEM.

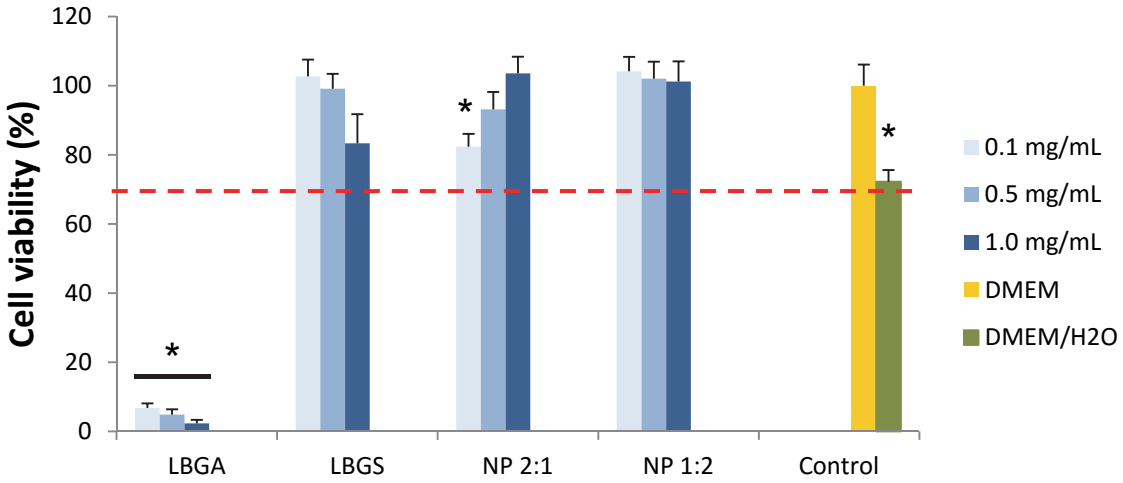

Figure 3.16 – Caco-2 cell viability measured by the MTT assay after 24 h exposure to increasing concentrations of ammonium Locust Bean Gum (LBGA) derivative, sulfate Locust Bean Gum (LBGS) derivative and LBGA/LBGS nanoparticles (NP). Data represent mean ± SEM (n ≥ 3, six replicates per experiment at each concentration). Dashed line indicates 70%. * $P < 0.05$ compared with DMEM.

Curiously, the same figures also demonstrate that the exposure of the cells to the formulation LBGA/LBGS 2:1 (w/w) resulted in an increase of cell viability with the increase of nanoparticle concentration at 3 h and at 24 h ($P < 0.05$). This was unexpected and may be due to the fact that LBG is a polysaccharide with capacity to promote cell proliferation in some cell lines, as reported in the literature (229). Despite the formulation LBGA/LBGS 2:1 (w/w) could improve cell proliferation with increasing concentrations, formulation LBGA/LBGS 1:2 (w/w), generally induced constant cell viability near 100%, irrespective of the concentration.

Comparing with the control (DMEM + H_2O) it is observed that the nanoparticles generally elicit higher cell viability, varying between 82% and 100% ($P < 0.05$). The most remarkable observation in the whole set of cell viability assessment is that, in spite of the strong decrease in cell viability induced by the contact with LBGA, this effect was completely reverted when the cells are exposed to a nanoparticulate form of the derivative. This was also observed in works using an ammonium derivative of pullulan, in which the derivative elicited around 40% cell viability upon 24 h of exposure, while nanoparticles produced with the polymer registered increased cell viabilities to values of 70% - 80% (58, 59). The different impact on cell viability generated by LBGA in form of polymer and of nanoparticles is possibly explained by a differential contact of each of the materials with the cells. While the polymer in form of a solute is presented as an extended chain and, thus, has a higher surface of contact with the cells, nanoparticles have

comparatively a lower contact. Additionally, the number of positive charges available for interaction with the negatively charged cells upon complexation with LBGS is significantly decreased, thus decreasing the potential toxicity (226). This reinforces the need to evaluate separately the carriers and the raw materials, as the former may exhibit different properties, that may encompass different risks (228).

These preliminary results suggest an absence of overt toxicity of LBG-only nanoparticles, thus potentiating possible applications, although it is recognized that further studies need to be performed to reach a more accurate conclusion in this regard.

3.4. Conclusions

LBG demonstrated to be a good substrate for the production of charged derivatives, permitting the synthesis of ammonium, sulfated and carboxylated LBG. Several characterization techniques were used to confirm the presence of the new chemical groups introduced in each new derivative.

Using a method of polyelectrolyte complexation, the produced derivatives were applied in the preparation of different formulations of LBG-based nanoparticles, reported herein for the first time. When the negatively charged derivatives (sulfated and carboxylated LBG) were used, chitosan was the applied positively charged polyelectrolite. In turn, ammonium LBG was complexed with sulfated LBG to obtain LBG-only nanoparticles. The physicochemical characteristics of nanoparticles were highly dependent on their composition and on the charge ratios applied in each complexation being performed. Generally, the observed characteristics, with sizes around 200-400 nm in certain cases, and tailorable zeta potential according to setup conditions, are suggested as adequate for drug delivery applications.

A preliminary toxicological evaluation of LBG derivatives and the produced nanoparticles was performed, assessing both the metabolic activity and the cell membrane integrity of representative intestinal cells (Caco-2 cells) after an exposure of up to 24 h to concentrations as higher as 1 mg/mL. Severe cytotoxicity was found for the ammonium derivative of LBG, but this was clearly reverted after the assembly of nanoparticles, which evidenced a very mild effect on Caco-2 cell viability. The results as a whole indicate the possibility to use the synthesized LBG derivatives to produce nanoparticles for drug delivery applications.

This page was intentionally left in blank

CHAPTER 4

LOCUST BEAN GUM NANOPARTICLES: APPLICATION IN ORAL IMMUNIZATION

The information presented in this chapter was submitted for publication in International Journal of Pharmaceutics:

Braz, L., Camacho, A., Grenha, A., Ferreira, D., Rosa da Costa, A.M., Gamazo, C., Sarmento, B., Chitosan/Sulfated Locust Bean Gum nanoparticles: *in vitro* and *in vivo* evaluation towards an application in oral immunization, submitted for publication

This page was intentionally left in blank

4. Chitosan/Sulfated Locust Bean Gum nanoparticles: *in vitro* and *in vivo* evaluation towards an application in oral immunization

4.1. Introduction

The search for alternative vaccination approaches that may circumvent the limitations of parenteral delivery is not new. Mucosal vaccination has thus been gaining popularity in the recent decades and some mucosal vaccines are currently available in the market (175, 230). Apart from leading to higher patient's compliance, as the discomfort associated with parenteral administration is avoided, mucosal vaccines permit an easier chain of distribution, mainly because a cold-chain is not necessary, which is relevant for developing countries (119, 137). The oral route is the one gathering higher interest concerning this alternative vaccination concept, not only because of the general advantages associated with oral administration, but also due to relevant features of the intestine for immunization. In this regard, a special mention is due to the gut associated mucosal tissue (GALT), which has sites where immune responses are initiated and effector sites where adaptive immune responses are executed (175). The Peyer's patches existing in the GALT comprise the main location of immune cells associated to the intestinal mucosa (154) and are separated from the intestinal lumen by the follicle associated epithelium (FAE) (159). FAE is composed of enterocytes, goblet cells and microfold cells (M cells) (136, 154), the latter being reported to have a thinner mucus layer, and good ability for antigen uptake and transport to antigen presenting cells (APCs) (231). Apart from these anatomical specificities, mucosal sites are considered locations of primary access for most human pathogens (138), many accessing the organism through the mouth. As mucosal immunization is expected to elicit both systemic and mucosal immunity, the development of the latter at the intestinal level becomes a relevant tool towards limiting or preventing pathogen entry, thus inhibiting the consequent infection (139, 140).

Notwithstanding the evident ability of the intestinal area for antigen recognition, antigens are biopharmaceuticals, thus being highly sensitive molecules that require specific precautions regarding their formulation and delivery. Indeed, the protein-based structure hinders the possibility of a direct oral administration, mainly because of the low gastric pH and the high content of proteases (232, 233). Suitable particles are therefore demanded for a successful oral immunization approach and nanoparticles have been indicated many times as very useful in mediating this process. Apart from providing the associated antigens with protection from the harsh gastrointestinal conditions referred above, their

small size is expected to permit an intimate contact with the epithelial surface, where cells with relevant roles in the generation of an immune response are located (234). In addition, nanoparticles may also act as immunomodulator adjuvants, meaning that the particles further mediate the development of the immune response. The particles may facilitate both the antigen uptake and internalization by GALT and, also, the antigenic cross-presentation by APCs (235). The use of The use of particle vehicles exhibiting targeting moieties that have a favoured interaction with epithelial glycoconjugates that are specifically activated by pathogens, such as the TLR family or the mannose receptor, has been proposed as a strategy that mimics microbial behaviour in the development of immune responses (235).

The uptake of particles is reported to primarily occur via the M cells (175), which have been referred to provide a privileged contact with mannose residues (80, 169) and, therefore, might be used as privileged target for mannose-containing particles. Locust bean gum (LBG) is a polysaccharide of the class of galactomannans, thus having a chemical structure composed of both galactose and mannose units (64), as depicted in **Figure 1.2**, from chapter 1 (general introduction). Therefore, it potentially has the ability to provide the said privileged contact between the particle and the M cells.

This paper proposes the design of nanoparticles based on LBG and chitosan, another polysaccharide, to be used as antigen particles for oral immunization purposes. A negatively charged derivative of LBG was produced (sulfated LBG) to enable the production of nanoparticles by polyelectrolyte complexation. Two model antigens were associated to the nanoparticles, an antigenic complex of *Salmonella enterica* serovar Enteritidis and ovalbumin; and *in vivo* studies were performed.

4.2. Materials and methods

4.2.1. Materials

Chitosan (CSup) in the form of hydrochloride salt (Protasan® UP Cl 113, deacetylation degree = 75% – 90%, molecular weight < 200 *k*Da), was purchased from Pronova Biopolymer (Sandvika, Norway). Locust bean gum (LBG) was a kind gift from Industrial Farense (Faro, Portugal). Immunogenic subcellular extract obtained from whole *Salmonella* Enteritidis cells (HE) was kindly provided by Professor Carlos Gamazo (University of Navarra, Spain). Ovalbumin (OVA), bovine serum albumin (BSA), phosphotungstate dibasic hydrate, glycerol, phosphate buffered saline (PBS) pH 7.4

tablets, Dulbecco's modified Eagle's medium (DMEM), penicillin/streptomycin (10000 units/mL, 10000 µg/mL), non-essential amino acids, L-glutamine 200 mM, trypsin-EDTA solution (2.5 g/L trypsin, 0.5 g/L EDTA), trypan blue solution (0.4%), thiazolyl blue tetrazolium bromide (MTT), lactate dehydrogenase (LDH) kit, sodium dodecyl sulfate (SDS), Ponceau S red staining solution, protease inhibitor cocktail, dimethyl sulfoxide (DMSO), HCl 37%, H_2O_2, 4-chloro-1-naphtol, NaCl, KH_2PO_4 and NaOH were purchased from Sigma-Aldrich (Germany). XT sample buffer, Criterion XT bis-tris gel, XT MOPS running buffer, Coomassie blue and Tris-glycine buffer were provided by Bio-Rad (USA) and PBS-tween (PBS-T) and 3-ethylbenzthiazoline-6-sulfonic acid (ABTS) by VWR (Portugal). Fetal bovine serum (FBS) was obtained from Gibco (USA), molecular mass markers (Novex Sharp Pre-stained Protein Standard) from Invitrogen (Germany). Peroxidase-conjugated goat anti-mouse IgG1, IgG2a and IgA antibodies were purchased from Nordic Immunology (Netherlands) and skimmed milk from Continente (Portugal). Ultrapure water (Mili-Q Plus, Milipore Iberica, Madrid, Spain) was used throughout. All other chemicals were reagent grade.

4.2.2. Cell line

The Caco-2 cell line was obtained from the American Type Culture Collection (Rockville, USA) and used between passages 77-93. Cell cultures were grown in 75 cm^2 flasks in a humidified 5% CO_2/95% atmospheric air incubator at 37 ºC. Cell culture medium was DMEM supplemented with 10% (v/v) FBS, 1% (v/v) L-glutamine solution, 1% (v/v) non-essential amino acids solution and 1% (v/v) penicillin/streptomycin. Medium was changed every 2-3 days and cells were subcultured weekly.

4.2.3. Production of Locust Bean Gum-based nanoparticles

All nanoparticles (NP) were prepared by polyelectrolyte complexation method which consists in the electrostatic interaction between the positive and negative charges of the different polymers (35).

4.2.3.1. CSup/LBGS nanoparticles

Nine mass ratios of CSup/LBGS (1:1; 1:1.25; 1:1.5; 1:1.75; 1:2; 1:3; 1:3.25; 1:3.5 and 1:4) were used to prepare the nanoparticles by polyelectrolyte complexation. The stock solution of CSup, dissolved in ultrapure water, was prepared to reach a final concentration of 1.0 mg/mL, while LBGS was dissolved in ultrapure water, at final concentration of 4.0 mg/mL. The solutions were filtered with a 0.45 µm filter prior to use. The formulations were prepared by slowly adding 1.8 ml of LBGS to 1.0 ml of CSup under gentle magnetic stirring at room temperature, as shown in **Figure 1.1** (chapter 1, general introduction). The concentration of CSup was kept constant at 1.0 mg/mL for the preparation of all formulations, but that of LBGS was modified to obtain the different ratios.

After the addition of the LBGS solutions to the CSup solution was possible to see, almost immediately, the Tyndall effect evidencing the formation of nanoparticles. The suspensions of nanoparticles were mixed by magnetic stirring for 10 min and then centrifuged in eppendorfs with a layer of 10 µL of glycerol, in order to facilitate the following step of ressuspension. The isolation of nanoparticles was performed by centrifugation (Thermo Scientific-Heraeus Fresco 17, Germany) at 16 000 x *g*, for 30 min at 15 ºC. After discarding the supernatants, the nanoparticles were ressuspended with 200 µL of ultrapure water.

4.2.3.2. Association of a bacterial antigenic complex to CSup/LBGS nanoparticles

An antigenic complex, HE, consisting of vesicles of outer membrane, was obtained from *Salmonella* Enteritidis. Its association was performed to the CSup/LBGS 1:1.5 and 1:2 (w/w) nanoparticle formulations, which selection was mainly driven by the production yield. The stock solution of the HE antigenic complex was prepared by dissolving it in ultrapure water (0.4 mg/mL) using the ultra-sound bath during 15 min at room temperature. The solution was filtered with a 0.22 µm low protein binding filter (Millex® - GV, Millipore, Spain) prior to use. The NP-HE were prepared using the same methodology used for the unloaded nanoparticles, but the concentration of LBGS solutions were adjusted using different concentrations of HE solutions, in order to obtain a theoretical content of 2%, 4% or 8% (w/w) of the total amount of polymers.

4.2.3.3. Association of OVA to CSup/LBGS nanoparticles

The association of OVA was performed to the CSup/LBGS 1:2 (w/w) nanoparticle formulation. The stock solution of OVA was prepared by dissolving it in ultrapure water (0.3 mg/mL) under magnetic stirring during 15 min at room temperature. The solution was filtered with a 0.22 µm low protein binding filter (Millex® - GV, Millipore, Spain) prior to use. The NP-OVA was prepared using the same methodology used for the unloaded nanoparticles, but the concentration of LBGS solution was adjusted using the stock OVA solution, in order to obtain a theoretical content of 8% (w/w) of the total amount of polymers.

4.2.4. Characterization of CSup/LBGS nanoparticles

4.2.4.1. Size, zeta potential and polidispersion index

The size, zeta potential and polidispersion index (PdI) determination of the nanoparticles was performed on freshly prepared samples. Size and PdI were measured by dynamic light scattering and zeta potential was measured by laser Doppler anemometry, using a Zetasizer Nano ZS (Malvern instruments, UK). To prepare the samples, 20 µL of each formulation were diluted in 1 mL of ultrapure water.

4.2.4.2. Production yield

For determination of nanoparticle production yield, the nanoparticles were prepared as described in the previous sections but without the use of the 10 µL of glycerol. After discarding the supernatant of each formulation, the pellets were frozen and then dried on a freeze-dryer (Alpha RVC, Germany). The yield of nanoparticle production (PY) was calculated as follows:

PY = (Nanoparticle sediment weight/Total solids weight) x 100

where nanoparticle sediment weight is the weight after freeze-drying and total solids weight is the total amount of solids added for nanoparticle formation.

4.2.4.3. Association efficiency

HE and OVA encapsulated in nanoparticles were quantified in each sample using the Micro BCA Protein Assay Kit (Pierce, USA), which provides a colorimetric method optimized to quantify reduced amounts of protein (0.5-20 µg/mL). A purple-coloured water-soluble reaction product is formed by the chelation of two molecules of BCA with one cuprous ion (Cu^{+1}), which exhibits a strong absorbance at 562 nm that is linear with increasing protein concentrations. High absorbance is therefore interpreted as high protein concentration.

Different calibration curves were performed for each formulation (NP-HE or NP-OVA) using ultrapure water as solvent. Supernatants obtained upon centrifugation of the nanoparticle production media were incubated with the MicroBCA reagent (2 h, 37 ºC) in a 96-well plate. After that time, samples were analysed by spectrophotometry (Infinite M200 Tecan, Austria) at 562 nm. The supernatants of unloaded nanoparticles were used for blank correction.

The protein association efficiency (AE) and loading capacity (LC) were calculated as follows:

AE (%) = [(Total antigen amount – Free antigen amount)/Total antigen amount] x 100

LC (%) = [Total antigen amount – Free antigen amount)/Nanoparticle weight] x 100

4.2.4.4. Morphological analysis

The morphological examination of CSup/LBGS nanoparticles was conducted by transmission electron microscopy (TEM; JEM-1011, JEOL, Japan). The samples were stained with 2% (w/v) phosphotungstic acid and placed on copper grids with carbon films (Ted Pella, USA) for TEM observation.

4.2.5. *In vitro* evaluation of CSup/LBGS nanoparticles

4.2.5.1. Evaluation of the structural integrity and antigenicity of the loaded antigens

4.2.5.1.1. HE-loaded CSup/LBGS nanoparticles

The integrity of HE antigens upon association was confirmed using SDS polyacrylamide gel electrophoresis (SDS-PAGE) analysis. Pellets of fresh NP-HE and free HE were dispersed in electrophoresis sample buffer (XT sample buffer) at a concentration of 1 mg of HE/mL. The mixtures were left in ultrasound bath for 15 min and then heated at 100 ºC for 10 min. After centrifugation (16 000 x *g*, 30 min, 15 ºC) the supernatants were collected and heated at 100 ºC for 10 min. SDS-PAGE was performed with Criterion XT bis-tris gel, run with XT MOPS running buffer at 200 mA for 1 h and finally stained with Coomassie blue.

The antigenicity study was performed by immunoblotting using sera from a pool of mice experimentally immunized with HE (40 µg, subcutaneously). After SDS-PAGE, the gel was transferred to a nitrocellulose membrane (pore size of 0.45 mm; Whatman®, UK) by using a semidry electroblotter (Bio-Rad, USA) at 200 mA for 30 min, in a transfer buffer (0.2 M glycine; 24 mM Tris; 20% methanol, pH 8.3). The blot was placed in blocking buffer (3% skimmed milk PBS) overnight at 4 ºC. After washing with PBS-Tween (PBS-T) the blot was incubated with serum diluted 1:100 in PBS-T with 1% (w/v) skimmed milk for 3 h. After washing with PBS-T, the blot was incubated for 1 h at room temperature with the peroxidase-conjugated goat anti-mouse IgG1 (Nordic Immunology) diluted 1:100 in PBS-T with 1% (w/v) BSA. The blot was washed with PBS-T and developed by incubation in a solution containing H_2O_2 and 4-chloro-1-naphtol for 3 min in the dark.

The apparent molecular masses of the proteins present in the antigenic extract were determined by comparing their electrophoretic mobility with that of molecular mass markers.

4.2.5.1.2. OVA-loaded CSup/LBGS nanoparticles

The integrity of OVA antigen upon association was confirmed by an SDS-PAGE analysis. Pellets of fresh NP-OVA and OVA were dispersed in electrophoresis sample buffer (XT sample buffer) at a concentration of 1 mg of OVA/mL. The mixtures were left in ultrasound

bath for 15 min and then heated at 100 ºC for 10 min. After centrifugation (16 000 x *g*, 30 min, 15 ºC) the supernatants were collected and heated at 100 ºC for 10 min. SDS-PAGE was performed in 10% polyacrylamide gel, run with tris-glycine buffer at 200 mA for 1 h and transferred to a nitrocellulose membrane, as indicated below. Finally, the membrane was stained with Ponceau S red staining solution and images were taken using the ChemiDoc XRS+ imaging system (Bio-Rad, USA) after several washes with ultrapure water.

The antigenicity study was performed by immunoblotting using sera from a pool of mice experimentally immunized with OVA (20 µg, subcutaneously). After SDS-PAGE, the gel was transferred to a nitrocellulose membrane (pore size of 0.45 mm; Whatman®, UK) at 200 mA for 1 h, in a transfer buffer (0.2 M glycine; 24 mM Tris; 20% methanol, pH 8.3) (wet transfer). The blot was placed in blocking buffer (5% skimmed milk PBS) during 3 h. After washing with PBS-T, the blot was incubated with serum diluted 1:100 in PBS-T with 1% (w/v) skimmed milk for 2 h at room temperature and then overnight at 4 ºC. After another washing step with PBS-T, the blot was incubated for 1 h at room temperature with the peroxidase-conjugated goat anti-mouse IgG1 diluted 1:100 in PBS-T with 1% (w/v) BSA. The blot was again washed with PBS-T and developed by incubation in a solution containing H_2O_2 and 4-chloro-1-naphtol for 15 min in the dark.

The apparent molecular masses of the proteins present in the antigen were determined by comparing their electrophoretic mobility with that of molecular mass markers.

4.2.5.2. Stability evaluation on storage

Aliquots of unloaded nanoparticle formulations (1:1; 1:1.5 and 1:2) and HE-loaded formulations (1:1.5 and 1:2) were stored at 4 ºC. Nanoparticle size and zeta potential were monitored as a function of time for 6 months, using the methodology described above ($n \geq 3$).

4.2.5.3. *In vitro* release in SGF and SIF

HE and OVA release profiles were determined in simulated gastric fluid (SGF) and simulated intestinal fluid (SIF) (236). In these studies, 2.5 mg of NP-HE and 7.02 mg of NP-OVA were incubated in SGF or SIF (37 ºC, 100 rpm), and at appropriate time intervals samples were collected, centrifuged (16 000 x *g*, 10 min, 15 ºC) and the released HE or

OVA determined by the microBCA (Pierce, USA) assay. Unloaded nanoparticles were submitted to the same conditions and used as blank. All experiments were performed at least in triplicate (n ≥ 3).

4.2.5.4. Safety evaluation of unloaded nanoparticles

The *in vitro* cell viability and cytotoxicity of CSup/LBGS nanoparticles, as well as that of the raw materials involved in nanoparticle production, was assessed by the metabolic assay MTT and the LDH release assay, respectively.

The cells were seeded at a density of 1×10^4 cells/well in 96-well plates, in 100 µL of the same medium used for culture in cell culture flasks, and were grown at 37 °C in a 5% CO_2 atmosphere for 24 h before use. The effect on cell viability induced by three different concentrations (0.1, 0.5 and 1.0 mg/mL) of unloaded nanoparticles, as well as that of raw materials involved in nanoparticle production, was evaluated over 3 h and 24 h. A SDS solution (2%, w/v) was used as a positive control of cell death, while cells incubated with DMEM served as negative control. An additional control (DMEM+H_2O) consisting in a mixture of DMEM and H_2O in the same ratio used for the samples was used, in order to evaluate the contribution of materials on cell viability. All formulations and controls were prepared as solution/suspensions in pre-warmed cell culture medium without FBS immediately before application to the cells.

To initiate the assay, culture medium of cells at 24 h in culture was replaced by 100 µL of fresh medium without FBS containing the test samples or controls. A constant ratio (3:1) between the culture medium and the solution/suspension of the materials was used. After 3 or 24 h of cell exposure, samples/controls were removed and 30 µL of the MTT solution (0.5 mg/mL in PBS, pH 7.4) was added to each well. After 2 h, any generated formazan crystals were solubilised with 50 µL of DMSO. Upon complete solubilisation of the crystals, the absorbance of each well was measured by spectrophotometry (Infinite M200, Tecan, Austria) at 540 nm and corrected for background absorbance using a wavelength of 650 nm (186).

The relative cell viability (%) was calculated as follows:

$$\text{Viability (\%)} = (A - S)/(CM - S)\times 100$$

where A is the absorbance obtained for each of the concentrations of the test substance, S is the absorbance obtained for the 2% SDS and CM is the absorbance obtained for

untreated cells (incubated with cell culture medium). The latter reading was assumed to correspond to 100% cell viability. The assay was performed at least for three occasions with six replicates at each concentration of test substance in each instance.

Considering the mild effect observed in the MTT assay, the LDH release assay was performed on polymeric solutions and nanoparticle suspensions, after 24 h exposure to a concentration of 1.0 mg/mL. This is a colorimetric assay that quantitatively measures LDH, a stable cytosolic enzyme that is released upon cell lysis. Released LDH in culture supernatants was measured with a 30-min coupled enzymatic assay that results in the conversion of a tetrazolium salt into a red formazan product. The amount of color formed is proportional to the number of lysed cells (187).

Samples from the culture medium in the seeding plates were centrifuged (16 000 x *g*, 5 min, 15 ºC), and 50 µL was collected and reacted with 100 µL of the LDH release reagent at room temperature and protected from light. The reaction was stopped after 30 min by adding 15 µL HCl 1N. Absorbance was measured by spectrophotometry at a wavelength of 490 nm with background correction at 690 nm. The relative LDH release (%) was calculated as follows, considering 100% release for samples incubated with the lysis solution (positive control of cell death):

$$\text{LDH release (\%)} = A_{test}/A_{control} \times 100$$

where A_{test} is the absorbance of the test sample and $A_{control}$ is the absorbance of positive control of cell death. The assay was performed in at least three occasions, with three replicates in each instance.

4.2.6. *In vivo* evaluation of the immune response in BALB/c mice

4.2.6.1. HE-loaded CSup/LBGS nanoparticles

The experiments were performed in compliance with the regulations of the responsible committee of the University of Navarra (Pamplona, Spain) and in strict accordance with good animal practice under the Declaration of Helsinki and the Directive 2010/63/EU. Six groups of five female BALB/c mice (20 ± 1 g), 6 weeks old (Harlan Iterfauna Ibérica, Spain), were starved 7 h before immunization and only allowed free access to water. The groups were immunized orally with 200 µL of: 200 µg of HE in PBS, 200 µg of HE encapsulated in NP (NP-HE in PBS), 2.33 mg of unloaded nanoparticles (NP in PBS); and

subcutaneously with 50 µL of: 40 µg of HE in PBS, 40 µg of HE encapsulated in NP (NP-HE in PBS), 466.25 µg of unloaded nanoparticles (NP in PBS). Blood samples and faeces were collected weekly from week 0 to 5 post immunization, centrifuged (10 000 x *g*, 10 min, room temperature) and stored at -20 ºC until being analyzed. The faeces, before centrifugation, were vortexed in PBS with 3% (w/v) of skimmed milk (100 mg/mL), and stored, after centrifugation, with addition of a protease inhibitor cocktail (10 µL/mL).

Specific antibodies (IgG1 and IgG2a from sera; IgA from feaces) against HE were determined by ELISA using 96 microtiter plates (Nunc MaxiSorp, Thermo Scientific). For that purpose, wells were coated overnight with 1 µg of HE in PBS at 4 ºC and then blocked with 1% (w/v) BSA (sera samples) or 3% (w/v) skimmed milk in PBS–T for 1 h at room temperature (faeces samples). After washing with PBS-T, samples were added diluted 1:40 (oral immunization) or 1:100 (S.C. immunization) in PBS-T and incubated at 37 ºC, for 4 h (serum); or diluted 1:2 in PBS-T and incubated overnight at 4 ºC (faeces). Then, washed wells were incubated for 1 h at room temperature with antibodies peroxidase-conjugated goat anti-mouse IgG1, IgG2a or IgA. For the color development, the substrate-chromogen used was H_2O_2-ABTS and after 15 min (serum) or 30 min (faeces) the absorbance was determined at λ_{max} 405 nm.

4.2.6.2. OVA-loaded CSup/LBGS nanoparticles

The experiments were performed in strict accordance with good animal practice under the Declaration of Helsinki, the Directive 2010/63/EU and the Portuguese law DL 113/2013. Four groups of six female BALB/c mice (20 ± 1 g), 6 weeks old (Instituto Gulbenkian de Ciência, Portugal), were starved 7 h before immunization and only allowed free access to water. The groups were immunized orally with 200 µL of: 100 µg of OVA, 100 µg of OVA encapsulated in NP (NP-OVA); and subcutaneously with 50 µL of: 20 µg of OVA, 20 µg of OVA encapsulated in NP (NP-OVA). Blood samples and faeces were collected at weeks 0, 1, 2, 4 and 6 post immunization, centrifuged (10 000 x *g*, 10 min, room temperature) and stored at -20 ºC until being analyzed. The faeces, before centrifugation, were vortexed in PBS with 3% (w/v) of skimmed milk (100 mg/mL), and stored, after centrifugation, with addition of a protease inhibitor cocktail (10 µL/mL).

Specific antibodies (IgG1 and IgG2a from sera; IgA from feaces) against OVA were determined by ELISA using 96 microtiter plates (Nunc MaxiSorp, Thermo Scientific). For that purpose, wells were coated overnight with 1 µg of OVA in PBS at 4 ºC and then blocked with 1% (w/v) BSA (sera samples) or 3% (w/v) skimmed milk in PBS–T for 1 h at

room temperature (faeces samples). After washing with PBS-T, a pool of samples were added in twofold serial dilutions in PBS-T starting with 1:40, and incubated at 37 ºC, for 4 h (serum); or starting with 1:1 and incubated overnight at 4 ºC (faeces). Then, washed wells were incubated for 1 h at room temperature with antibodies peroxidase-conjugated goat anti-mouse IgG1, IgG2a or IgA. For the color development, the substrate-chromogen used was H_2O_2-ABTS and after 15 min (serum) or 30 min (faeces) the absorbance was determined at λ_{max} 405 nm. The end titers were determined as the dilution of sample giving the mean O.D. ≥ 0.2 the obtained from untreated mice sera.

4.2.7. Statistical analyses

The t-test and the one-way analysis of variance (ANOVA) with the pair wise multiple comparison procedures (Holm-Sidak method) were performed to compare two or multiple groups, respectively. All analyses were run using the SigmaStat statistical program (Version 3.5, SyStat, USA) and differences were considered to be significant at a level of $P < 0.05$.

4.3. Results and discussion

4.3.1. Characterization of unloaded CSup/LBGS nanoparticles

Several formulations of LBG-based nanoparticles were produced by a very mild polyelectrolyte complexation, according to a procedure detailed in the experimental section. Polyelectrolyte complexation is a process that involves electrostatic interaction between oppositely charged groups. This procedure takes the advantage of occurring in a hydrophilic environment with mild preparation conditions, avoiding the use of organic solvents or high shear forces that might compromise the stability of encapsulated materials (108, 194). LBG is a natural polymer with neutral charge, which hinders the application of the mentioned methodology to directly obtain nanoparticles. In order to overcome that relevant limitation, a sulfate derivative of LBG was produced, exhibiting a negative charge. When CSup and LBGS solutions are mixed, an electrostatic interaction is established between the negatively charged sulfate groups of LBGS and the positively charged amino groups of CSup, leading to nanoparticle formation (**Figure 1.1**). Considering the pH of the involved solutions (4.3 for CSup and 5.6 for LBGS), the polymers display positive and negative charges, respectively. In the case of CSup, a

degree of deacetylation of 86%, to which corresponds 0.86 positive charges per monomer, and a M_w of 113 kDa, have been reported (237). The mean molar mass for the monomer (198 g/mol) may be obtained by ponderation of the molar masses of the acetylated and deacetylated units. In turn, for LBGS a C:S molar ratio of 26.76 was determined, to which corresponds a DS of 1.22 and a mean molar mass of 932 g/mol for the monomer. An M_w of 27 kDa was determined by GPC analysis.

As the aim of this work was to disclose the effect of LBGS in the production of nanoparticles, the produced formulations accounted with a similar or higher amount of this polymer comparing with CSup. Nine formulations of CSup/LBGS nanoparticles were produced with polymeric mass ratios varying within 1:1 and 1:4. After the preparation procedures, nanoparticles were characterized in terms of size, polydispersion index (PdI), zeta potential and production yield. The detailed results are shown in **Table 4.1**.

Table 4.1 - Physicochemical characteristics and production yield of CSup/LBGS unloaded nanoparticles (mean ± SD; n ≥ 3). Different letters represent significant differences in each parameter ($P < 0.05$).

CSup/LBGS (w/w)	Size (nm)	PdI	Zeta potential (mV)	Production yield (%)
1:1	174.8 ± 13.1 [a]	0.10 ± 0.005	+13.0 ± 2.7 [b]	9.1 ± 5.0 [c]
1:1.25	183.0 ± 4.7 [a]	0.10 ± 0.03	+14.5 ± 1.3 [b]	n.d.
1:1.5	184.0 ± 4.1 [a]	0.09 ± 0.01	+13.0 ± 0.8 [b]	12.5 ± 3.9 [c]
1:1.75	182.5 ± 5.0 [a]	0.09 ± 0.01	+13.3 ± 1.0 [b]	n.d.
1:2	183.0 ± 6.1 [a]	0.13 ± 0.02	+13.5 ± 0.6 [b]	30.2 ± 2.8 [d]
1:3	198.0 ± 26.0 [a]	0.12 ± 0.01	+13.0 ± 1.0 [b]	n.d.
1:3.25	pp	-	-	-
1:3.5	pp	-	-	-
1:4	pp	-	-	-

CSup: ultrapure chitosan; LBGS: sulfated locust bean gum; n.d.: not determined; PdI: polydispersity index; pp: precipitate

Formulations with a higher amount of LBGS (ratios ≥ 1:3.25, w/w) resulted in precipitation. Considering that a constant amount of CSup is used to produce all the formulations, the observed precipitation is possibly due to the presence of an excess of anionic charges, which neutralize CSup positive charges and, thus, reduce or eliminate electrostatic repulsion, leading to precipitation. For all the other tested mass ratios, a clear Tyndall effect was observed upon mixing the two polysaccharides, indicating the presence of colloidal particles. Nanoparticles were thus successfully obtained for mass ratios varying between 1:1 and 1:3. Surprisingly, the size of the particles did not present significant variations among the tested ratios, being in all cases of approximately 180 nm. The ratio 1:3 resulted in nanoparticles with an average size of 198 nm but the standard deviation increased 4-5 times (26 nm), which suggests the beginning of the destabilization of the process of nanoparticle formation, which is reinforced by the precipitation occurred in the following ratio (1:3.25, w/w). The absence of variations was not expected, as varying the amount of one of the polymers, and therefore the amount of charges, should result in different nanoparticle characteristics. The nanoparticles evidenced a very narrow PdI (around 0.1) and a positive zeta potential around +13 mV. As observed for the size, it was also unexpected that the zeta potential did not vary with the alteration of the mass ratios. This effect is better analyzed considering the charge ratios involved in each formulation. By dividing the charge of each repeating unit by its molar mass, a charge per mass ratio is obtained for each polymer. In a 1/*n* formulation of CSup/LBGS, the -/+ charge ratio is calculated by:

-/+ charge ratio = *n* . charge per mass (LBGS) / charge per mass (CSup)

Figure 4.1 demonstrates the influence of -/+ charge ratio on the zeta potential. As observed, the charge ratio varies between 0.30 and 0.91 without significant effect on the resulting zeta potential. This pattern is relatively similar to that observed in the nanoparticles presented in the previous chapter, when charge ratios vary without reaching a value around 1. In these CSup/LBGS nanoparticles, on reaching -/+ charge ratios of 0.98, 1.06 and 1.21 precipitation occurred. Although this behavior was unexpected, it has been reported in other works regarding polysaccharide nanoparticles produced by the same methodology (58, 59, 195, 238, 239).

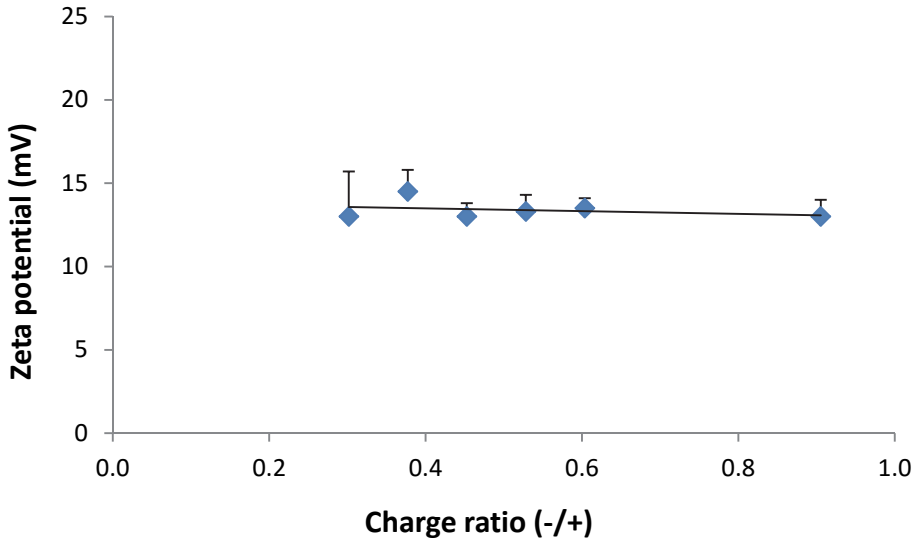

Figure 4.1 – Effect of charge ratio (-/+) on the zeta potential of CSup/LBGS nanoparticles.

It was previously demonstrated that the process leading to the assembly of polyelectrolyte complexes has two major steps: the rapid formation of molecular or primary complex particles, and a subsequent phase corresponding to the aggregation of primary particles to secondary particles. While the primary particles are held together by long-range electrostatic interactions, the formation of secondary particles involves short-range dispersive interactions (240, 241). In this case, considering the differences between the charge densities of the two polysaccharides (0.86 charges/monomer in CSup and 0.24 charges/monomer in LBGS), a very inefficient charge pairing should be expected. Therefore, and also regarding the differences in the molecular weights of the polysaccharides, in formulations 1:1 to 1:1.5, a reduced number of primary complexes should form. The poor charge neutralization should result in enhanced electrostatic repulsion between primary particles, leading to low dispersive attraction and smaller particle sizes, as well as to low yields. By increasing the amount of LBGS, towards the 1:2 formulation, a larger number of primary particles form, which should tend to aggregate in larger particles as the (-/+) charge ratio increases to 0.60. However, that was not the case, with all formulations presenting almost invariant particle sizes, which should mean that more particles formed; thus, the slight increase in yield observed in the latter formulation (241). The fact that all formulations present similar surface potentials of ~13 mV, seems to corroborate this hypothesis, as this potential should correspond to a repulsive electrostatic force overcoming the dispersive interactions and therefore preventing the particles from growing further. This behavior was observed in other works (238), normally associated to the use of CSup. Therefore, another possible explanation may reside in conformational

features of CS when the free base form is dissolved in acetic acid or when the hydrochloride salt is dissolved in water.

Taking into account the previous observations regarding the similarity of physicochemical characteristics and the suggested destabilization starting in formulation CSup/LBGS 1:3 (w/w), it was decided to determine the production yield of nanoparticles 1:1, 1:1.5 and 1:2 (w/w). While no significant differences were observed between the first two, with yields of 9-13%, the latter registered a much higher yield around 30% ($P < 0.05$). This is the trend that is usually observed (39, 195, 242, 243) and reflects the fact that, up to a certain limit, when increased amounts of LBGS are incorporated, the occurrence of electrostatic interactions is also increased, resulting in the formation of a higher number of nanoparticles (106).

In order to restrict the number of formulations for the subsequent tasks, and considering that the production yield was the most differentiating characteristic of the nanoparticles, it was decided to select the formulations CSup/LBGS 1:1.5 and 1:2 (w/w) for the rest of the studies. **Figure 4.2** displays the morphological characterization of representative nanoparticles (CSup/LBGS 1:2, w/w). This was performed by TEM and revealed a solid and compact structure, showing a tendency to exhibit a spherical-like shape.

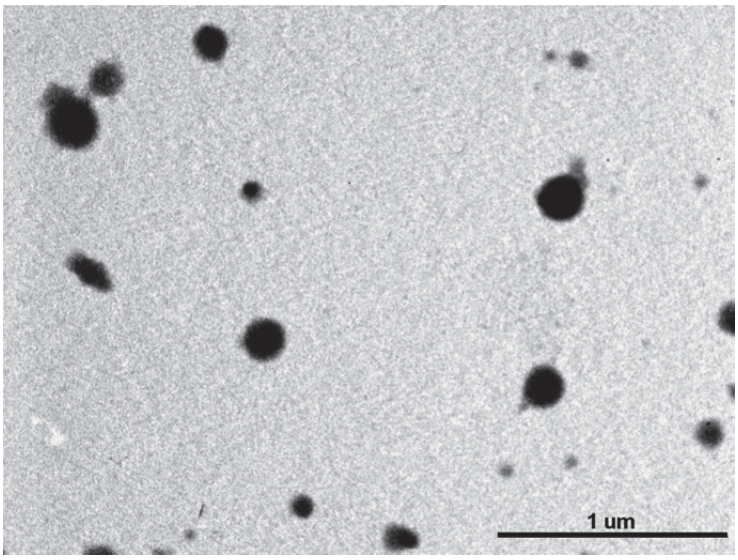

Figure 4.2 - TEM microphotograph of CSup/LBGS 1:2 (w/w) nanoparticles.

4.3.2. Characterization of loaded nanoparticles

Bearing in mind the main objective of proposing CSup/LBGS nanoparticles for oral vaccination, the first approach regarding the association of an antigen relied on using an immunogenic subcellular extract obtained from whole *Salmonella* Enteritidis cells (HE) (244, 245). After performing the *in vivo* studies, which results are reported in a subsequent section (section 4.3.4), the need to test soluble antigens was identified, in order to permit a more clear evaluation of the real adjuvant properties of the formulated nanoparticles. Therefore, in a second stage of the work the protein ovalbumin (OVA) was associated as model antigen. Additionally, as being one of the mostly used molecules for the antigen effect, it enables further comparisons with the literature. As pertinent information, the HE extracts are mainly composed of proteins (29%) and lipopolysaccharides (59%) (246). It is well reported in the literature that lipopolysaccharide fractions have great ability to generate immunological responses, since they are prototypical PAMP's (247). Therefore, taking into account that OVA is a protein, devoid of PAMP components, it is assumed as less immunogenic than HE.

4.3.2.1. HE-loaded CSup/LBGS

As said above, the first demonstration of the usefulness of the developed nanoparticles to act as adjuvants in a vaccination strategy relies on the determination of their ability to associate antigens. In order to verify this, different amounts of the bacterial HE antigens were tested and the resulting nanoparticles characterized. Departing from initial concentrations of 2%, 4% and 8% (w/w) of the total amount of the polymers, an effective and similar association was observed in all cases. In fact, the association efficiency varied within 29-36% (**Table 4.2**), independently of both the initial concentration of antigen and the formulation. These resulted in loading capacities up to 12%. Taking into account that HE is negatively charged when in the LBGS-HE solution, and also considering the high density of free amino groups present in the chitosan solution, it could be assumed that the main factor affecting HE association to the nanoparticles was an electrostatic interaction. This is in agreement with many other works reporting the association of protein-based macromolecules to nanoparticles produced by polyelectrolyte complexation (40, 106, 248, 249). In turn, although it could be expected that HE and LBGS might compete in their interaction with chitosan, the obtained results do not show an influence of LBGS content on HE association. This may be due to the fact that LBGS could also interact with HE by means of hydrophobic interactions, hydrogen bonding and other intermolecular forces

(242). The absence of a concentration-dependent effect regarding HE was also unexpected, although it has been observed in other works (39, 106).

Table 4.2 – Physicochemical characteristics, production yield and association efficiency of HE antigens in CSup/LBGS nanoparticles (mean ± SD; n ≥ 3). Different letters represent significant differences in each parameter, evaluated separately for each mass ratio ($P < 0.05$).

CSup/LBGS (w/w)	HE (%)	Size (nm)	PdI	Zeta potential (mV)	Production yield (%)	Association efficiency (%)	Loading capacity (%)
1:1.5	0	184.0 ± 4.1 [a]	0.09 ± 0.01	+13.0 ± 0.8 [e]	12.5 ± 3.9 [i]	-	-
	2	191.5 ± 7.8 [a]	0.11 ± 0.02	+10.0 ± 1.4 [f]	9.6 ± 6.3 [i]	31.2 ± 7.4 [k]	6.4 ± 1.5 [m]
	4	190.0 ± 11.3 [a]	0.10 ± 0.01	+10.0 ± 1.4 [f]	13.1 ± 3.8 [i]	29.0 ± 2.6 [k]	8.5 ± 0.8 [m]
	8	196.5 ± 2.1 [b]	0.08 ± 0.01	+9.5 ± 0.7 [f]	15.5 ± 0.0 [i]	25.3 ± 3.2 [k]	12.1 ± 1.5 [n]
1:2	0	183.0 ± 6.1 [c]	0.13 ± 0.02	+13.5 ± 0.6 [g]	30.2 ± 2.8 [j]	-	-
	2	192.0 ± 9.9 [c]	0.11 ± 0.00	+10.5 ± 0.7 [h]	28.5 ± 5.2 [j]	35.5 ± 9.7 [l]	2.4 ± 0.7 [o]
	4	193.0 ± 11.3 [c]	0.13 ± 0.02	+11.5 ± 0.7 [h]	29.6 ± 3.9 [j]	34.8 ± 3.3 [l]	4.5 ± 0.4 [p]
	8	202.5 ± 10.6 [d]	0.13 ± 0.03	+12.5 ± 0.7 [g]	30.1 ± 3.7 [j]	31.9 ± 4.0 [l]	7.8 ± 1.0 [q]

CSup: ultrapure chitosan; HE: antigenic extract from *Salmonella* Enteritidis; LBGS: sulfated locust bean gum; PdI: polydispersity index

Table 4.2 further displays the physicochemical characteristics of HE-loaded CSup/LBGS nanoparticles. The size of the particles was around 190-200 nm independently of the specific formulation and the amount of HE associated. When comparing with the corresponding unloaded nanoparticles, which had a size of 183-184 nm, no significant differences were generally observed. An exception was only observed when 8% HE was associated, for both formulations, with sizes reaching approximately 200 nm ($P < 0.05$), but this observation is considered to be devoid of physiological relevance. The PdI of the nanoparticles remained remarkably low after association of HE (around 0.1) and a very slight decrease of 2-3 mV in zeta potential was generally observed ($P < 0.05$). Regarding the latter, the only exception was for the formulation 1:2, again when 8% HE was associated (zeta potential of +12.5 mV), in which no significant variation was observed comparing with the equivalent unloaded nanoparticles. Regarding the yield of the process of nanoparticle production, it was also observed an absence of effect upon association of HE antigens, independently of the used concentration. Considering that size and zeta potential values remained approximately similar after the association of the antigen, the maintenance of the production yield is indicative of displacement of the polymers to permit the incorporation of the active molecule.

Taking into account the properties exhibited by HE-loaded nanoparticles, it was decided to select the formulation CSup/LBGS 1:2 with 8% of HE associated, to perform subsequent studies. This selection was driven by the presence of a higher theoretical amount of LBG and HE antigens. The morphological examination of this specific formulation was performed by TEM (**Figure 4.3**) and revealed the maintenance of the solid and compact structure of the unloaded nanoparticles, also showing a tendency to exhibit a spherical-like shape.

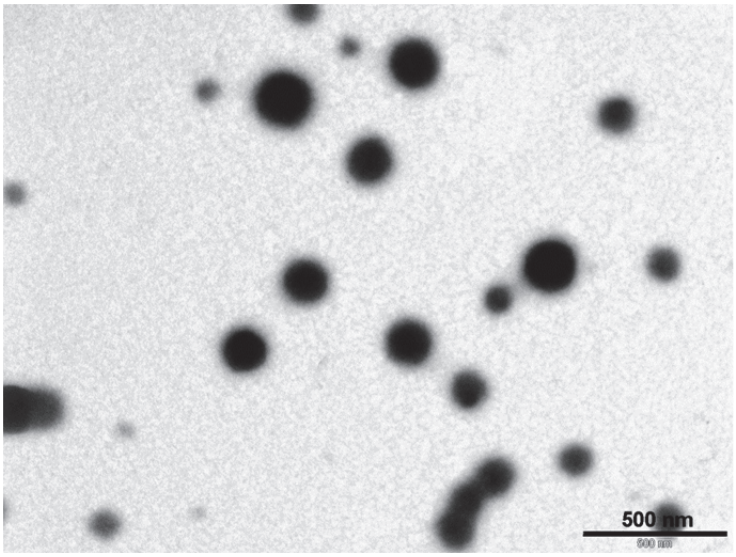

Figure 4.3 – TEM microphotograph of HE-loaded CSup/LBGS (1:2, w/w; 8% HE) nanoparticles.

As shown in **Table 4.2**, the developed HE-loaded CSup/LBGS nanoparticles evidence adequate physicochemical properties for the objective of oral delivery aimed at mucosal vaccination, with a size around 200 nm and a positive zeta potential. In fact, the size is small enough to permit an intimate contact with epithelial surfaces, which is maximal at 50–500 nm (20, 21). In turn, the positive zeta potential further potentiates the interaction with epithelia, as this is negatively charged and, thus, an electrostatic interaction is enabled. In summary, these characteristics are expected to provide a prolonged retention of nanoparticles close to epithelial surfaces, potentiating the uptake by M cells and/or antigen release.

4.3.2.2. OVA-loaded CSup/LBGS

As mentioned above, the need to associate a second antigen was identified and OVA was selected for this end. Considering that CSup/LBGS nanoparticles 1:2 (w/w) containing 8% HE had been previously selected for further studies, the production of OVA-loaded nanoparticles respected the same composition, in order to effectively evaluate the particle contribution as vaccination adjuvant. As stated in **Table 4.3**, OVA was successfully encapsulated with a similar efficiency as that for HE (26.4%), which resulted in a loading of 5.2%. Regarding the physicochemical characteristics of OVA-loaded nanoparticles, there are no statistically significant differences in size when comparing with unloaded particles, while a slight decrease of zeta potential around 4 mV was observed ($P < 0.05$).

The production yield registered a significant increase from 30% to 38% ($P < 0.05$). When a comparison with HE-loaded nanoparticles is performed, considering the corresponding formulation, it should be highlighted that OVA-loaded nanoparticles have a significantly lower size (179 nm vs 203 nm) and higher production yield (38% vs 30%) ($P < 0.05$). A significant difference was also found for zeta potential, but only decreasing around 3 mV ($P < 0.05$).

Naturally, the literature does not report similar nanoparticles, as LBG is being proposed for the first time herein, but chitosan-based nanoparticles have been suggested many times regarding oral vaccination (250-257). Occasionally, ovalbumin was the tested antigen (252), resulting in nanoparticle size around 300 nm and a strong positive zeta potential (+43 mV). As said above, the positive zeta potential is a desirable characteristic to mediate and favor the interaction with the epithelium. In our work, the proposed nanoparticles present a lower zeta potential, but also a lower size, which further benefits this interaction, due to an increased surface area.

Table 4.3 – Physicochemical characteristics, production yield end association efficiency of OVA in CSup/LBGS nanoparticles (mean ± SD; n ≥ 3). Different letters represent significant differences in each parameter ($P < 0.05$).

CSup/LBGS (w/w)	OVA (%)	Size (nm)	PdI	Zeta potential (mV)	Production yield (%)	Association efficiency (%)	Loading capacity (%)
1:2	0	183.0 ± 6.1 [a]	0.13 ± 0.02	+13.5 ± 0.6 [b]	30.2 ± 2.8 [d]	-	-
	8	178.6 ± 6.8 [a]	0.13 ± 0.02	+9.0 ± 1.0 [c]	37.9 ± 4.1 [e]	26.4 ± 3.8	5.2 ± 0.7

CSup: ultrapure chitosan; LBGS: sulfated locust bean gum; OVA: ovalbumin; PdI: polydispersity index

4.3.3. *In vitro* evaluation of Locust Bean Gum-based nanoparticles

4.3.3.1. Evaluation of the structural integrity and antigenicity of the loaded antigens

As detailed above, the association of either HE or OVA into nanoparticles was performed by means of a mild ionic interaction. Along with the determination of the ability of the developed nanoparticles to associate the selected antigens, it is also of utmost importance to ensure that the particles and the procedure used for their production enable the preservation of the structural integrity and antigenicity of the encapsulated molecules. SDS-PAGE analysis followed by immunoblotting was the method used to perform this evaluation.

The results of this evaluation are depicted in **Figure 4.4** and **Figure 4.5**, for HE and OVA, respectively. Regarding HE, SDS-PAGE results shown in **Figure 4.4-b** demonstrate that the procedure used for HE entrapment did not affect the structural integrity of the molecules, as no additional fragments are observed in the HE released from nanoparticles (lane 2) when compared with the control HE solution (lane 1).

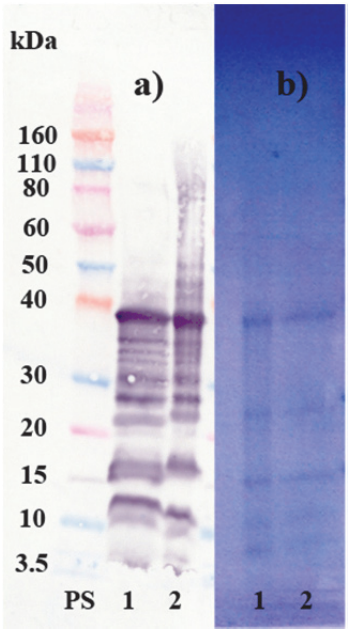

Figure 4.4 – Immunoblot (a) and SDS-PAGE (b) analyses of free HE (1) and HE released from HE-loaded CSup/LBGS nanoparticles (2) (PS: standard proteins).

Moreover, the immunoblot membrane shown in **Figure 4.4-a** demonstrated that the HE-specific antibodies from sera of a pool of mice experimentally immunized with HE, recognized the antigen epitopes in a similar way as for the control HE solution. This confirms that the antigenicity of the HE antigenic complex was not altered after the entrapment into the nanoparticles.

Concerning the association of OVA, similar results were observed. As demonstrated in **Figure 4.5**, the SDS-PAGE of OVA released from nanoparticles (**Figure 4.5-a**) showed identical bands for the entrapped (lane 2) and native OVA (lane 1) and there were no additional bands indicating the presence of aggregates or fragments greater or less than 45K (molecular weight of OVA). Hence, the data suggest that the structural integrity of ovalbumin was not significantly affected by the entrapment procedure. The antigenicity of OVA was also not modified after association, as the immunoblot bands from OVA solution (**Figure 4.5-b**, lane 1) and OVA released from nanoparticles (**Figure 4.5-b**, lane 2) were identical.

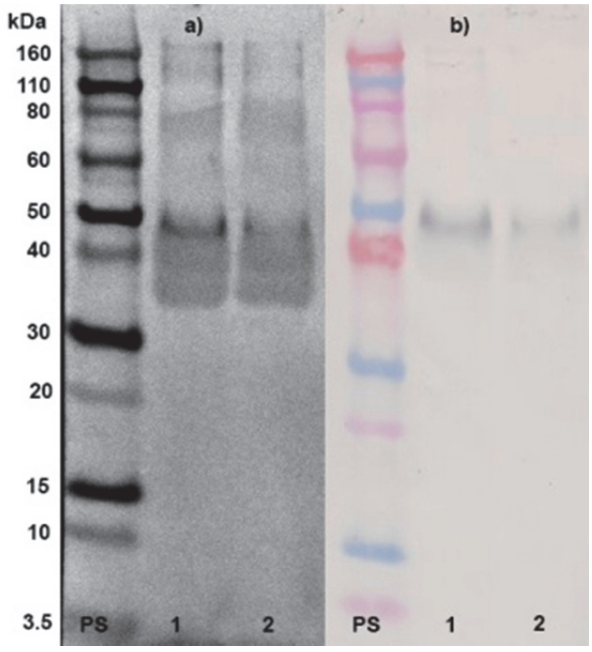

Figure 4.5 – SDS-PAGE (a) and immunoblot (b) analyses of free OVA (1) and OVA released from OVA-loaded CSup/LBGS nanoparticles (2) (PS: standard proteins).

Altogether, these results indicate the adequacy of polyelectrolyte complexation as a method to provide the association of antigens in polymeric nanoparticles, reinforcing results already available in the literature. In fact, several works reporting the preparation of

nanoparticles using methodologies involving electrostatic interaction and using materials such as chitosan, its derivatives and alginate, have demonstrated to provide protection to various model antigens including inactivated influenza virus (258), bovine serum albumin (259), tetanus toxoid (260) and diphtheria toxoid (261).

4.3.3.2. Stability evaluation on storage

Nanoparticles are usually formulated as aqueous suspensions, as in this work, and one of the most reported limitations of these systems relies on their tendency for aggregation. Both physical (aggregation/particle fusion) and chemical issues (hydrolysis of polymer and chemical reactivity) are known to play significant roles in this context, thus contributing for the low stability that is frequently reported for colloidal drug carriers (262-264). The main reason for this phenomenon is the higher attractive potential existing between two particles coming into contact, when comparing with the kinetic energy that could induce their separation (265). The natural tendency for aggregation during the storage period is, therefore, one of the most important limitations preventing nanoparticle applications (266, 267). In this regard, the use of charged nanoparticles might prevent aggregation and has been proposed as strategy to increase nanoparticle stability. Although in this work nanoparticles do not exhibit a strong surface charge as compared with other chitosan-based nanoparticle formulations (56, 57, 59, 195, 268), there is still a positive surface charge that might help on this effect.

In order to study the nanoparticle behavior on storage, the size and zeta potential of HE-loaded and unloaded CSup/LBGS nanoparticles in the aqueous suspension were monitored along time. The rationale of conducting this assay in water was the interest in obtaining information on nanoparticle stability in the resuspension medium. Several formulations were evaluated for both HE-loaded and unloaded nanoparticles and similar behaviors were observed. **Figure 4.6** represent the results obtained for the formulation 1:2 (w/w) but are representative of the observations performed for the other formulations (1:1 and 1:1.5). It was observed that, both formulations perfectly maintain the initial physicochemical characteristics when stored at 4 ºC, no alterations being observed either on size or zeta potential for up to 6 months. These results demonstrate the physical stability of the developed nanoparticles, suggesting that the zeta potential is sufficiently high to induce repulsion on nanoparticles. Chitosan-based nanoparticles have been reported to exhibit physicochemical stability in similar time intervals (59, 195, 269, 270).

However, a direct comparison with locust bean gum based nanoparticles is not possible - as no such system was reported before.

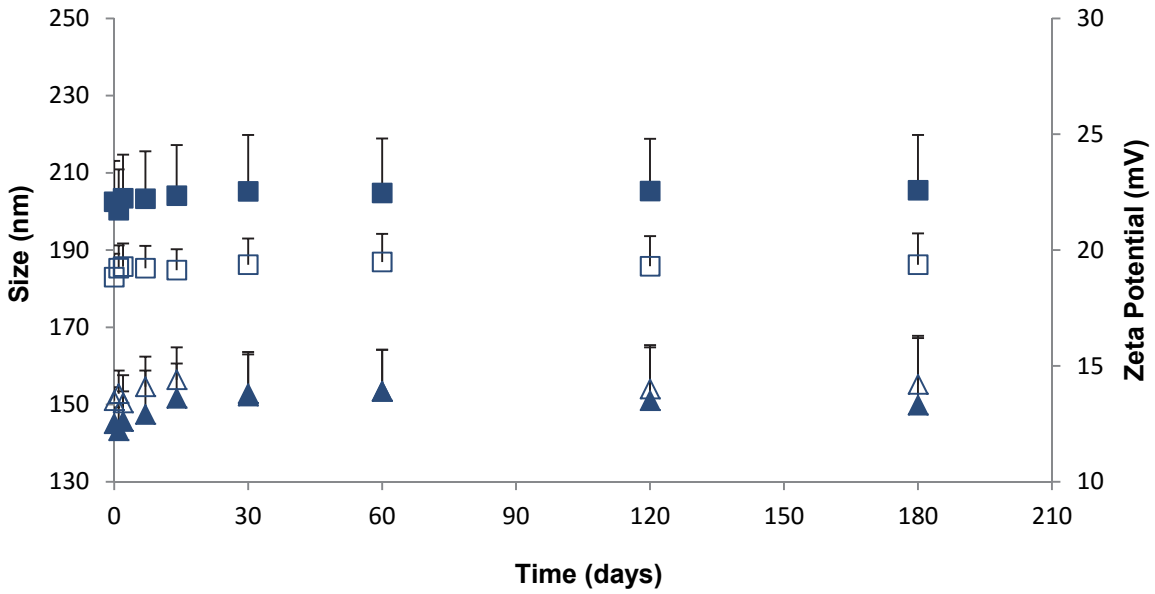

Figure 4.6 – Size (square marks) and zeta potential (triangular marks) evolution as function of time upon storage at 4 ºC of CSup/LBGS 1:2 (w/w) unloaded nanoparticles (empty marks) and HE-loaded nanoparticles (8% w/w; filled marks); (mean ± SD, n ≥ 3).

4.3.3.3. *In vitro* release in SGF and SIF

Considering the design of these nanoparticles for an oral vaccination approach, it is adequate to determine the release of the encapsulated antigens in media simulating both the gastric (SGF) and intestinal (SIF) environments. In this association approach it is important that the nanoparticles not only provide protection to the antigens regarding the harsh conditions of the gastric medium, but also prevent the release of the antigens, in order to maximize the antigen internalization by the M cells mediated by the particle.

Figure 4.7 shows the release profile of HE and OVA in SGF and SIF. As can be observed, HE is considered to not present significant release in any of the tested media. In fact, in SGF it releases a maximum amount of 7.5% in 2 h, while releasing 4.3% in SIF after 4 h. Moreover, although it might not be relevant from a physiological point of view, HE release at the end of 24 h was 21.6% ± 2.0 and 13.2% ± 4.8 in SGF and SIF, respectively. In turn, OVA presented a rather different behavior. In this case, the release in the SGF was of 45.0% at the end of 2 h, and 3.0% in SIF at the end of 4 h.

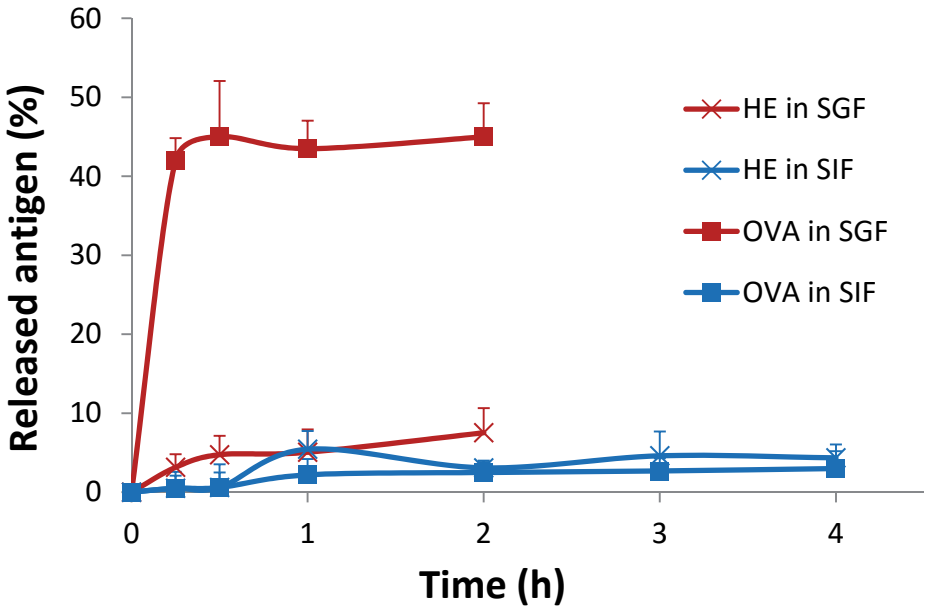

Figure 4.7 – Antigen released overtime from CSup/LBGS nanoparticles in simulated gastric fluid (SGF) and simulated intestinal fluid (SIF), at 37 ºC (mean ± SD; n ≥ 3).

Considering what was stated above, in the case of OVA-loaded nanoparticles, it could be assumed that a high amount of encapsulated OVA releases in the harsh conditions of gastric environment, affecting the biological activity of the molecule. This difference observed for HE-loaded and OVA-loaded nanoparticles could be hypothetically explained by a greater association of HE into the particle, contrasting with a substantial adsorption of OVA onto its surface. Although the determined physicochemical properties do not confirm these effects, it should be reminded that a very small amount of protein is being associated (theoretical load of 8% (w/w)). OVA release at the end of 24 h was 75.5% ± 13.1 and 9.8% ± 1.5 in SGF and SIF, respectively. It is remarkable that an insignificant amount of antigen was observed to release in SIF in both cases. This means that a great amount of antigen remains associated to the nanoparticles until they reach the contact with the Peyer patches, where the nanoparticles are expected to have a favored contact with the M cells, which will potentiate the immunological response.

Despite the existence of many works proposing the application of nanoparticles in oral immunization, a limited number of works reports the use of either HE or OVA as model antigens. Works reporting release studies are even narrower and, from those, none involves polyelectrolyte complexation or ionic gelation. One sole work studied HE release, registering 10% release in SGF (after 30 min) and 12% in SIF (after 3 h) from Gantrez®

AN nanoparticles (271), values slightly higher than those obtained in our study. The release of OVA was studied from poly(d,l-lactide-co-glycolide) (PLGA)-based nanoparticles. Pegylated PLGA-based nanoparticles which were surface decorated with RGD molecules to target M cells (OVA association efficiency of 30 – 50%) registered 5% release after 2 h of incubation in gastric medium (HCl 0.1 M) and 10 – 20% in intestinal medium (154). In turn, PLGA-lipid nanoparticles conjugated with ulex europaeus agglutinin-1 and containing the Toll-like receptor agonist monophosphoryl lipid A (95% OVA association efficiency), released 17% of the protein after 2 h incubation in gastric acid medium (0.1 M HCl) and 3 h in intestinal medium (PBS pH 6.8) (272). Comparatively, our work registered higher release of this protein after cumulative contact with the two media, but we expect that the remaining amount suffices for an adequate immunization effect.

While no studies report the release of OVA as model antigen from chitosan nanoparticles proposed for oral immunization, there are some works on chitosan-based microparticles. The results are however uneven, certainly as a result of different methods of preparation of microparticles and the use of diverse chitosan molecules. In fact, different works reported either immediate release of OVA in SGF (273), or only 50% in 2 h (274). The latter behavior is similar to that registered in our work, where 45% released in 2 h. The results regarding the release in SIF or PBS pH 7.3 were more coincident, where a maximum release of 10% - 20% was determined after 1 h (273) (159, 274). This is not far from the 3% registered in our work at the end of 4 h.

4.3.3.4. Safety evaluation of unloaded nanoparticles

Assessing the biocompatibility of drug delivery systems is a major issue in designing drug carriers (52, 197, 198). Although the toxic effects of formulations can only be accurately determined by *in vivo* assays, several *in vitro* tests can be performed in adequate cell lines to give the first indications on the systems cytotoxicity (197, 201). Additionally, current international guidelines indicate the need to contextualize biocompatibility with a specific route of administration and dose of the material (198). Moreover, the materials composing the matrix of the particles and the particle itself should be regarded as different entities. In line with this assumption, these should be evaluated separately, since the particle structure, among others, might affect the final toxicological behavior (198, 228). According to the guidelines issued by the International Organization for Standardization (ISO), testing biocompatibility implies the performance of a complete set of assays,

addressing at first cellular morphology, membrane integrity and metabolic efficiency, among other tests (197, 199-201). In this work we performed two of the most used assays to test the cytotoxicity of materials, namely the metabolic assay MTT and the membrane integrity assay based on LDH release. The MTT assay assesses cell metabolic efficiency, relying on the evaluation of enzymatic function. To do so, after the exposure to the matrix materials used for the nanoparticles production or the nanoparticles themselves, cells are incubated with yellow tetrazolium (MTT) salts which are reduced to purple-blue formazan crystals by active mitochondrial dehydrogenases (197). In this manner, a higher concentration of the formazan dye corresponds to a higher amount of metabolically active cells, which is usually interpreted as higher cell viability. The LDH release assay provides a mean to determine the amount of LDH in cell culture medium upon exposure to potentially toxic substances. As LDH is a cytoplasmic enzyme, its presence in the cell culture medium is an indicator of irreversible cell death due to cell membrane damage (202, 203). The assay thus evaluates cell membrane integrity and complements the results obtained by the MTT assay.

In this work, Caco-2 cells were used to evaluate the toxicological profile of CSup, LBGS and the nanoparticles resulting from the combination of these polymers. **Figure 4.8** and **Figure 4.9** represent the Caco-2 cell viability obtained after exposure to the mentioned materials at different concentrations, for a period of 3 h and 24 h. The overall observation of the results reveals a mild effect on cell viability from both the polymers and nanoparticles, considered to be devoid of biological relevance. In fact, all samples resulted in viabilities above 70% after 3 h or 24 h of exposure, when tested at concentrations varying within 0.1 and 1.0 mg/mL. At 3 h cell viability remained above 88% in all cases (**Figure 4.8**), the lower values being observed for the raw material LBGS, although not to a statistically significant level. As observed in the previous chapter for LBG and LBG derivatives, prolonging the exposure until 24 h resulted in slight alterations (**Figure 4.9**). These were actually considered very mild, as cell viability did not decrease below 70% in any case. This value is that considered by ISO 10993-5 (201) as the level below which a toxic effect occurs. The only observation deserving a mention is that the exposure to the highest concentration tested (1.0 mg/mL) of CSup and the nanoparticle formulation, decreased cell viability to around 70% and 90%, respectively ($P < 0.05$).

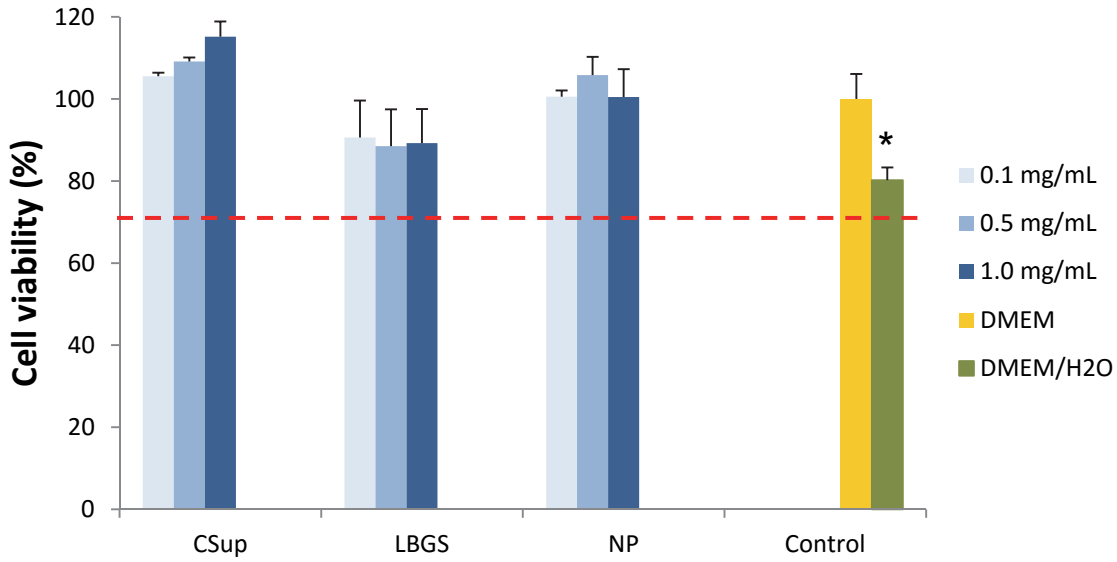

Figure 4.8 – Caco-2 cell viability measured by the MTT assay after 3 h exposure to increasing concentrations of Chitosan (CSup), sulfate Locust Bean Gum (LBGS) derivative and CSup/LBGS nanoparticles (NP). Data represent mean ± SEM (n ≥ 3, six replicates per experiment at each concentration). Dashed line indicates 70%. * $P < 0.05$ compared with DMEM.

A control was used that consists in a mixture of DMEM and H_2O in the same ratio used for the samples, taking into account that both the raw materials and the nanoparticles were solubilized/suspended in water and diluted with cell culture medium prior to incubation with the cells. This enables a real evaluation on the contribution of these materials on the final cell viability. As observed in **Figure 4.8** and **Figure 4.9**, the cell viability induced by this control varied between 80 and 72% when tested at 3 h and 24 h. While at 3 h CSup and nanoparticles comparatively induced higher cell viability (100% or more), after 24 h the incubation with 1.0 mg/mL of CSup was found to decrease cell viability (71%) to a level comparable to that of this control (DMEM + H_2O). Remarkably, focusing on the concentration of 1.0 mg/mL, the cell viability obtained by exposure to the nanoparticles was higher than that registered for CSup assessed individually and the control of DMEM + H_2O ($P < 0.05$).

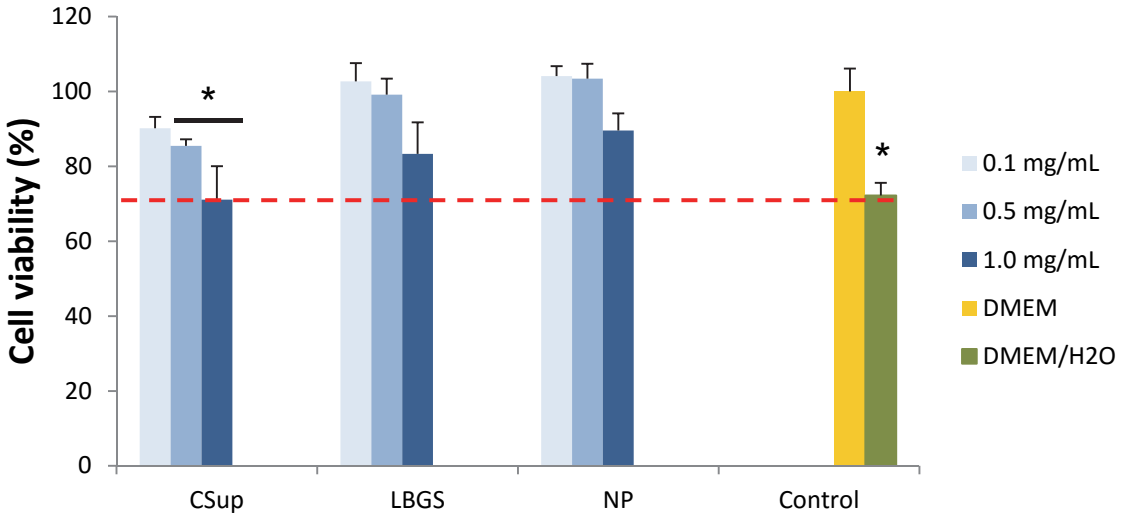

Figure 4.9 – Caco-2 cell viability measured by the MTT assay after 24 h exposure to increasing concentrations of Chitosan (CSup), sulfate Locust Bean Gum (LBGS) derivative and CSup/LBGS nanoparticles (NP). Data represent mean ± SEM (n ≥ 3, six replicates per experiment at each concentration). Dashed line indicates 70%. * $P < 0.05$ compared with DMEM.

LBG-based nanoparticles are now being reported for the first time. Therefore, the literature does not report any information regarding the cytotoxic effect of the particles, hindering the establishment of any comparison. In contrast, chitosan-based nanoparticles have been reported for a long time. As chitosan is one of the most used polymers in drug delivery, nanocarriers other than nanoparticles have been proposed, such as nanocapsules and nanoemulsions, for instance. This diversity affects viability results (108), but even when similar carriers are at play, it is frequently difficult to establish valid comparisons taking into account the large variety of chitosan molecules (chitosan base/salt(s), molecular weight, deacetylation degree, etc.) which is also known to have a role on cell viability (275). Notwithstanding these limitations, the general outcome regarding chitosan-based nanoparticles is a very mild effect on Caco-2 cells viability. Attempting to perform a direct and accurate comparison, other works assessing a nanoparticle concentration of 1.0 mg/mL reported similar results to those found in this work, both at 3 h (276) and 24 h (277, 278).

As mentioned above, the quantification of LDH released by the cells provides a complementary indication on the cytotoxicity of materials to which the cells were exposed to. If the materials affect the integrity of cell membrane, the leaking of this cytoplasmic enzyme occurs and its quantification is enabled. The loss of intracellular LDH and its release to the culture medium is therefore an indicator of irreversible cell death due to cell

membrane damage (202, 203). In this study, the amount of LDH released by Caco-2 cells exposed to CSup/LBGS nanoparticles was determined, using as control both the incubation with cell culture medium (negative control of cell death) and the exposure to a lysis buffer (positive control of cell death, assumed as 100%). The latter corresponds to the maximum amount of cytoplasmic enzyme that can be released, while the former is the minimum. As observed in **Figure 4.10**, the exposure to the raw materials CSup and LBGS induced the release of an amount of LDH (around 25%) that is comparable to that of the negative control, as no statistically significant differences were detected. On the contrary, the contact with CSup/LBGS nanoparticles resulted in an unexpected increased level of LDH release (43%; $P < 0.05$), which is indicative of cytotoxicity.

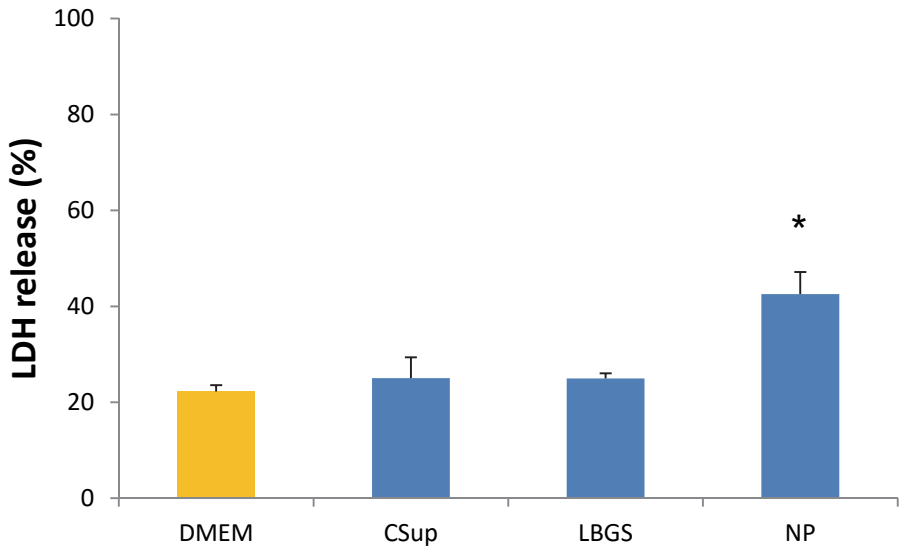

Figure 4.10 – Caco-2 cell viability measured by the LDH release assay after 24 h exposure to 1 mg/mL solutions of Chitosan (CSup), sulfate Locust Bean Gum (LBGS) derivative and CSup/LBGS nanoparticles (NP). Data represent mean ± SEM (n ≥ 3, three replicates per experiment). * $P < 0.05$ compared with DMEM.

If a direct correlation between LDH release and cell death is assumed, the contact with the nanoparticles results in approximately 60% cell viability, comparing with the 80% elicited by DMEM. Surprisingly, this does not correspond with the observations resulting from the MTT assay, in which a cell viability of 90% was observed for this condition. One possible explanation is that these nanoparticles act as metabolic enhancers, thus although with a lower number of available cells (as indicated by the LDH assay), MTT conversion into formazan is accelerated, resulting in the overestimation of the cell viability.

This difference in the results of the two assays reinforces the need to perform various and different tests to conclude on the cytotoxic profile of nanoparticles.

4.3.4. *In vivo* evaluation of the immune response in BALB/c mice

After verifying the ability of LBG derivatives to produce nanoparticles with capacity to associate antigens of interest and evaluating the cytotoxicity of the nanoparticles in an intestinal model, an *in vivo* assay was designed and setup to evaluate the adjuvant effect of the particles towards an immunization strategy. Two different model antigens were used, HE and OVA, and the immunization experiments performed with each antigen were conducted in different laboratories, applying different methodologies for the analysis of results. In the former (HE) a serum dilution was selected and the O.D. for each animal was determined, the data being presented as mean ± SEM. In the latter (OVA), a pool with the samples of different animals was used and data presented as log2 titers.

4.3.4.1. HE-loaded CSup/LBGS nanoparticles

The immunization of mice was performed by either oral or subcutaneous route, in order to permit a comparison of effects. Serum and faeces from the mice were collected before the immunization and at weeks 1-5 post immunization. The collection of both types of samples enables the determination of immune responses at both the systemic (IgG1 and IgG2a) and mucosal (IgA) levels. The results obtained upon oral immunization are shown in **Figure 4.11**. The transversal observation is that, as expected, unloaded particles did not induce any type of immune response. Concerning the systemic antibody response (**Figure 4.11 – A and B**) no statistical differences were observed between the groups corresponding to free HE (which is the control) and the NP-HE groups. Moreover, the results also show that, five weeks after immunization, a similar Th1/Th2-mediated antibody response for both formulations was elicited. Regarding this, it is important to refer that the literature reports that to achieve a protective response against *Salmonella* Enteritidis infection, a balance between antibody response and cellular mediated immune response is demanded (279, 280). In this way, a balance between Th1 and Th2 type responses is required, and *Salmonella* attenuated vaccines are reported to normally induce Th1 type responses, being less effective at inducing Th2 type responses (281-283). In this study, the nanoparticle formulation of HE (NP-HE) induced the required balanced Th1/Th2 response since the beginning of the study, which can be explained by

the presence of mannose groups, as was suggested in a study performed with mannosylated nanoparticles (120, 284). In that work it was verified that mannosylated nanoparticles induced a more balanced Th1/Th2 response comparing with non-mannosylated nanoparticles, an effect justified by the authors to be due to the high tropism of mannosylated particles for uptake by PPs rich in APCs (271). In our work, the presence of mannose groups in LBG may possibly mediate a stronger interaction of LBG nanoparticles with the M cells of PPs, contributing to the observed balance in the Th1/Th2 response.

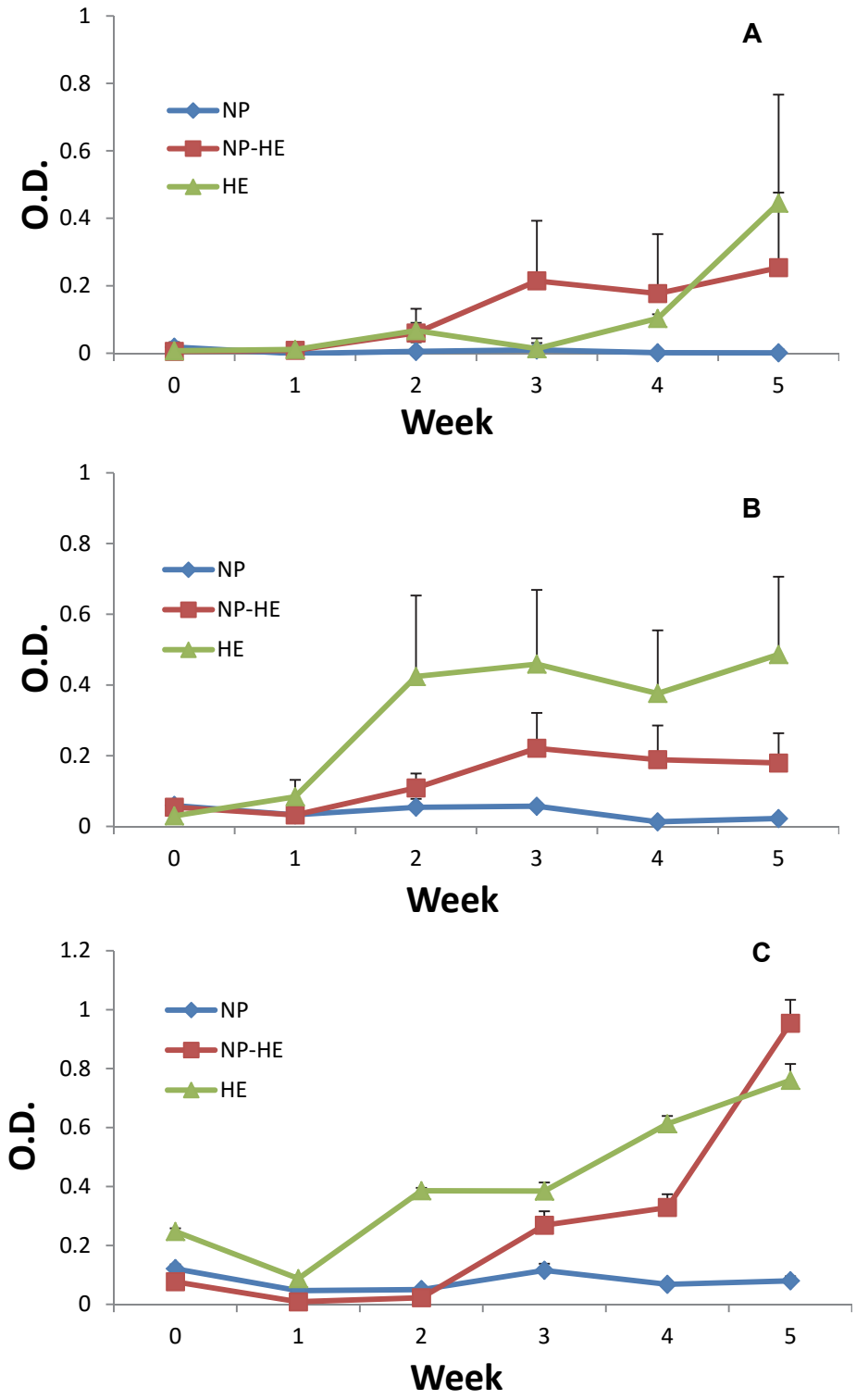

Figure 4.11 – Immunogenicity of HE after oral administration in mice. Serum A) IgG1 and B) IgG2a systemic response, and C) IgA mucosal response after oral immunization of 5 female BALB/c mice with 200 µg of HE solution (HE), 200 µg of encapsulated HE (NP-HE) and the corresponding mass of blank nanoparticles (NP). In the HE group the results of one mouse were rejected due to the high initial absorbance (week 0) (mean ± SEM; n ≥ 4).

The mucosal antibody response (**Figure 4.11 – C**) was also determined and, between weeks 2 and 4, it is observed a higher response from the group immunized with free HE compared with the NP-HE group ($P < 0.05$). Five weeks after immunization a shift is observed, with the NP-HE group presenting a higher response than the HE group ($P < 0.05$).

When the formulations were administered via the subcutaneous route an antibody response profile was elicited for HE and NP-HE groups (**Figure 4.12**). It was also observed that both groups elicited identical Th1/Th2 antibody immune responses from the first week on (**Figure 4.12 – A and B**).

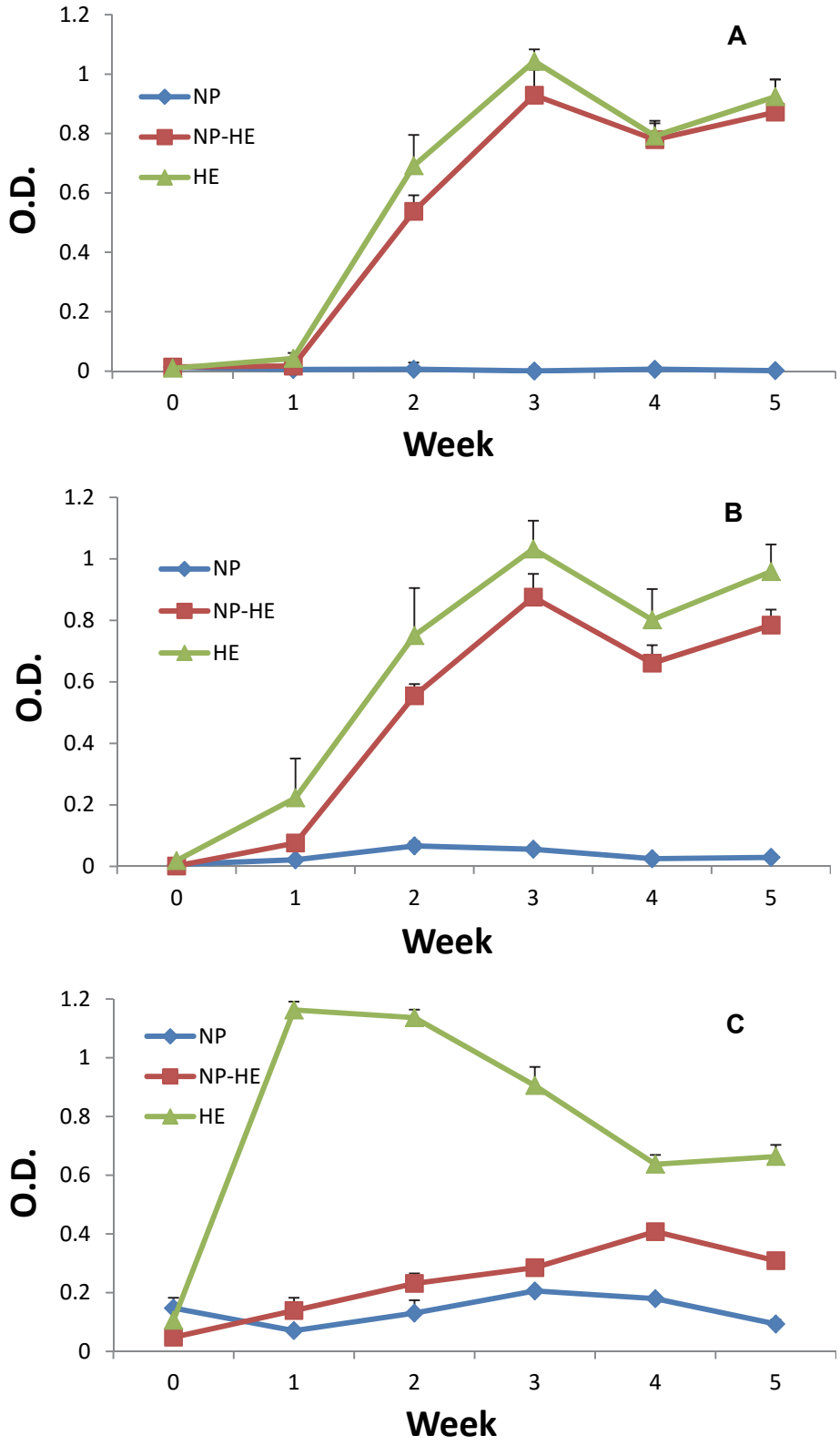

Figure 4.12 – Immunogenicity of HE after S.C. administration in mice. Serum A) IgG1 and B) IgG2a systemic response, and C) IgA mucosal response after S.C. immunization of 5 female BALB/c mice with 40 μg of HE solution (HE), 40 μg of encapsulated HE (NP-HE) and the corresponding mass of blank nanoparticles (NP) (mean ± SEM; n = 5).

However, free HE induced a much higher IgA response than NP-HE ($P < 0.05$), particularly until week 3 (**Figure 4.12 – C**). It could be argued that free HE is immediately available to induce a mucosal response, comparing with HE encapsulated into nanoparticles. Similarly to what was observed for the oral route, unloaded nanoparticles did not produce an immune response.

A relevant observation regarding the obtained results relies on the confirmation of the mildness of the nanoparticle production method, as the results indicate that the association process did not alter the immunogenicity of HE antigens. Nevertheless, although in fact no differences were generally observed to a statistically significant level, the trend indicates that free HE has a more favorable performance, when comparing with encapsulated antigens. Overall, the results suggest that HE antigens are possibly too robust and capable of inducing a strong immune response when administered in free form, thus not potentiating the observation of an adjuvant effect by the nanoparticles. This fact may be explained by the particulate nature of HE (liposome-like), and the high content of LPS in the HE extract. It is known that LPS is recognized by TLR-4 (150). Considering the hypothesis that the majority of the HE antigens in the nanoparticle formulation is entrapped into the matrix, the recognition by DCs will be preferably made by the mannose receptor, which is a C-type lectin receptor (152). It is reported that the uptake of antigens by C-type lectin receptors does not necessarily result in the induction of potent effector T-cells, although it facilitates the antigen-presentation capacity of DCs. Moreover, uptake of antigen by C-type lectin receptors without any TLR binding may induce antigen-specific tolerance. In contrast, TLR binding usually leads to DCs maturation and activation resulting in a robust activation of immune responses and the induction of effector T-cells (285).

It seems, thus, that the presence of mannose units in LBG nanoparticles, potentially recognized by the M cells and expected to improve the immune response, was not as good as the effect of the particulate antigen itself. Therefore, a need was identified to select and test a second antigen. For this effect, the same formulation of nanoparticles was associated with OVA and administered under the same protocol.

4.3.4.2. OVA-loaded CSup/LBGS nanoparticles

In order to evaluate the effect of OVA-loaded nanoparticles, these were administered by oral or subcutaneous routes, as was performed for HE-loaded nanoparticles. Taking into account the results described above for the unloaded particles, it was considered

unnecessary to include a group of animals immunized with unloaded particles. Therefore, only two groups were established, corresponding to OVA-loaded nanoparticles and free OVA, as a control. Similarly to the previous assay, serum and faeces from the mice were collected before the immunization and at weeks 1-6 post immunization.

Figure 4.13 and **Figure 4.14** show the serum titers of IgG1 and IgG2a (systemic response), and IgA (mucosal response) after an oral or subcutaneous immunization of mice by a single dose of OVA-loaded nanoparticles or free OVA. Overall, it is observed the adjuvant effect of nanoparticle formulations compared to free OVA in both routes. Focusing on the oral immunization (**Figure 4.13**), the elicited IgG1 specific response (Th2) was significant after OVA immunization, either free or encapsulated. Nanoparticles did not improve the effect of OVA regarding Th2 activation (IgG1, **Figure 4.13 – A**), but, however, a strong improvement was observed regarding Th1 activation (IgG2a, **Figure 4.13 – B**), as the respective area under the curve (AUC) was five times higher than that determined for free OVA. Intestinal immune system has a predisposition towards Th2 cell responses since antigen presentation by DCs from PPs are characterized by the production of IL-4, IL-6, and IL-10, which inhibit a Th1 response (286). It is also important to refer that soluble antigens usually elicit high levels of IgG1 antibodies (Th2 response), but very low levels of IgG2a (Th1 response) (287). Therefore, under these circumstances, the role of the adjuvant becomes critical in order to achieve a more balanced Th1/Th2 response. A similar positive effect of association was apparent regarding the mucosal response (IgA), as shown in **Figure 4.13 – C**. In this respect, OVA-loaded nanoparticles registered a 3-fold higher AUC when comparing with free OVA.

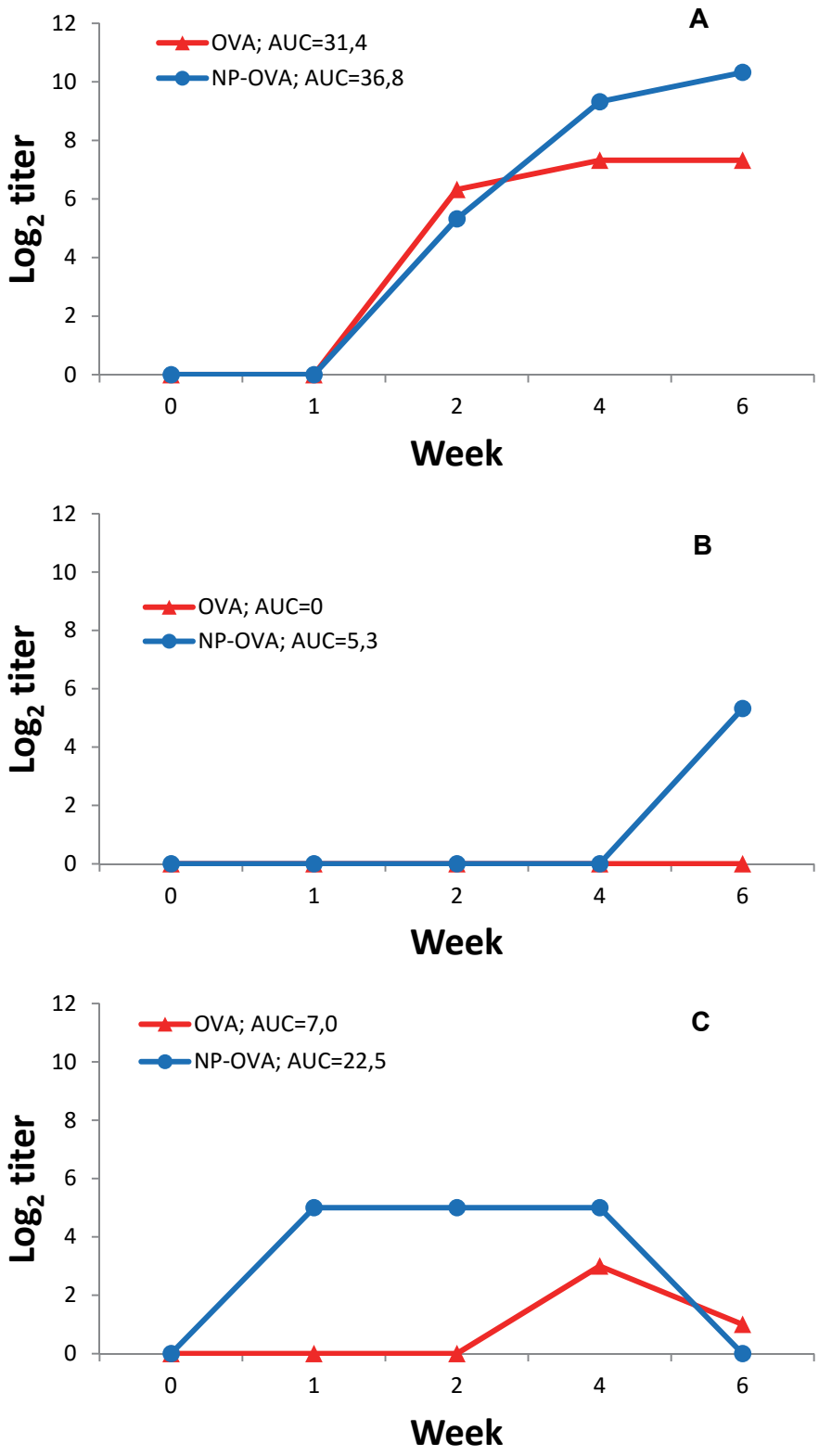

Figure 4.13 – Immunogenicity of OVA after oral administration in mice. Serum anti-OVA A) IgG1; B) IgG2a and C) faecal anti-OVA IgA response in BALB/c mice (n = 6) after oral immunization with 100 µg of OVA solution (OVA) or 100 µg of encapsulated OVA (NP-OVA). Antibody titers were determined in pooled serum samples at days 0, 7, 14, 21 and 28 post-administration.

When considering the determined AUC, a comparable mucosal response was elicited when the formulation was administered by subcutaneous route (**Figure 4.14 – C**). However, the pattern registered for the responses was markedly different. In fact, while the oral immunization induced a response that was detected from week one, the response obtained upon subcutaneous immunization was only observed starting from week two to four. In turn, the subcutaneous administration of nanoencapsulated OVA showed a similar activation of Th2 (IgG1, **Figure 4.14 – A**) and Th1 (IgG2a, **Figure 4.14 – B**) to that described for free OVA.

After oral immunization, OVA-loaded nanoparticles showed a predominant Th2 response compared to the slightly elicited Th1 one (AUC_{Th2} was seven times higher than AUC_{Th1}), consistent with results obtained by others (252, 284, 288-290). On the contrary, subcutaneous immunization with OVA-loaded nanoparticles elicited a more balanced Th1 and Th2 response. In order to perform a semi-quantitative comparison between the nanoparticle formulation and the free OVA, the AUC of the titers representing the systemic immune response (AUC_{Th1}, AUC_{Th2}) were measured and summed. Regarding the oral immunization, an increase of 34% in the total AUC was accounted for the encapsulated OVA. In turn, this association only induced a 13% increase in the response after subcutaneous immunization. This is possibly justified by the presence of mannose units in LBG nanoparticles, potentiating a stronger interaction with M cells and the mediation of a stronger immune response when the nanoparticles are administered by the oral route.

The mucosal IgA antibodies obtained after oral immunization with OVA-loaded nanoparticles were higher than after subcutaneous administration. This phenomenon may be related to the effective uptake of nanoparticles by gut Peyer's patches, obviously only possible after oral delivery, and the passage of the particulate system to lymphocytes causing an effective generation of mucosal IgA. However, it should be taken into account that a 5-fold higher dose of antigen was administered by oral route.

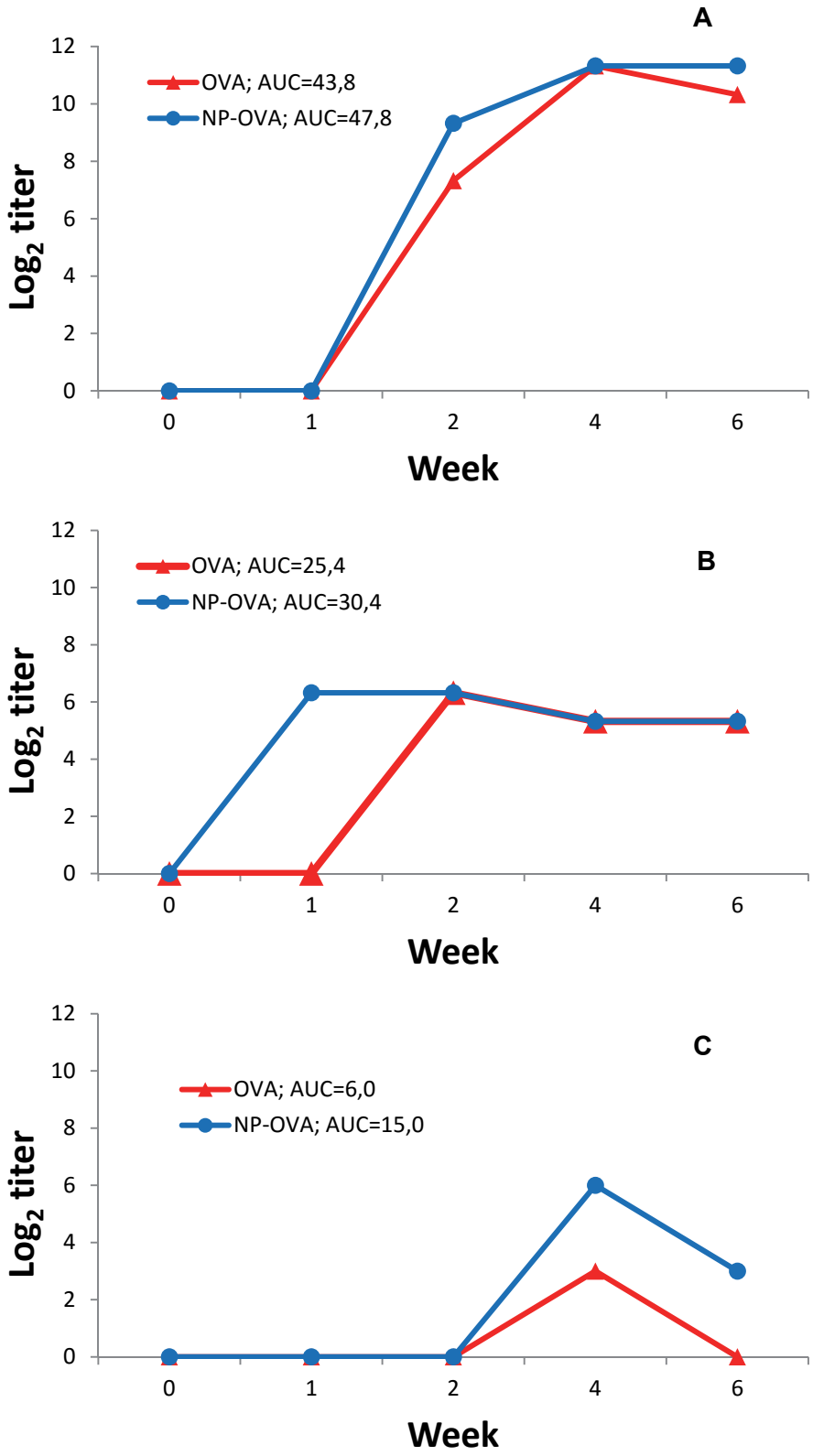

Figure 4.14 – Immunogenicity of OVA after S.C. administration in mice. Serum anti-OVA A) IgG1; B) IgG2a and C) faecal anti-OVA IgA response in BALB/c mice (n = 6) after S.C. immunization with 20 µg of OVA solution (OVA) or 20 µg of encapsulated OVA (NP-OVA). Antibody titers were determined in pooled faecal samples at days 0, 7, 14, 21 and 28 post-administration.

Considering the *in vivo* results as a whole, CSup/LBGS nanoparticles did not demonstrate an extra-adjuvant effect when the self-adjuvant multicomponent HE was used to immunize; in contrast, a significant adjuvant effect was demonstrated when using OVA as a model antigen. This is certainly a consequence of the fact that HE is a particulate antigen and stronger immunological responses are known to be generated to this type of antigens in comparison with soluble ones, like OVA. Therefore, the suitability of CSup/LBGS nanoparticles to provide an adjuvant effect in oral immunization is suggested, although it is strongly dependent on the used antigen. Both the presence of mannose units in LBG, which target M cells and DC's, and the mucoadhesive characteristics of CSup, are thought to have played a role in the improved response mediated by nanoparticles. Additionally, results obtained by others suggest that targeting to M cells and/or mucosal DCs should be the way to achieve a better and/or more balanced immune response (252, 284, 288-290). It is worth to mention that the oral immunization performed in these *in vivo* assays, truly evaluates the system capability, since it was made by oral gavage (not intraduodenally) and no prior administration of sodium bicarbonate solution, in order to neutralize the acid environment of the stomach, was made. The role of M cells and mucosal DCs to achieve the adjuvant properties suggested herein should be demonstrated.

4.4. Conclusions

This work reports for the first time the production of nanoparticles based on locust bean gum, demonstrating the ability of the produced sulfate derivative of locust bean gum to form nanoparticulate complexes with chitosan by means of an electrostatic interaction. The produced nanoparticles were proposed as adjuvants in oral immunization, efficiently associating two model antigens (HE antigenic complex and OVA) without compromising their structural integrity. Displaying a size around 180 - 200 nm and a positive zeta potential, the antigen-loaded nanoparticles were deemed adequate for the proposed application in oral immunization. These characteristics, along with the mannose content of LBG and the bioadhesive properties of chitosan, are expected to mediate both a prolonged contact with the intestinal mucosa and a favored interaction with intestinal M cells and mucosal DC's. Nanoparticles were also demonstrated to be stable in suspension for at least 3 months when stored at 4 ºC. The cytotoxic assessment performed in Caco-2 cells revealed no alterations at the level of cell metabolic activity upon exposure to the nanoparticles, but a mild negative effect on cell membrane integrity was observed. The *in vivo* proof of concept demonstrated the adjuvant effect of the proposed system when OVA

was used as soluble antigen model, although this effect was not observed when a particulate antigen like HE was tested. Nanoparticles were found to elicit a balanced Th1/Th2 immune response, which is a relevant effect towards an effective immunological protection. Additionally and as expected, nanoparticles were capable of inducing not only a systemic response, but also a response at the mucosal level.

This page was intentionally left in blank

CHAPTER 5

GENERAL CONCLUSIONS AND PERPECTIVES

This page was intentionally left in blank

5. General conclusions

The results of the work presented in this thesis indicate the potential of the polymeric nanoparticulate system based on polysaccharides for an application in oral immunization, especially for soluble antigens.

In a more detailed manner, the described results permitted the following conclusions:

- Locust bean gum (LBG) is a neutral polysaccharide with a chemical composition corresponding to a galactomannan. Its high content in OH groups enabled the performance of chemical modifications to attribute charged functions to the molecule, resulting in the synthesis of charged derivatives of LBG. Sulfated (LBGS), carboxylated (LBGC) and ammonium LBG (LBGA) derivatives were synthesized;

- Varied methods were applied for the characterization of LBG and its derivatives, which demonstrated the effective functionalization of the original polysaccharide. The charged LBG derivatives permitted the production of LBG-based nanoparticles by a mild method of polyelectrolyte complexation. Chitosan (CS or CSup)/LBGS, CS/LBGC and LBGA/LBGS nanoparticles were developed;

- CSup/LBGS nanoparticles were selected to deepen the studies, demonstrating to be stable up to 180 days when stored at 4 ºC;

- Two model antigens (a particulate cellular extract of *Salmonella* Enteritidis, HE, and a soluble antigen, ovalbumin) were effectively associated to CSup/LBGS nanoparticles without any deleterious effect on their structural integrity, while their antigenicity was retained. The nanoparticles exhibited adequate physicochemical properties for an application in oral immunization and demonstrated to restrain the release of the antigens. In this regard, HE had very limited release in either simulated gastric or intestinal fluids and ovalbumin released a maximum of 40% in simulated gastric medium;

- The determination of the cytotoxic profile of LBG derivatives revealed severe cytotoxicity of the ammonium derivative towards a model of the intestinal epithelium (Caco-2 cells), contrasting to a very mild effect of either original LBG or the negatively charged derivatives (LBGS and LBGC). This toxicological effect was reverted when LBGA was converted to nanoparticulate form (LBGA/LBGS nanoparticles). CSup/LBGS nanoparticles induced cell viabilities around 100% in a test of metabolic activity, although an assessment of membrane integrity evidenced higher cytotoxicity, thus reinforcing the need to widen the set of assays used to determine the toxicological profile of the formulations;

- *In vivo* studies demonstrated the adjuvant effect of the CSup/LBGS nanoparticles in obtaining an immunological response (systemic and mucosal) after oral immunization. This effect was only provided when the soluble antigen ovalbumin was used, contrasting with an absence of effect when the particulate antigen HE was tested. Nanoparticles were further found to elicit a balanced Th1/Th2 immune response, which is a relevant observation regarding an effective immunological protection.

Future perspectives

In the sequence of the studies described in this thesis and the drawn conclusions, there is great room for further testing and improving. One of the greatest challenges of nanoparticle design concerns the scaling up of their production. As seen in the description of results, the final properties of nanoparticles produced by polyelectrolyte complexation are sensitive to small alterations, such as a slight variation in concentration. The use of a larger scale does not permit such a good control, comparing with the lab scale, over all the parameters (stirring speed, addition of one solution over other, etc.) and some of the desired features of nanoparticles can be lost (291). Interestingly, the controlled scaled up production of chitosan nanoparticles by ionic gelation with tripolyphosphate was reported by using a static mixer, indicating the value of the device in this regard (292). It would be interesting to test and optimize conditions for scaling of the nanoparticle production. Another important challenge regarding nanoparticle production relies on their stabilization. In most cases nanoparticles are produced in aqueous medium, as is the case of CSup/LBGS nanoparticles. Although we have demonstrated that their physicochemical properties remain unaltered up to 180 days when stored at 4 ºC, longer shelf-life is needed. Additionally, storage and transport costs need to be reduced as possible, requiring the preparation of solid forms of nanoparticles. This may be done by freeze-drying and our group has endeavored several strategies that improve the stability of protein-loaded nanoparticles, which could be applied in this case. These include not only freeze-drying in presence of different cryo- and lyoprotectants like sugars (sucrose, glucose, trehalose, mannitol), cyclodextrins, surfactants (polyvinylalcohol, Pluronic®) (26), but also using annealing as a strategy to optimize lyophilization (293).

One of the limitations identified in the work is the relatively low association efficiency. Therefore, establishing strategies that could improve that parameter would also be an important advancement. As the method of nanoparticle production and antigen association involves electrostatic interactions, an adequate approach would consist in

testing varied pH values, playing with the exhibited charges and establishing the conditions of maximized association. Additionally, it would be important to test other soluble antigens of interest for oral delivery, such as toxins, to demonstrate the adjuvant effect of the nanoparticles. Distribution in gastrointestinal tract and uptake by Peyer's patches using fluorescently labelled antigen/nanoparticle can be studied to unveil the establishment of a real interaction with the M cells. Moreover, it would be beneficial to perform *in vivo* tests in other animals, such as dogs or pigs, which have organic functions closer to those of humans and permit a more realistic approach of the real effect of nanoparticles (294).

This page was intentionally left in blank

References

1. Rader RA. (Re)defining biopharmaceutical. Nat Biotechnol. 2008;26(7):743-51.
2. Alonso MJ. Nanomedicines for overcoming biological barriers. Biomed Pharmacother. 2004;58:168-72.
3. Kammona O, Kiparissides C. Recent advances in nanocarrier-based mucosal delivery of biomolecules. J Control Release. 2012;161(3):781-94.
4. Courrier H, Butz N, Vandamme T. Pulmonary drug delivery systems: recent developments and prospects. Crit Rev Ther Drug Carrier Syst. 2002;19:425-98.
5. Caon T, Jin L, Simões CMO, Norton RS, Nicolazzo JA. Enhancing the buccal mucosal delivery of peptide and protein therapeutics. Pharm Res. 2014;32(1):1-21.
6. Antosova Z, Mackova M, Kral V, Macek T. Therapeutic application of peptides and proteins: parenteral forever? Trends Biotechnol. 2009;27(11):628-35.
7. Casettari L, Illum L. Chitosan in nasal delivery systems for therapeutic drugs. J Control Release. 2014;190:189-200.
8. de la Fuente M, Csaba N, Garcia-Fuentes M, Alonso MJ. Nanoparticles as protein and gene carriers to mucosal surfaces. Nanomed. 2008;3:845-57.
9. Li H, Yu Y, Faraji-Dana S, Li B, Lee C, Kang L. Novel engineered systems for oral, mucosal and transdermal drug delivery. J Drug Target. 2013;21(7):611-29.
10. Cleland JL, Daugherty A, Mrsny R. Emerging protein delivery methods. Curr Opin Biotechnol. 2001;12(2):212-9.
11. Chiellini F, Piras AM, Errico C, Chiellini E. Micro/nanostructured polymeric systems for biomedical and pharmaceutical applications. Nanomed. 2008;3(3):367-93.
12. Takeuchi H, Yamamoto H, Kawashima Y. Mucoadhesive nanoparticulate systems for peptide drug delivery. Adv Drug Deliver Rev. 2001;47(1):39-54.
13. ISO. Nanotechnologies - Vocabulary - Part 2: Nano-objects. International Organization for Standardization; 2015.
14. Mudshinge SR, Deore AB, Patil S, Bhalgat CM. Nanoparticles: Emerging carriers for drug delivery. Saudi Pharm J. 2011;19(3):129-41.
15. Singh R, Lillard Jr J. Nanoparticle-based targeted drug delivery. Exp Mol Pathol. 2009;86:215-23.
16. Zhao L, Seth A, Wibowo N, Zhao C-X, Mitter N, Yu C, et al. Nanoparticle vaccines. Vaccine. 2014;32(3):327-37.
17. das Neves J, Nunes R, Machado A, Sarmento B. Polymer-based nanocarriers for vaginal drug delivery. Adv Drug Deliver Rev. 2015;92:53-70.
18. Elsabahy M, Wooley KL. Design of polymeric nanoparticles for biomedical delivery applications. Chem Soc Rev. 2012;41(7):2545-61.

19. Csaba N, Garcia-Fuentes M, Alonso MJ. The performance of nanocarriers for transmucosal drug delivery. Expert Opin Drug Deliv. 2006;3(4):463-78.
20. Desai MP, Labhasetwar V, Amidon GL, Levy RJ. Gastrointestinal uptake of biodegradable microparticles: effect of particle size. Pharm Res. 1996;13(12):1838-45.
21. Jani P, Halbert GW, Langridge J, Florence AT. Nanoparticle uptake by the rat gastrointestinal mucosa: quantitation and particle size dependency. J Pharm Pharmacol. 1990;42(12):821-6.
22. Yih TC, Al-Fandi M. Engineered nanoparticles as precise drug delivery systems. J Cell Biochem. 2006;97(6):1184-90.
23. Lopes M, Shrestha N, Correia A, Shahbazi M-A, Sarmento B, Hirvonen J, et al. Dual chitosan/albumin-coated alginate/dextran sulfate nanoparticles for enhanced oral delivery of insulin. J Control Release. 2016;232:29-41.
24. Araújo F, Shrestha N, Shahbazi M-A, Fonte P, Mäkilä EM, Salonen JJ, et al. The impact of nanoparticles on the mucosal translocation and transport of GLP-1 across the intestinal epithelium. Biomaterials. 2014;35(33):9199-207.
25. Dombu CY, Betbeder D. Airway delivery of peptides and proteins using nanoparticles. Biomaterials. 2013;34(2):516-25.
26. Fonte P, Reis S, Sarmento B. Facts and evidences on the lyophilization of polymeric nanoparticles for drug delivery. J Control Release. 2016;225:75-86.
27. Chan H-K, Kwok PCL. Production methods for nanodrug particles using the bottom-up approach. Adv Drug Deliver Rev. 2011;63(6):406-16.
28. Wais U, Jackson AW, He T, Zhang H. Nanoformulation and encapsulation approaches for poorly water-soluble drug nanoparticles. Nanoscale. 2016;8(4):1746-69.
29. Wang J, Byrne JD, Napier ME, DeSimone JM. More effective nanomedicines through particle design. Small. 2011;7(14):1919-31.
30. Fan W, Yan W, Xu Z, Ni H. Formation mechanism of monodisperse, low molecular weight chitosan nanoparticles by ionic gelation technique. Colloids and Surfaces B: Biointerfaces. 2012;90:21-7.
31. Canelas DA, Herlihy KP, DeSimone JM. Top-down particle fabrication: Control of size and shape for diagnostic imaging and drug delivery. Wiley Interdiscip Rev Nanomed Nanobiotechnol. 2009;1(4):391-404.
32. Pinto Reis C, Neufeld RJ, Ribeiro AJ, Veiga F. Nanoencapsulation I. Methods for preparation of drug-loaded polymeric nanoparticles. Nanomed: Nanotechnol. 2006;2(1):8-21.
33. Lima AC, Sher P, Mano JF. Production methodologies of polymeric and hydrogel particles for drug delivery applications. Expert Opin Drug Deliv. 2012;9(2):231-48.

34. Calvo P, Remuñán-López C, Vila-Jato JL, Alonso MJ. Novel hydrophylic chitosan-polyethylene oxide nanoparticles as protein carriers. J Appl Polym Sci. 1997;63:125-32.

35. Bhattarai N, Gunn J, Zhang M. Chitosan-based hydrogels for controlled, localized drug delivery. Adv Drug Deliv Rev. 2010;62(1):83-99.

36. Poncelet D. Microencapsulation: fundamentals, methods and applications. In: Blitz J, Gun'ko V, editors. Surface Chemistry in Biomedical and Environmental Science. Dordrecht: Springer; 2005. p. 23-4.

37. Kissel T, Maretscheck S, Packhäuser C, Schnieders J, Seidel N. Microencapsulation techniques for parenteral depot systems and their application in the pharmaceutical industry. In: Benita S, editor. Microencapsulation: Methods and industrial applications. New York: Taylor & Francis; 2006. p. 99-122.

38. Sarmento B, Martins S, Ribeiro A, Veiga F, Neufeld R, Ferreira D. Development and comparison of different nanoparticulate polyelectrolyte complexes as insulin carriers. Int J Pept Res Ther. 2006;12:131-8.

39. Grenha A, Gomes ME, Rodrigues M, Santo VE, Mano JF, Neves NM, et al. Development of new chitosan/carrageenan nanoparticles for drug delivery applications. J Biomed Mater Res A. 2010;92A(4):1265-72.

40. Sarmento B, Ribeiro A, Veiga F, Ferreira D. Development and characterization of new insulin containing polysaccharide nanoparticles. Colloids and Surfaces B: Biointerfaces. 2006;53:193-202.

41. Agnihotri SA, Mallikarjuna N, Aminabhavi T. Recent advances on chitosan-based micro- and nanoparticles in drug delivery. J Control Release. 2004;100:5-28.

42. Tiyaboonchai W. Chitosan nanoparticles: a promising system for drug delivery. Naresuan Univer J. 2003;11:51-66.

43. Carvalho EL, Grenha A, Remunan-Lopez C, Alonso MJ, Seijo B. Mucosal delivery of liposome-chitosan nanoparticle complexes. Methods Enzymol. 2009;465:289-312.

44. Karewicz A, Bielska D, Nowakowska M. Modified polysaccharides as versatile materials in controlled delivery of anti-degenerative agents. Curr Pharm Des. 2012;18:2518-35.

45. Anwunobi A, Emeje M. Recent applications of natural polymers in nanodrug delivery. J Nanomed Nanotechnol. 2011;S4:2-7.

46. Beneke C, Viljoen A, Hamman J. Polymeric plant-derived excipients in drug delivery. Molecules. 2009;14:2602-20.

47. Pollard M, Kelly R, Fischer P, Windhab E, Eder B, Amadò R. Investigation of molecular weight distribution of LBG galactomannan for flours prepared from individual seeds, mixtures, and commercial samples. Food Hydrocoll. 2008;22:1596–606.

48. Mizrahy S, Peer D. Polysaccharides as building blocks for nanotherapeutics. The Chemistry Society Reviews. 2012;41:2623-40.

49. d'Ayala GG, Malinconico M, Laurienzo P. Marine derived polysaccharides for biomedical applications: chemical modification approaches. Molecules. 2008;13:2069-106.

50. Zhang H, Ma Y, Sun X. Recent developments in carbohydrate-decorated targeted drug/gene delivery. Med Res Rev. 2010;30(2):270-89.

51. Rodrigues S, Grenha A. Activation of macrophages: Establishing a role for polysaccharides in drug delivery strategies envisaging antibacterial therapy. Curr Pharm Des. 2015;21:4869-87.

52. Liu Z, Jiao Y, Wang Y, Zhou C, Zhang Z. Polysaccharides-based nanoparticles as drug delivery systems. Adv Drug Deliver Rev. 2008;60(15):1650-62.

53. dos Santos MA, Grenha A. Polysaccharide nanoparticles for protein and peptide delivery: Exploring less-known materials. In: Rossen D, editor. Advances in Protein Chemistry and Structural Biology. Volume 98: Academic Press; 2015. p. 223-61.

54. Copetti G, Grassi M, Lapasin R, Pricl S. Synergistic gelation of xanthan gum with locust bean gum: a rheological investigation. Glycoconj J. 1997;14:951-61.

55. Malafaya P, Silva G, Reis R. Natural–origin polymers as carriers and scaffolds for biomolecules and cell delivery in tissue engineering application. Adv Drug Deliver Rev. 2007;59:207–33.

56. Oyarzun-Ampuero FA, Brea J, Loza MI, Torres D, Alonso MJ. Chitosan–hyaluronic acid nanoparticles loaded with heparin for the treatment of asthma. Int J Pharm. 2009;381(2):122-9.

57. Goycoolea FM, Lollo G, Remuñán-López C, Quaglia F, Alonso MJ. Chitosan-alginate blended nanoparticles as carriers for the transmucosal delivery of macromolecules. Biomacromolecules. 2009;10(7):1736-43.

58. Dionísio M, Braz L, Corvo M, Lourenço JP, Grenha A, da Costa AMR. Charged pullulan derivatives for the development of nanocarriers by polyelectrolyte complexation. Int J Biol Macromol. 2016;86:129-38.

59. Dionísio M, Cordeiro C, Remuñán-López C, Seijo B, Rosa da Costa AM, Grenha A. Pullulan-based nanoparticles as carriers for transmucosal protein delivery. Eur J Pharm Sci. 2013;50(1):102-13.

60. Kawamura Y. Carob Bean Gum Chemical and Technical Assessment. Joint FAO/WHO Expert Committee on Food Additives, 2008.

61. Rowe R, Sheskey P, Owen S. Handbook of Pharmaceutical Excipients. 6 ed. London: Pharmaceutical Press; 2009.

62. Prajapati VD, Jani GK, Moradiya NG, Randeria NP, Nagar BJ. Locust bean gum: A versatile biopolymer. Carbohydr Polym. 2013;94(2):814-21.

63. Barak S, Mudgil D. Locust bean gum: Processing, properties and food applications - A review. Int J Biol Macromol. 2014;66:74-80.

64. Dionísio M, Grenha A. Locust bean gum: exploring its potential for biopharmaceutical applications. J Pharm Bioall Sci. 2012;4(3):75-85.

65. Andrade C, Azero E, Luciano L, Gonçalves M. Solution properties of the galactomannans extracted from the seeds of Caesalpinia pulcherrima and Cassia javanica: comparison with locust bean gum. Int J Biol Macromol. 1999;26:181–5.

66. Rinaudo M. Main properties and current applications of some polysaccharides as biomaterials. Polym Int. 2008;57:397–430.

67. Picout D, Ross-Murphy S, Jumel K, Harding S. Pressure cell assisted solution characterization of polysaccharides. 2. Locust bean gum and tara gum. Biomacromolecules. 2002;3:761-7.

68. Sébastien G, Christophe B, Mario A, Pascal L, Michel P, Aurore R. Impact of purification and fractionation process on the chemical structure and physical properties of locust bean gum. Carbohydr Polym. 2014;108:159-68.

69. Mathur V, Mathur N. Fenugreek and other less known legume galactomannan-polysaccharides: Scope for developments. J Sci Ind Res. 2005;64.

70. Alves MM, Antonov YA, Gonçalves MP. The effect of structural features of gelatin on its thermodynamic compatibility with locust bean gum in aqueous media. Food Hydrocoll. 1999;13(2):157-66.

71. Garcia-Ochoa F, Casas J. Viscosity of locust bean (Ceratonia siliqua) gum solutions. J Sci Food Agr. 1992;59:97-100.

72. Lavazza M, Formantici C, Langella V, Monti D, Pfeiffer U, Galante YM. Oxidation of galactomannan by laccase plus TEMPO yields an elastic gel. J Biotechnol. 2011;156(2):108-16.

73. Bouzouita N, Khaldi A, Zgoulli S, Chebil L, Chekki R, Chaabouni MM, et al. The analysis of crude and purified locust bean gum: A comparison of samples from different carob tree populations in Tunisia. Food Chem. 2007;101(4):1508-15.

74. Dakia P, Blecker C, Robert C, Whatelet B, Paquot M. Composition and physicochemical properties of locust bean gum extracted from whole seeds by acid or water dehulling pre-treatment. Food Hydrocoll. 2008;22:807–18.

75. Surana S, Munday D, Cox P, Khan K. Relationship between swelling, erosion and drug release in hydrophilic natural gum mini-matrix formulations. Eur J Pharm Sci. 1998;6:207-17.

76. Pollard M, Kelly R, Wahl C, Fischer KP, Windhab E, Eder B, et al. Investigation of equilibrium solubility of a carob galactomannan. Food Hydrocoll. 2007;21:683-92.
77. Urdiain M, Doménech-Sánchez A, Albertí S, Benedí V, Rosselló J. Identification of two additives, locust bean gum (E-410) and guar gum (E- 412), in food products by DNA-based methods. Food Addit Contam A. 2004;21(7):619 - 25.
78. Wang F, Wang YJ, Sun Z. Conformational role of xanthan in its interaction with locust bean gum. J Food Sci. 2002;67(7):2609-14.
79. Sudhakar Y, Kuotsu K, Bandyopadhyay AK. Buccal bioadhesive drug delivery - A promising option for orally less efficient drugs. J Control Release. 2006;114:15-40.
80. Alonso-Sande M, Teijeiro-Osorio D, Remuñán-López C, Alonso MJ. Glucomannan, a promising polysaccharide for biopharmaceutical purposes. Eur J Pharm Biopharm. 2009;72(2):453-62.
81. Jain A, Gupta Y, Jain S. Perspectives of biodegradable natural polysaccharides for site-specific drug delivery to the colon. J Pharm Pharm Sci. 2007;10(1):86-128.
82. Bauer A, Kesselhut A. Novel pharmaceutical excipients for colon targeting. STP Pharmaceutical Sciences. 1995;5:54-9.
83. Malik K, Arora G, Singh I. Locust bean gum as superdisintegrant - Formulation and evaluation of nimesulide orodispersible tablets. Polim Med. 2011;41(1):17-28.
84. Kurita K. Chitin and chitosan: functional biopolymers from marine crustaceans. Mar Biothecnol. 2006;8:203-26.
85. Knaul JZ, Bui VT, Creber KAM, Kasaai MR. Characterization of deacetylated chitosan and chitosan molecular weight review. Can J Chem. 1998;76(11):1699-706.
86. Rinaudo M. Chitin and chitosan: Properties and applications. Prog Polym Sci. 2006;31(7):603-32.
87. Ravi Kumar MNV. A review of chitin and chitosan applications. React Funct Polym. 2000;46(1):1-27.
88. Muzzarelli R. Chitin. In: Aspinall GO, editor. The polysaccharides. Orlando: Academic Press; 1985. p. 417-50.
89. Singh D, Ray A. Biomedical applications of chitin, chitosan and their derivatives. Rev Macromol Chem Physic. 2000;C40:69-83.
90. Zalloum HM, Mubarak MS. Antioxidant polymers: Metal chelating agents. In: Cirilo G, Iemma F, editors. Antioxidant Polymers. New Jersey: John Wiley & Sons, Inc.; 2012. p. 87-114.
91. Sorlier P, Denuziere A, Viton C, Domard A. Relation between the degree of acetylation and the electrostatic properties of chitin and chitosan. Biomacromolecules. 2001;2(3):765-72.

92. Dong YM, Qiu WB, Ruan Y, Wu Y, Wang M, Xu CY. Influence of molecular weight on critical concentration of chitosan/formic acid liquid crystalline solution. Polym J. 2001;33(5):387-9.

93. Yamamoto H, Kuno Y, Sugimoto S, Takeuchi H, Kawashima Y. Surface-modified PLGA nanosphere with chitosan improved pulmonary delivery of calcitonin by mucoadhesion and opening of the intercellular tight junctions. J Control Release. 2005;102(2):373-81.

94. Cho Y, Jang J, Park C, Ko S. Preparation and solubility in acid and water of partially deacetylated chitins. Biomacromolecules. 2000;1(609-614).

95. Fernández-Urrusuno R, Calvo P, Remuñán-López C, Vila-Jato JL, José Alonso M. Enhancement of nasal absorption of insulin using chitosan nanoparticles. Pharm Res. 1999;16(10):1576-81.

96. De Campos AM, Sánchez A, Alonso MaJ. Chitosan nanoparticles: a new vehicle for the improvement of the delivery of drugs to the ocular surface. Application to cyclosporin A. Int J Pharm. 2001;224(1–2):159-68.

97. Al-Qadi S, Grenha A, Carrión-Recio D, Seijo B, Remuñán-López C. Microencapsulated chitosan nanoparticles for pulmonary protein delivery: In vivo evaluation of insulin-loaded formulations. J Control Release. 2012;157:383-90.

98. Shrestha N, Araújo F, Shahbazi M-A, Mäkilä E, Gomes MJ, Airavaara M, et al. Oral hypoglycaemic effect of GLP-1 and DPP4 inhibitor based nanocomposites in a diabetic animal model. J Control Release. 2016;232:113-9.

99. Fernanda A, Filipa A, Ana Vanessa N, Sara Baptista da S, Jose das N, Domingos F, et al. Chitosan formulations as carriers for therapeutic proteins. Curr Drug Discov Technol. 2011;8(3):157-72.

100. Tharanathan RN, Kittur FS. Chitin — The undisputed biomolecule of great potential. Crit Rev Food Sci Nutr. 2003;43(1):61-87.

101. Hirano S, Seino H, Akiyama Y, Nonaka I. Bio-compatibility of chitosan by oral and intravenous administrations. Polym Mater Sci Eng. 1988;59:897-901.

102. Dornish M, Hagen A, Hansson E, Peucheur C, Vedier F, Skaugrud O. Safety of Protasan: ultrapure chitosan salts for biomedical and pharmaceutical use. In: Domard A, Roberts G, Varum K, editors. Advances in chitin science. Lyon: Jacques Andre Publisher; 1997. p. 664-70.

103. Lehr C-M, Bouwstra JA, Schacht EH, Junginger HE. In vitro evaluation of mucoadhesive properties of chitosan and some other natural polymers. Int J Pharm. 1992;78:43-8.

104. Artursson P, Lindmark T, Davis SS, Illum L. Effect of chitosan on the permeability of monolayers of intestinal epithelial cells (Caco-2). Pharm Res. 1994;11:1358-61.

105. Borchard G, Lueβen HL, de Boer AG, Verhoef JC, Lehr C-M, Junginger HE. The potential of mucoadhesive polymers in enhancing intestinal peptide drug absorption. III: Effects of chitosan-glutamate and carbomer on epithelial tight junctions in vitro. J Control Release. 1996;39(2–3):131-8.

106. Fernández-Urrusuno R, Romani D, Calvo P, Vila-Jato J, Alonso M. Development of a freeze-dried formulation of insulin-loaded chitosan nanoparticles intended for nasal administration. STP Pharma Sciences. 1999;9:429–36.

107. Prego C, García M, Torres D, Alonso MJ. Transmucosal macromolecular drug delivery. J Control Release. 2005;101(1–3):151-62.

108. Prego C, Torres D, Alonso MJ. The potential of chitosan for the oral administration of peptides. Expert Opin Drug Deliv. 2005;2:843-54.

109. Shrestha N, Shahbazi M-A, Araújo F, Zhang H, Mäkilä EM, Kauppila J, et al. Chitosan-modified porous silicon microparticles for enhanced permeability of insulin across intestinal cell monolayers. Biomaterials. 2014;35(25):7172-9.

110. Sogias IA, Williams AC, Khutoryanskiy VV. Why is chitosan mucoadhesive? Biomacromolecules. 2008;9(7):1837-42.

111. Chen M-C, Mi F-L, Liao Z-X, Hsiao C-W, Sonaje K, Chung M-F, et al. Recent advances in chitosan-based nanoparticles for oral delivery of macromolecules. Adv Drug Deliver Rev. 2013;65(6):865-79.

112. Yeh T-H, Hsu L-W, Tseng MT, Lee P-L, Sonjae K, Ho Y-C, et al. Mechanism and consequence of chitosan-mediated reversible epithelial tight junction opening. Biomaterials. 2011;32(26):6164-73.

113. Kakutani H, Kondoh M, Fukasaka M, Suzuki H, Hamakubo T, Yagi K. Mucosal vaccination using claudin-4-targeting. Biomaterials. 2010;31:5463-71.

114. Poland GA, Jacobson RM. Understanding those who do not understand: a brief review of the anti-vaccine movement. Vaccine. 2001;19(17–19):2440-5.

115. Gangarosa EJ, Galazka AM, Wolfe CR, Phillips LM, Miller E, Chen RT, et al. Impact of anti-vaccine movements on pertussis control: the untold story. The Lancet. 1998;351(9099):356-61.

116. Murray CJL, Lopez AD. Alternative projections of mortality and disability by cause 1990-2020: global burden of disease study. The Lancet. 1997;349:1498-509.

117. Kieny MP, Excler JL, Girard M. Research and development of new vaccines against infectious diseases. Am J Public Health. 2004;94:1931-5.

118. Amanna IJ, Slifka MK. Contributions of humoral and cellular immunity to vaccine-induced protection in humans. Virology. 2011;411:206-15.

119. Chadwick S, Kriegel C, Amiji M. Nanotechnology solutions for mucosal immunization. Adv Drug Deliver Rev. 2010;62:394-407.

120. Irache JM, Salman HH, Gomez S, Espuelas S, Gamazo C. Poly(anhydride) nanoparticles as adjuvants for mucosal vaccination. Front Biosci (Schol Ed). 2010;2:876-90.

121. Crotty S, Lohman BL, Lu FXS, Tang SB, Miller CJ, Andino R. Mucosal immunization of cynomolgus macaques with two serotypes of live poliovirus vectors expressing simian immunodeficiency virus antigens: Stimulation of humoral, mucosal, and cellular immunity. J Virol. 1999;73:9485-95.

122. Peek LJ, Middaugh CR, Berkland C. Nanotechnology in vaccine delivery. Adv Drug Deliver Rev. 2008;60:915-28.

123. Putra N. Design, manufacturing and testing of a portable vaccine carrier box employing thermoelectric module and heat pipe. J Med Eng Technol. 2009;33:232-7.

124. Coffin CS, Saunders C, Thomas CM, Loewen AH, Ghali WA, Campbell NR. Validity of ICD-9-CM administrative data for determining eligibility for pneumococcal vaccination triggers. Am J Med Qual. 2005;20:158-63.

125. Corbel MJ, Das RG, Lei D, Xing DK, Horiuchi Y, Dobbelaer R. WHO Working Group on revision of the Manual of Laboratory Methods for Testing DTP Vaccines-Report of two meetings held on 20-21 July 2006 and 28-30 March 2007, Geneva, Switzerland. Vaccine. 2008;26:1913-21.

126. Webster DE, Gahan ME, Strugnell RA, Wasselingh SL. Advances in oral vaccine delivery options: what is on the horizon? Am J Drug Deliv. 2003;1:227-40.

127. Vogel FR. Adjuvants in perspective. Dev Biol Stand. 1998;92:241-8.

128. Mills KHG. Regulatory T cells: Friend or foe in immunity to infection? Nat Rev Immunol. 2004;4(11):841-55.

129. Waite J, Skokos D. Th17 response and inflammatory autoimmune diseases. Int J Inflam. 2012;2012:1-10.

130. Corthay A. How do regulatory T cells work? Scand J Immunol. 2009;70(4):326-36.

131. Garcon N, Segal L, Tavares F, Van Mechelen M. The safety evaluation of adjuvants during vaccine development: The AS04 experience. Vaccine. 2011;29:4453-9.

132. Mbow ML, De Gregorio E, Valiante NM, Rappuoli R. New adjuvants for human vaccines. Curr Opin Immunol. 2010;22:411-6.

133. Hammer SM, Sobieszczyk ME, Janes H, Karuna ST, Mulligan MJ, Grove D, et al. Efficacy trial of a DNA/rAd5 HIV-1 preventive vaccine. N Engl J Med. 2013;369(22):2083-92.

134. Roy A, Eisenhut M, Harris RJ, Rodrigues LC, Sridhar S, Habermann S, et al. Effect of BCG vaccination against Mycobacterium tuberculosis infection in children: systematic review and meta-analysis. Br Med J. 2014;349:1-11.

135. RTS SCTP. Efficacy and safety of RTS,S/AS01 malaria vaccine with or without a booster dose in infants and children in Africa: final results of a phase 3, individually randomised, controlled trial. The Lancet. 2015;386(9988):31-45.
136. Lavelle EC, O'Hagan DT. Delivery systems and adjuvants for oral vaccines. Expert Opin Drug Deliv. 2006;3:747-62.
137. Sarti F, Perera G, Hintzen F, Kotti K, Karageorgiou V, Kammona O, et al. In vivo evidence of oral vaccination with PLGA nanoparticles containing the immunostimulant monophosphoryl lipid A. Biomaterials. 2011;32:4052-7.
138. Mann JF, Shakir E, Carter KC, Mullen AB, Alexander J, Ferro VA. Lipid vesicle size of an oral influenza vaccine delivery vehicle influences the Th1/Th2 bias in the immune response and protection against infection. Vaccine. 2009;27:3643-9.
139. Ogra PL, Faden H, Welliver RC. Vaccination strategies for mucosal immune responses. Clin Microbiol Rev. 2001;14:430-45.
140. Baca-Estrada ME, Foldvari M, Babiuk SL, Babiuk LA. Vaccine delivery: lipid-based delivery systems. J Biotechnol. 2000;83:91-104.
141. Lee VHL, Yang JJ. Oral drug delivery. In: Hillery AM, Lloyd AW, Swarbrick J, editors. Drug delivery and targeting: for pharmacists and pharmaceutical scientists. 1 ed. London: Taylor & Francis; 2001. p. 145-83.
142. Srivastava I, Singh M. DNA vaccines: focus on increasing potency and efficacy. Int J Pharm Med. 2005;19:15-28.
143. des Rieux A, Fievez V, Garinot M, Schneider YJ, Preat V. Nanoparticles as potential oral delivery systems of proteins and vaccines: a mechanistic approach. J Control Release. 2006;116:1-27.
144. Jepson MA, Clark MA, Hirst BH. M cell targeting by lectins: a strategy for mucosal vaccination and drug delivery. Adv Drug Deliver Rev. 2004;56:511-25.
145. Wattendorf U, Merkle HP. PEGylation as a tool for the biomedical engineering of surface modified microparticles. J Pharm Sci. 2008;97:4655-69.
146. Murphy K. Janeway's Immunobiology. 8 ed. New York: Garland Science; 2012.
147. Pyż E, Marshall ASJ, Gordon S, Brown GD. C-type lectin-like receptors on myeloid cells. Ann Med. 2006;38(4):242-51.
148. Takeda K, Kaisho T, Akira S. Toll-like receptors. Annu Rev Immunol. 2003;21(1):335-76.
149. Ebner S, Ehammer Z, Holzmann S, Schwingshackl P, Forstner M, Stoitzner P, et al. Expression of C-type lectin receptors by subsets of dendritic cells in human skin. Int Immunol. 2004;16(6):877-87.
150. Gi M, Im W, Hong S. Dendritic cells as danger-recognizing biosensors. Sensors. 2009;9(9):6730-51.

151. Dambuza IM, Brown GD. C-type lectins in immunity: recent developments. Curr Opin Immunol. 2015;32:21-7.
152. Kerrigan AM, Brown GD. C-type lectins and phagocytosis. Immunobiology. 2009;214(7):562-75.
153. Geijtenbeek TBH, Gringhuis SI. Signalling through C-type lectin receptors: shaping immune responses. Nat Rev Immunol. 2009;9(7):465-79.
154. Garinot M, Fievez V, Pourcelle V, Stoffelbach F, des Rieux A, Plapied L, et al. PEGylated PLGA-based nanoparticles targeting M cells for oral vaccination. J Control Release. 2007;120:195-204.
155. Engering AJ, Cella M, Fluitsma DM, Hoefsmit ECM, Lanzavecchia A, Pieters J. Mannose receptor mediated antigen uptake and presentation in human dendritic cells. In: Ricciardi-Castagnoli P, editor. Dendritic Cells in Fundamental and Clinical Immunology. 3. Boston, MA: Springer US; 1997. p. 183-7.
156. Kapsenberg ML. Dendritic-cell control of pathogen-driven T-cell polarization. Nat Rev Immunol. 2003;3(12):984-93.
157. Nutt SL, Hodgkin PD, Tarlinton DM, Corcoran LM. The generation of antibody-secreting plasma cells. Nat Rev Immunol. 2015;15(3):160-71.
158. Shlomchik MJ, Weisel F. Germinal center selection and the development of memory B and plasma cells. Immunol Rev. 2012;247(1):52-63.
159. van der Lubben IM, Verhoef JC, Borchard G, Junginger HE. Chitosan for mucosal vaccination. Adv Drug Deliver Rev. 2001;52:139-44.
160. Plapied L, Vandermeulen G, Vroman B, Preat V, des Rieux A. Bioadhesive nanoparticles of fungal chitosan for oral DNA delivery. Int J Pharm. 2010;398:210-8.
161. Azizi A, Kumar A, Diaz-Mitoma F, Mestecky J. Enhancing oral vaccine potency by targeting intestinal M cells. PLoS Pathog. 2010;6(11):e1001147.
162. Tyrer PC, Ruth Foxwell A, Kyd JM, Otczyk DC, Cripps AW. Receptor mediated targeting of M-cells. Vaccine. 2007;25(16):3204-9.
163. Brayden DJ, Jepson MA, Baird AW. Keynote review: intestinal Peyer's patch M cells and oral vaccine targeting. Drug Discov Today. 2005;10:1145-57.
164. Kraehenbuhl JP, Neutra MR. Epithelial M cells: differentiation and function. Annu Rev Cell Dev Biol. 2000;16:301-32.
165. Owen RL. Uptake and transport of intestinal macromolecules and microorganisms by M cells in Peyer's patches--a personal and historical perspective. Semin Immunol. 1999;11:157-63.
166. Maldonado-Contreras AL, McCormick BA. Intestinal epithelial cells and their role in innate mucosal immunity. Cell Tissue Res. 2011;343:5-12.

167. Dahan S, Roth-Walter F, Arnaboldi P, Agarwal S, Mayer L. Epithelia: lymphocyte interactions in the gut. Immunol Rev. 2007;215:243-53.
168. Pukanud P, Peungvicha P, Sarisuta N. Development of mannosylated liposomes for bioadhesive oral drug delivery via M cells of Peyer's patches. Drug Deliv. 2009;16(5):289-94.
169. Tomizawa H, Aramaki Y, Fujii Y, Hara T, Suzuki N, Yachi K, et al. Uptake of phosphatidylserine lipossomes by rat Peyer's patches following intraluminal administration. Pharm Res. 1993;10(4):549-52.
170. Kadiyala I, Loo Y, Roy K, Rice J, Leong KW. Transport of chitosan-DNA nanoparticles in human intestinal M-cell model versus normal intestinal enterocytes. Eur J Pharm Sci. 2010;39:103-9.
171. des Rieux A, Ragnarsson EG, Gullberg E, Preat V, Schneider YJ, Artursson P. Transport of nanoparticles across an in vitro model of the human intestinal follicle associated epithelium. Eur J Pharm Sci. 2005;25:455-65.
172. Jung T, Kamm W, Breitenbach A, Hungerer KD, Hundt E, Kissel T. Tetanus toxoid loaded nanoparticles from sulfobutylated poly(vinyl alcohol)-graft-poly(lactide-co-glycolide): evaluation of antibody response after oral and nasal application in mice. Pharm Res. 2001;18:352-60.
173. McClean S, Prosser E, Meehan E, O'Malley D, Clarke N, Ramtoola Z, et al. Binding and uptake of biodegradable poly-DL-lactide micro- and nanoparticles in intestinal epithelia. Eur J Pharm Sci. 1998;6:153-63.
174. Fischer S, Merkle HP, Gander B. Micro- and nano-particles for vaccines: exploiting basic principles of the immune system. In: Ravi Kumar MNV, editor. Handbook of Particulate Drug Delivery. 2. Valencia: American Scientific Publishers; 2008. p. 311-24.
175. Davitt CJH, Lavelle EC. Delivery strategies to enhance oral vaccination against enteric infections. Adv Drug Deliver Rev. 2015;91:52-69.
176. Arca HC, Gunbeyaz M, Senel S. Chitosan-based systems for the delivery of vaccine antigens. Expert Reviews of Vaccines. 2009;8:937-53.
177. Dey P, Sa B, Maiti S. Carboxymethyl ethers of locust bean gum - A review. Int J Pharm Pharm Sci. 2011;3(2):4-7.
178. Kaity S, Ghosh A. Carboxymethylation of locust bean gum: Application in interpenetrating polymer network microspheres for controlled drug delivery. Ind Eng Chem Res. 2013;52(30):10033-45.
179. Sierakowski MR, Milas M, Desbrières J, Rinaudo M. Specific modifications of galactomannans. Carbohydr Polym. 2000;42:51-7.
180. da Silva Perez D, Montanari S, Vignon MR. TEMPO-mediated oxidation of cellulose III. Biomacromolecules. 2003;4(5):1417-25.

181. Cunha PLR, Maciel JS, Sierakowski MR, Paula RCMd, Feitosa JPA. Oxidation of cashew tree gum exudate polysaccharide with TEMPO reagent. J Braz Chem Soc. 2007;18:85-92.

182. Wang J, Yang T, Tian J, Liu W, Jing F, Yao J, et al. Optimization of reaction conditions by RSM and structure characterization of sulfated locust bean gum. Carbohydr Polym. 2014;114:375-83.

183. Maiti S, Chowdhury M, Chakraborty A, Ray S, Sa B. Sulfated locust bean gum hydrogel beads for immediate analgesic effect of tramadol hydrochloride. J Sci Ind Res. 2014;73:21-8.

184. Yuan H, Zhang W, Li X, Lu X, Li N, Gao X, et al. Preparation and in vitro antioxidant activity of k-carrageenan oligosaccharides and their oversulfated, acetylated, and phosphorylated derivatives. Carbohydr Res. 2005;340:685-92.

185. Simkovic I, Yadav MP, Zalibera M, Hicks KB. Chemical modification of corn fiber with ion-exchanging groups. Carbohydr Polym. 2009;76:250-4.

186. Carmichael J, DeGraff WG, Gazdar AF, Minna JD, Mitchell JB. Evaluation of a tetrazolium-based semiautomated colorimetric assay: assessment of chemosensitivity testing. Cancer Res. 1987;47(4):936-42.

187. Braydich-Stolle L, Hussain S, Schlager JJ, Hofmann MC. In vitro cytotoxicity of nanoparticles in mammalian germline stem cells. Toxicol Sci. 2005;88(2):412-9.

188. Mihai D, Mocanu G, Carpov A. Chemical reactions on polysaccharides: I. Pullulan sulfation. Eur Polym J. 2001;37(3):541-6.

189. Alban S, Schauerte A, Franz G. Anticoagulant sulfated polysaccharides: Part I. Synthesis and structure–activity relationships of new pullulan sulfates. Carbohydr Polym. 2002;47(3):267-76.

190. Mähner C, Lechner MD, Nordmeier E. Synthesis and characterisation of dextran and pullulan sulphate. Carbohydr Res. 2001;331(2):203-8.

191. Rekha MR, Sharma CP. Blood compatibility and in vitro transfection studies on cationically modified pullulan for liver cell targeted gene delivery. Biomaterials. 2009;30(34):6655-64.

192. Qin C, Xiao Q, Li H, Fang M, Liu Y, Chen X, et al. Calorimetric studies of the action of chitosan-N-2-hydroxypropyl trimethyl ammonium chloride on the growth of microorganisms. Int J Biol Macromol. 2004;34(1–2):121-6.

193. Nakanishi K, Goto T, Ohashi M. Infrared spectra of organic ammonium compounds. Bull Chem Soc Jpn. 1957;30(4):403-8.

194. Grenha A. Chitosan nanoparticles: a survey of preparation methods. J Drug Target. 2012;20(4):291-300.

195. Rodrigues S, da Costa AM, Grenha A. Chitosan/carrageenan nanoparticles: effect of cross-linking with tripolyphosphate and charge ratios. Carbohydr Polym. 2012;89(1):282-9.
196. Crouzier T, Picart C. Ion pairing and hydration in polyelectrolyte multilayer films containing polysaccharides. Biomacromolecules. 2009;10(2):433-42.
197. Rodrigues S, Dionísio M, Remuñán-López C, Grenha A. Biocompatibility of chitosan carriers with application in drug delivery. J Funct Biomater. 2012;3:615-41.
198. Gaspar R, Duncan R. Polymeric carriers: Preclinical safety and the regulatory implications for design and development of polymer therapeutics. Adv Drug Deliver Rev. 2009;61(13):1220-31.
199. ISO. Biological evaluation of medical devices Part 1: Evaluation and testing. International Organization for Standardization; 2009.
200. ISO. Biological evaluation of medical devices Part 3: Tests for genotoxicity, carcinogenicity, and reproductive toxicity. International Organization for Standardization; 2003.
201. ISO. Biological evaluation of medical devices Part 5: Tests for in vitro cytotoxicity. International Organization for Standardization; 2009.
202. Racher AJ, Looby D, Griffiths JB. Use of lactate dehydrogenase release to assess changes in culture viability. Cytotechnology. 1990;3(3):301-7.
203. Fotakis G, Timbrell JA. In vitro cytotoxicity assays: comparison of LDH, neutral red, MTT and protein assay in hepatoma cell lines following exposure to cadmium chloride. Toxicol Lett. 2006;160(2):171-7.
204. Balimane PV, Chong S, Morrison RA. Current methodologies used for evaluation of intestinal permeability and absorption. J Pharmacol Toxicol Methods. 2000;44(1):301-12.
205. Fernandes MB, Gonçalves JE, Scotti MT, de Oliveira AA, Tavares LC, Storpirtis S. Caco-2 cells cytotoxicity of nifuroxazide derivatives with potential activity against Methicillin-resistant Staphylococcus aureus (MRSA). Toxicol In Vitro. 2012;26(3):535-40.
206. Kamiloglu S, Capanoglu E, Grootaert C, Van Camp J. Anthocyanin absorption and metabolism by human intestinal caco-2 cells - A review. Int J Mol Sci. 2015;16(9):21555-74.
207. Shah P, Jogani V, Bagchi T, Misra A. Role of caco-2 cell monolayers in prediction of intestinal drug absorption. Biotechnol Prog. 2006;22(1):186-98.
208. Sarmento B, Andrade F, Silva SBd, Rodrigues F, das Neves J, Ferreira D. Cell-based in vitro models for predicting drug permeability. Expert Opin Drug Metab Toxicol. 2012;8(5):607-21.

209. Sujja-areevath J, Munday DL, Cox PJ, Khan KA. Relationship between swelling, erosion and drug release in hydrophillic natural gum mini-matrix formulations. Eur J Pharm Sci. 1998;6:207–17.

210. Coviello T, Alhaique F, Dorigo A, Matricardi P, Grassi M. Two galactomannans and scleroglucan as matrices for drug delivery: preparation and release studies. Eur J Pharm Biopharm. 2007;66(2):200-9.

211. Malik K, Arora G, Singh I. Taste masked microspheres of ofloxacin: Formulation and evaluation of orodispersible tablets. Sci Pharm. 2011;79(3):653-72.

212. Tobyn MJ, Staniforth JN, Baichwal AR, McCall TW. Prediction of physical properties of a novel polysaccharide controlled release system. I. Int J Pharm. 1996;128:113-22.

213. Sandolo C, Coviello T, Matricardi P, Alhaique F. Characterization of polysaccharide hydrogels for modified drug delivery. Eur Biophys J. 2007;36(7):693-700.

214. Colombo P, Conte U, Gazzaniga A, Maggi L, Sangalli ME, Peppas NA, et al. Drug release modulation by physical restrictions of matrix swelling. Int J Pharm. 1990;63(1):43-8.

215. Conte U, Maggi L. Modulation of the dissolution profiles from Geomatrix® multi-layer matrix tablets containing drugs of different solubility. Biomaterials. 1996;17(9):889-96.

216. Syed I, Mangamoori L, Rao Y. Formulation and characterization of matrix and triple-layer matrix tablets for oral controlled drug delivery. Int J Pharm Pharm Sci. 2010;2(3):137-43.

217. Jana S, Gandhi A, Sheet S, Sen KK. Metal ion-induced alginate–locust bean gum IPN microspheres for sustained oral delivery of aceclofenac. Int J Biol Macromol. 2015;72:47-53.

218. Dey P, Sa B, Maiti S. Impact of gelation period on modified locust bean-alginate interpenetrating beads for oral glipizide delivery. Int J Biol Macromol. 2015;76:176-80.

219. Ngwuluka NC, Choonara YE, Kumar P, du Toit LC, Modi G, Pillay V. A co-blended locust bean gum and polymethacrylate-NaCMC matrix to achieve zero-order release via hydro-erosive modulation. AAPS PharmSciTech. 2015;16(6):1377-89.

220. Zhao F, Zhao Y, Liu Y, Chang X, Chen C, Zhao Y. Cellular uptake, intracellular trafficking, and cytotoxicity of nanomaterials. Small. 2011;7(10):1322-37.

221. Fröhlich E. The role of surface charge in cellular uptake and cytotoxicity of medical nanoparticles. Int J Nanomedicine. 2012;7:5577-91.

222. Turcotte RF, Lavis LD, Raines RT. Onconase cytotoxicity relies on the distribution of its positive charge. The FEBS journal. 2009;276(14):3846-57.

223. Ilinskaya O, Dreyer F, Mitkevich V, Shaw K, Pace C, Makarov A. Changing the net charge from negative to positive makes ribonuclease Sa cytotoxic. Protein Sci. 2002;11(10):2522-5.

224. Bhattacharjee S, de Haan L, Evers N, Jiang X, Marcelis A, Zuilhof H, et al. Role of surface charge and oxidative stress in cytotoxicity of organic monolayer-coated silicon nanoparticles towards macrophage NR8383 cells. Part Fibre Toxicol. 2010;7(25):2-12.

225. Platel A, Carpentier R, Becart E, Mordacq G, Betbeder D, Nesslany F. Influence of the surface charge of PLGA nanoparticles on their in vitro genotoxicity, cytotoxicity, ROS production and endocytosis. J Appl Toxicol. 2016;36(3):434-44.

226. Huang M, Khor E, Lim L-Y. Uptake and cytotoxicity of chitosan molecules and nanoparticles: Effects of molecular weight and degree of deacetylation. Pharm Res. 2004;21(2):344-53.

227. Constantin M, Fundueanu G, Cortesi R, Esposito E, Nastruzzi C. Aminated polysaccharide microspheres as DNA delivery systems. Drug Deliv. 2003;10(3):139-49.

228. Aillon KL, Xie Y, El-Gendy N, Berkland CJ, Forrest ML. Effects of nanomaterial physicochemical properties on in vivo toxicity. Adv Drug Deliver Rev. 2009;61(6):457-66.

229. Perestrelo AR, Grenha A, Rosa da Costa AM, Belo JA. Locust bean gum as an alternative polymeric coating for embryonic stem cell culture. Mater Sci Eng C Mater Biol Appl. 2014;40:336-44.

230. Caetano LA, Almeida AJ, Gonçalves LMD. Approaches to tuberculosis mucosal vaccine development using nanoparticles and microparticles: A review. J Biomed Nanotechnol. 2014;10(9):2295-316.

231. Yamamoto M, Pascual DW, Kiyono H. M cell-targeted mucosal vaccine strategies. In: Kozlowski AP, editor. Mucosal vaccines: Modern concepts, strategies, and challenges. Berlin, Heidelberg: Springer Berlin Heidelberg; 2012. p. 39-52.

232. Kristensen M, Nielsen HM. Cell-penetrating peptides as carriers for oral delivery of biopharmaceuticals. Basic Clin Pharmacol Toxicol. 2016;118(2):99-106.

233. Truong-Le V, Lovalenti PM, Abdul-Fattah AM. Stabilization challenges and formulation strategies associated with oral biologic drug delivery systems. Adv Drug Deliver Rev. 2015;93:95-108.

234. Sharma R, Agrawal U, Mody N, Vyas SP. Polymer nanotechnology based approaches in mucosal vaccine delivery: Challenges and opportunities. Biotechnol Adv. 2015;33(1):64-79.

235. Gamazo C, Martín-Arbella N, Brotons A, Camacho AI, Irache JM. Mimicking microbial strategies for the design of mucus-permeating nanoparticles for oral immunization. Eur J Pharm Biopharm. 2015;96:454-63.

236. Convention TUSP. The United States Pharmacopeia XXXII/National Formulary XXVII. Rockville: The United States Pharmacopeial Convention; 2009.

237. Fernandez-Megia E, Novoa-Carballal R, Quiñoá E, Riguera R. Optimal routine conditions for the determination of the degree of acetylation of chitosan by 1H-NMR. Carbohydr Polym. 2005;61(2):155-61.

238. Rodrigues S, Cardoso L, da Costa A, Grenha A. Biocompatibility and stability of polysaccharide polyelectrolyte complexes aimed at respiratory delivery. Materials. 2015;8(9):5647-70.

239. Li Z, Gu L. Effects of mass ratio, pH, temperature, and reaction time on fabrication of partially purified pomegranate ellagitannin−gelatin nanoparticles. J Agric Food Chem. 2011;59(8):4225-31.

240. Müller M, Keßler B, Fröhlich J, Poeschla S, Torger B. Polyelectrolyte complex nanoparticles of poly(ethyleneimine) and poly(acrylic acid): Preparation and applications. Polymers. 2011;3(2):762-78.

241. Starchenko V, Müller M, Lebovka N. Growth of polyelectrolyte complex nanoparticles: Computer simulations and experiments. J Phys Chem C. 2008;112(24):8863-9.

242. de la Fuente M, Seijo B, Alonso MJ. Novel hyaluronan-based nanocarriers for transmucosal delivery of macromolecules. Macromol Biosci. 2008;8(5):441-50.

243. Teijeiro-Osorio D, Remunan-Lopez C, Alonso MJ. New generation of hybrid poly/oligosaccharide nanoparticles as carriers for the nasal delivery of macromolecules. Biomacromolecules. 2009;10(2):243-9.

244. Ochoa-Repáraz J, Sesma B, Álvarez M, Renedo MJ, Irache JM, Gamazo C. Humoral immune response in hens naturally infected with Salmonella Enteritidis against outer membrane proteins and other surface structural antigens. Vet Res. 2004;35(3):291-8.

245. Bonafonte MA, Solano C, Sesma B, Alvarez M, Montuenga L, García-Ros D, et al. The relationship between glycogen synthesis, biofilm formation and virulence in Salmonella enteritidis. FEMS Microbiol Lett. 2000;191(1):31-6.

246. Ochoa J, Irache JM, Tamayo I, Walz A, DelVecchio VG, Gamazo C. Protective immunity of biodegradable nanoparticle-based vaccine against an experimental challenge with Salmonella Enteritidis in mice. Vaccine. 2007;25(22):4410-9.

247. Werling D, Jungi TW. TOLL-like receptors linking innate and adaptive immune response. Vet Immunol Immunopathol. 2003;91(1):1-12.

248. Calvo P, Remunan-Lopez C, Vila-Jato JL, Alonso MJ. Chitosan and chitosan/ethylene oxide-propylene oxide block copolymer nanoparticles as novel carriers for proteins and vaccines. Pharm Res. 1997;14(10):1431-6.

249. Grenha A, Seijo B, Remuñán-López C. Microencapsulated chitosan nanoparticles for lung protein delivery. Eur J Pharm Sci. 2005;25:427-37.

250. Le Buanec H, Vetu C, Lachgar A, Benoit MA, Gillard J, Paturance S, et al. Induction in mice of anti-Tat mucosal immunity by the intranasal and oral routes. Biomed Pharmacother. 2001;55:316-20.

251. Borges O, Tavares J, de Sousa A, Borchard G, Junginger HE, Cordeiro-da-Silva A. Evaluation of the immune response following a short oral vaccination schedule with hepatitis B antigen encapsulated into alginate-coated chitosan nanoparticles. Eur J Pharm Sci. 2007;32:278-90.

252. Slütter B, Plapied L, Fievez V, Sande MA, Rieux Ad, Schneider Y-J, et al. Mechanistic study of adjuvant effect of biodegradable nanoparticles in mucosal vaccination. J Control Release. 2009;138:113-21.

253. Farhadian A, Dounighi NM, Avadi M. Enteric trimethyl chitosan nanoparticles containing hepatitis B surface antigen for oral delivery. Hum Vaccin Immunother. 2015;11(12):2811-8.

254. Abkar M, Lotfi AS, Amani J, Eskandari K, Ramandi MF, Salimian J, et al. Survey of Omp19 immunogenicity against Brucella abortus and Brucella melitensis: influence of nanoparticulation versus traditional immunization. Vet Res Commun. 2015;39(4):217-28.

255. Malik B, Goyal AK, Markandeywar TS, Rath G, Zakir F, Vyas SP. Microfold-cell targeted surface engineered polymeric nanoparticles for oral immunization. J Drug Target. 2012;20(1):76-84.

256. Mishra N, Khatri K, Gupta M, Vyas SP. Development and characterization of LTA-appended chitosan nanoparticles for mucosal immunization against hepatitis B. Artif Cells Nanomed Biotechnol. 2014;42(4):245-55.

257. Harde H, Agrawal AK, Jain S. Tetanus toxoids loaded glucomannosylated chitosan based nanohoming vaccine adjuvant with improved oral stability and immunostimulatory response. Pharm Res. 2015;32(1):122-34.

258. Dehghan S, Kheiri MT, Tabatabaiean M, Darzi S, Tafaghodi M. Dry-powder form of chitosan nanospheres containing influenza virus and adjuvants for nasal immunization. Arch Pharm Res. 2013;36(8):981-92.

259. Li XY, Li X, Kong XY, Shi S, Guo G, Zhang J, et al. Preparation of N-trimethyl chitosan-protein nanoparticles intended for vaccine delivery. J Nanosci Nanotechnol. 2010;10(8):4850-8.

260. Sayın B, Somavarapu S, Li XW, Thanou M, Sesardic D, Alpar HO, et al. Mono-N-carboxymethyl chitosan (MCC) and N-trimethyl chitosan (TMC) nanoparticles for non-invasive vaccine delivery. Int J Pharm. 2008;363(1–2):139-48.

261. Sarei F, Dounighi NM, Zolfagharian H, Khaki P, Bidhendi SM. Alginate nanoparticles as a promising adjuvant and vaccine delivery system. Indian J Pharm Sci. 2013;75(4):442-9.

262. Abdelwahed W, Degobert G, Stainmesse S, Fessi H. Freeze-drying of nanoparticles: Formulation, process and storage considerations. Adv Drug Deliver Rev. 2006;58(15):1688-713.

263. Chacón M, Molpeceres J, Berges L, Guzmán M, Aberturas MR. Stability and freeze-drying of cyclosporine loaded poly(D,L lactide–glycolide) carriers. Eur J Pharm Sci. 1999;8(2):99-107.

264. Kumar G, Shafiq N, Malhotra S. Drug-loaded PLGA nanoparticles for oral administration: Fundamental issues and challenges ahead. Crit Rev Ther Drug Carrier Syst. 2012;29(2):149-82.

265. Ikeda S, Zhong Q. Polymer and colloidal models describing structure-function relationships. Annu Rev Food Sci Technol. 2012;3(1):405-24.

266. Sameti M, Bohr G, Ravi Kumar MNV, Kneuer C, Bakowsky U, Nacken M, et al. Stabilisation by freeze-drying of cationically modified silica nanoparticles for gene delivery. Int J Pharm. 2003;266(1–2):51-60.

267. Wu L, Zhang J, Watanabe W. Physical and chemical stability of drug nanoparticles. Adv Drug Deliver Rev. 2011;63(6):456-69.

268. Borges O, Borchard G, Verhoef JC, de Sousa A, Junginger HE. Preparation of coated nanoparticles for a new mucosal vaccine delivery system. Int J Pharm. 2005;299:155-66.

269. Hafner A, Lovrić J, Voinovich D, Filipović-Grčić J. Melatonin-loaded lecithin/chitosan nanoparticles: Physicochemical characterisation and permeability through Caco-2 cell monolayers. Int J Pharm. 2009;381(2):205-13.

270. Morris GA, Castile J, Smith A, Adams GG, Harding SE. The effect of prolonged storage at different temperatures on the particle size distribution of tripolyphosphate (TPP) – chitosan nanoparticles. Carbohydr Polym. 2011;84(4):1430-4.

271. Salman HH, Gamazo C, Campanero MA, Irache JM. Salmonella-like bioadhesive nanoparticles. J Control Release. 2005;106:1-13.

272. Ma T, Wang L, Yang T, Ma G, Wang S. M-cell targeted polymeric lipid nanoparticles containing a toll-like receptor agonist to boost oral immunity. Int J Pharm. 2014;473(1–2):296-303.

273. Hori M, Onishi H, Machida Y. Evaluation of Eudragit-coated chitosan microparticles as an oral immune delivery system. Int J Pharm. 2005;297(1-2):223-34.

274. Maculotti K, Tira EM, Sonaggere M, Perugini P, Conti B, Modena T, et al. In vitro evaluation of chondroitin sulphate-chitosan microspheres as carrier for the delivery of proteins. J Microencapsul. 2009;26(6):535-43.

275. Prego C, Torres D, Alonso MJ. Chitosan nanocapsules as carriers for oral peptide delivery: Effect of chitosan molecular weight and type of salt on the *in vitro* behaviour and *in vivo* effectiveness. J Nanosci Nanotechnol. 2006;6:1-8.

276. da Silva LC, Garcia T, Mori M, Sandri G, Bonferoni MC, Finotelli PV, et al. Preparation and characterization of polysaccharide-based nanoparticles with anticoagulant activity. Int J Nanomedicine. 2012;7:2975-86.

277. Loh JW, Saunders M, Lim L-Y. Cytotoxicity of monodispersed chitosan nanoparticles against the Caco-2 cells. Toxicol Appl Pharmacol. 2012;262(3):273-82.

278. Zaki NM, Hafez MM. Enhanced antibacterial effect of ceftriaxone sodium-loaded chitosan nanoparticles against intracellular *Salmonella typhimurium*. AAPS PharmSciTech. 2012;13(2):411-21.

279. Harrison JA, Villarreal-Ramos B, Mastroeni P, Demarco de Hormaeche R, Hormaeche CE. Correlates of protection induced by live Aro- Salmonella typhimurium vaccines in the murine typhoid model. Immunology. 1997;90(4):618-25.

280. Sztein MB, Wasserman SS, Tacket CO, Edelman R, Hone D, Lindberg AA, et al. Cytokine production patterns and lymphoproliferative responses in volunteers orally Immunized with attenuated vaccine strains of Salmonella typhi. J Infect Dis. 1994;170(6):1508-17.

281. Okahashi N, Yamamoto M, VanCott JL, Chatfield SN, Roberts M, Bluethmann H, et al. Oral immunization of interleukin-4 (IL-4) knockout mice with a recombinant Salmonella strain or cholera toxin reveals that CD4+ Th2 cells producing IL-6 and IL-10 are associated with mucosal immunoglobulin A responses. Infect Immun. 1996;64(5):1516-25.

282. VanCott JL, Staats HF, Pascual DW, Roberts M, Chatfield SN, Yamamoto M, et al. Regulation of mucosal and systemic antibody responses by T helper cell subsets, macrophages, and derived cytokines following oral immunization with live recombinant Salmonella. J Immunol. 1996;156(4):1504-14.

283. Yang DM, Fairweather N, Button LL, McMaster WR, Kahl LP, Liew FY. Oral Salmonella typhimurium (AroA-) vaccine expressing a major leishmanial surface protein (gp63) preferentially induces T helper 1 cells and protective immunity against leishmaniasis. J Immunol. 1990;145(7):2281-5.

284. Salman HH, Irache JM, Gamazo C. Immunoadjuvant capacity of flagellin and mannosamine-coated poly(anhydride) nanoparticles in oral vaccination. Vaccine. 2009;27:4784-90.

285. van Kooyk Y. C-type lectins on dendritic cells: Key modulators for the induction of immune responses. Biochem Soc Trans. 2008;36(6):1478-81.

286. Jump RL, Levine AD. Murine Peyer's patches favor development of an IL-10-secreting, regulatory T cell population. J Immunol. 2002;168(12):6113-9.

287. Gutierro I, Hernández RM, Igartua M, Gascón AR, Pedraz JL. Size dependent immune response after subcutaneous, oral and intranasal administration of BSA loaded nanospheres. Vaccine. 2002;21(1–2):67-77.

288. Fievez V, Plapied L, Rieux Ad, Pourcelle V, Freichels H, Wascotte V, et al. Targeting nanoparticles to M cells with non-peptidic ligands for oral vaccination. Eur J Pharm Biopharm. 2009;73(1):16-24.

289. Salman HH, Gamazo C, Agueros M, Irache JM. Bioadhesive capacity and immunoadjuvant properties of thiamine-coated nanoparticles. Vaccine. 2007;25:8123-32.

290. Salman HH, Gamazo C, de Smidt PC, Russell-Jones G, Irache JM. Evaluation of bioadhesive capacity and immunoadjuvant properties of vitamin B(12)-Gantrez nanoparticles. Pharm Res. 2008;25:2859-68.

291. Paliwal R, Babu RJ, Palakurthi S. Nanomedicine scale-up technologies: Feasibilities and challenges. AAPS PharmSciTech. 2014;15(6):1527-34.

292. Dong Y, Ng WK, Shen S, Kim S, Tan RBH. Scalable ionic gelation synthesis of chitosan nanoparticles for drug delivery in static mixers. Carbohydr Polym. 2013;94(2):940-5.

293. Fonte P, Lino PR, Seabra V, Almeida AJ, Reis S, Sarmento B. Annealing as a tool for the optimization of lyophilization and ensuring of the stability of protein-loaded PLGA nanoparticles. Int J Pharm. 2016;503(1–2):163-73.

294. Sjögren E, Abrahamsson B, Augustijns P, Becker D, Bolger MB, Brewster M, et al. In vivo methods for drug absorption – Comparative physiologies, model selection, correlations with in vitro methods (IVIVC), and applications for formulation/API/excipient characterization including food effects. Eur J Pharm Sci. 2014;57:99-151.